The mobility of platinum-group elements in humic acid under surficial weathering conditions: an experimental study

Von der Naturwissenschaftlichen Fakultät der
Gottfried Wilhelm Leibniz Universität Hannover

zur Erlangung des Grades

Doktorin der Naturwissenschaften (Dr. rer. nat.)

genehmigte Dissertation

von

Emmylou Kotzé, M.Sc. (Südafrika)

2019

Referentin/ Referent: Prof. Dr. rer. nat. Francois Holtz

Korreferentin/ Korreferent: Dr. rer. nat. Stephan Schuth

Tag der Promotion: 02.12.2019

Table of Contents

Figures

Appendix

Tables

Appendix

Abstract

Although the platinum-group elements (PGE) are known to be mobile under certain conditions in the surficial weathering environment, their mobilization in the presence of humic substances is poorly constrained. In these experiments, platinum and palladium were mobilized and analyzed in solution using laboratory preparations of humic acid solutions, synthetic minerals, and naturally occurring chromitite samples. The composition of synthetic humic acid is an average of naturally occurring humic substances. Experiments were carried out using humic acid powder (HAP), humic acid sodium salt (HASS) and water as solutions. Synthetic powders of PdS, PtS_2, PdTe and $PdTe_2$ were used as substrate for the solutions, along with chromite concentrate and tailings material from the Thaba Mine, South Africa. These substrates were exposed to water, HAP and HASS in different concentrations and for different periods of time. Two series of experiments were carried out: short-term experiments and long-term experiments. The short-term experiments were split into three time-series: 1 hour, 20 hours and 100 hours. Each sample of each time-series was rotated continuously. The synthetic powders and chromite concentrate were each mixed with water, then 1 M HASS solution, and then 1 M HAP solution. The pH of the HAP and HASS solutions was fixed at 3 and 3.5, respectively. The long-term experiments involved mixing the substrates and solutions together, then letting these react undisturbed in a beaker for 320 days. Only HAP was used for the long-term experiments, with water as a control for selected powders. The concentration of HAP in these solutions was low, ranging from 0.1-10 ppm. The pH of each solution was found to be about 8, and was not artificially changed. Aliquots of each solution were taken at predetermined intervals. All solutions from this study were analyzed by sector-field inductively coupled plasma mass spectrometry (SF-ICP-MS). Due to the use of hydrochloric acid to fix pH in the short-term experiments, Pd and Pt may have been mobilized by means of chloride complexes rather than humic substances in these experiments, which showed that water was capa-

ble of mobilizing Pd and Pt as well as the humic acids. The long-term experiments, however, revealed a complex relationship between mineral type and strength of humic acid solution. While Pd was not mobilized significantly from PdTe and $PdTe_2$, several thousand μg/l of tellurium was mobilized from these powders. Tellurium oxide crystals were found on the residues of these experiments, and the palladium content of the initial palladium tellurides increased relative to tellurium. Palladium was mobilized from PdS at a rate of about 0.5 μg/l per day, reaching a final value of 162 μg/l in the strongest humic acid solution. Platinum, however, was taken into solution during the first few days, and then precipitated from solution due to a change in pH driven by the hydrolysis of platinum sulfide. In a hydrous environment, it seems that humic acid plays an important role in removing certain elements, causing others to be enriched in the weathered ore. Pd is more mobile than Pt in a humic acid solution, but in telluride minerals, Te is preferentially mobilized, and Pd stays behind, probably forming residual PGE minerals that are preserved in the weathering environment. Experiments on chromitite concentrate and tailings material showed that although the humic acids are capable of mobilizing Cr, it is not necessary for the chromite crystal to be broken down in order to liberate platinum-group elements. The PGE-bearing minerals are probably exposed to weathering once the interstitial silicate minerals of the chromitite are weathered. The results of the experiments on chromitite material confirmed that Pd and Pt could be leached by the humic substances in a simulated surficial environment. Along with the previous experiments, they suggest that the humic acids play an important role during weathering of PGE deposits.

Keywords: PGEs, humic acids, geochemistry, chromitites, ore deposits

Zusammenfassung

Obwohl die Platingruppenelemente (PGE) umgebungsbedingt durch Verwitterung auf der Erdoberfläche mobil werden können, ist deren Mobilisierung in der Präsenz von Huminstoffen bis heute kaum quantitativ untersucht worden. Anhand von Huminsäure-Standardlösungen, synthetischen Mineralien und natürlich vorkommenden Chromititproben wurden Platin und Palladium in diesen Versuchen in Lösung mobilisiert sowie analysiert. Die Zusammensetzung der synthetischen Huminsäuren beträgt eine durchschnittliche Approximation der natürlich vorkommenden Huminstoffe. Es wurden Versuche mit Huminsäurenpulver (humic acid powder, HAP), Huminsäurenatriumsalz (humic acid sodium salt, HASS) sowie Wasser als Lösungen durchgeführt. Als Substrat für die Lösungen wurden synthetische Pulver aus PdS, PtS2, PdTe und PdTe2 sowie Chromitkonzentrat und Tailingsmaterial aus der Thaba Mine, Südafrika, verwendet. Diese Substrate wurden Wasser, HAP und HASS in unterschiedlichen Konzentrationen und für unterschiedliche Zeitdauern ausgesetzt. Es wurden zwei Versuchsreihen durchgeführt: Kurzzeitversuche und Langzeitversuche. Die Kurzzeitversuche wurden in drei Zeitreihen aufgeteilt: 1 Stunde, 20 Stunden und 100 Stunden. Alle Proben wurden kontinuierlich mechanisch herumgedreht. Die synthetischen Pulver und das Chromitkonzentrat wurden zuerst mit Wasser, danach mit 1 M HASS-Lösung und schließlich mit 1 M HAP-Lösung gemischt. Die pH-Werte der HAP- und HASS-Lösungen wurden jeweils auf 3 bzw. 3,5 künstlich festgehalten. Bei den Langzeitversuchen wurden die Substrate und die Lösungen miteinander vermischt und anschließend 320 Tage lang ungestört im Becherglas gelassen, um die Reaktionen zu ermöglichen. Für die Langzeitversuche wurde ausschließlich HAP verwendet, in Begleitung von Wasser als Versuchskontrolle bei ausgewählten Pulvern. Die HAP-Konzentration in diesen Lösungen war bei 0,1-10 ppm gering. Der pH-Wert dieser Lösungen lag bei etwa 8 und wurde nicht künstlich verändert. Teilproben jeder Lösung

wurden in vorgegebenen Abständen entnommen. Alle Lösungen aus dieser Studie wurden mittels Sektorfeld-Massenspektrometrie mit induktiv gekoppeltem Plasma (SF-ICP-MS) analysiert. Aufgrund der Verwendung von Salzsäure zur Fixierung des pH-Wertes in den Kurzzeitversuchen ist es wahrscheinlich, dass Pd und Pt in diesen Versuchen nicht nur durch Huminstoffe, sondern auch durch Chloridkomplexe mobilisiert worden waren. Diese Tendenz zeigte, dass Pd und Pt nicht nur durch Huminsäuren mobilisiert werden können, sondern auch durch Wasser. Die Langzeitversuche zeigten jedoch einen komplexen Zusammenhang zwischen Mineralart und Konzentration der Huminsäurenlösung. Obwohl Pd nicht bedeutend aus PdTe und PdTe2 mobilisiert wurde, wurden aus diesen Pulvern mehrere Tausend µg/l Tellur mobilisiert. Auf den Rückständen dieser Versuche wurden Telluroxid-Kristalle gefunden, und der Palladiumgehalt der ursprünglichen Palladiumtelluride stieg dem Tellurgehalt gegenüber. Palladium wurde aus PdS mit einer Schnelligkeit von etwa 0,5 µg/l pro Tag mobilisiert und erreichte in der stärksten Huminsäurenlösung einen Endwert von 162 µg/l. In den ersten Tagen wurde Platin in die Lösung aufgenommen, scheidete aber aufgrund einer pH-Änderung, die durch die Hydrolyse von Platinsulfid erfolgte, etwas später aus. In einer wasserhaltigen Umgebung scheint es der Fall zu sein, dass Huminsäuren eine wichtige Rolle in der Befreiung bestimmter Elemente spielen, wodurch andere im verwitterten Erz angereichert werden. Pd ist in Huminsäurenlösung deutlich mobiler als Pt, allerdings wird aus Tellurid-Mineralien vorzugsweise Te mobilisiert, während Pd hinterlassen wird, wodurch restliche PGE-Mineralien vermutlich entstehen, die in der Verwitterungsumgebung erhalten bleiben. Versuche mit Chromititkonzentrat und Tailingsmaterial zeigten, dass die Huminsäuren zwar in der Lage sind, Cr zu mobilisieren, dass es aber unnötig ist, den Chromitkristall zu zerlegen, um Platingruppenelemente freizusetzen. Wahrscheinlich werden die PGE-haltigen Mineralien der Verwitterung erst ausgesetzt, wenn die interstitiellen Silikatminerale des Chromitits bereits verwittert sind. Die Versuche mit Chromititmaterial bestätigten, dass Pd und Pt durch die Huminstoffe in einer simulierten, erdoberflächenähnlichen Umgebung ausgelaugt werden

können. Zusammen mit anderen bisherigen Experimenten deuten die Ergebnisse darauf hin, dass die Huminsäuren eine wichtige Rolle bei der Verwitterung von PGE-Lagerstätten spielen.

Schlagwörter: PGEs, Huminsäure, Geochemie, Chromitite, Lagerstätten

1. Introduction

1.1. Why PGE?

The production of PGE (platinum group elements) for industry is critical from the viewpoint of European economies as well as countries around the world. The PGE have many uses not only as durable jewelry, but also in the chemical, electronic, glass production, automotive and medical sectors for their unique properties—biocompatibility, high melting temperature and conductivity, inertness and oxidation– and corrosion-resistance (Creamer, 2006). They are used for spark plugs, as treatment for cancer (as cisplatin and carboplatin), to produce glass and liquid crystal displays, in computers and smartphones, as catalysts in the manufacture of paints, textiles and acids, in autocatalytic systems to remove carbon monoxide, nitrous oxides and hydrocarbons from exhaust fumes, and in devices such as pacemakers and defibrillators (Creamer, 2006; Shaffer, 2015). Although the PGE can be recycled from jewelry, electronics and catalytic equipment (recycled Pt and Pd accounts for about 24% of their worldwide supply) (Shaffer, 2015), they are also mined extensively. In this thesis, PGM refers to "platinum group minerals," therefore, the minerals from which the PGE may be liberated.

Important PGM deposits which represent present and future resources of the PGE include the chromitites, (e.g. Gain, 1985) Merensky Reef (e.g. Naldrett et al., 2009) and Platreef (e.g. Ihlenfield & Keays, 2011) of the Bushveld Igneous Complex (BIC) in South Africa, the Ni-Cu-PGE-bearing mafic intrusions of Noril'sk-Talnakh, Russia, (e.g. Arndt et al., 2003) the Great Dyke of Zimbabwe, (e.g. Locmelis et al., 2010; Oberthür et al., 2015) the Sudbury Igneous Complex of Canada, (Dare et al., 2011) the similar orthomagmatic sulfide-PGE deposits associated with mafic–ultramafic igneous intrusions of Finland such as the Kilvenjärvi deposit, (Andersen et al., 2006) the Stillwater Layered Complex of Montana, U.S.A., (e.g. Godel & Barnes, 2008) the low-temperature hydrothermal platinum veins of the Waterberg

deposit, South Africa (e.g. McDonald et al., 1999) and the high-temperature hydrothermal mineralization of platinum at the Driekop dunite pipe in South Africa, (e.g. Tarkian & Stumpfl, 1975; Schiffries, 1982) nickel laterites occurring in tropical zones such as the Dominican Republic, (e.g. Aiglsperger et al., 2015) the Freetown Peninsula of Sierra Leone (e.g. Bowles, 1986; et al., 2017) and New Caledonia, associated with PGE-enriched chromitite of the New Caledonia Ophiolite Complex, (e.g. Augé & Marizot, 1995; Traoré et al., 2006) other alluvial deposits such as those found in Minas Gerais, Brazil (e.g. Cabral et al., 2007) and the oxidized portions of the Great Dyke, Zimbabwe, (e.g. Oberthür et al., 2003) and PGE placer deposits originating from certain intrusive complexes rich in PGE in Canada, (e.g. Barkov et al., 2005) Alaska (e.g. Tolstykh et al., 2002) and the Ural Mountains of Russia (e.g. Johan, 2006). Of these, the laterite and alluvial deposits in particular show possible interaction between the PGE and soil components such as soil organic matter, humic substances from plant remains (Aiglsperger et al., 2015; Bowles et al, 2017) and microbes (Cabral et al., 2011; Bowles et al., 2017). PGE enrichment occurs in soils associated with these laterite deposits even when the source rock is not unusually enriched in PGE (Aiglsperger et al., 2015). Because of the high demand for PGM in specific industrial sectors combined with the fact that PGE deposits can be difficult to access, the European Commission has classified PGM as part of the critical raw materials needed in the EU (European Commission, 2014). Within this context, it makes sense to examine non-traditional sources of PGE as possible future sources.

The PGE are economically recoverable from underground and open-cast mining at grades above 1-3 grams per ton (Cawthorn, 1999; Cramer, 2001), depending on the price of Pt and the other PGE, and also the ratio of Pt, Pd and Rh to the total PGE in the ore deposit. Some underground workings, particularly those of the BIC, contain PGE at a total grade of 7-9 g/t (Cawthorn et. al., 2002). Although oxidized deposits are theoretically still economic, some yielding concentrations such as 0.1-0.3 g/ton of combined Pt+Pd in the weathering zone of the

Freetown Layered Complex (Bowles, et. al., 2017), and 3-5 g/ton of Pt in the oxidized zone of the Great Dyke (Kraemer et. al., 2015) in alluvium that can easily be removed by open-pit mining, the mode of occurrence of the PGMs is such that the PGE cannot be easily recovered (Locmelis et. al., 2010; Oberthür et. al., 2013). A possible approach to exploiting oxide PGE deposits may be hydrometallurgical (selective leaching followed by electrolysis or precipitation) rather than pyrometallurgical (roasting, smelting) (Dreisinger, 2009; Evans & Spratt, 2000; Oberthür et. al., 2013; Kraemer et. al., 2015).

1.2. PGE in the surficial environment and the importance of humic substances

The PGE have been observed to be mobile under hydrothermal conditions at varying temperatures (e.g. Tarkian & Stumpfl, 1975; Schiffries, 1982; McDonald et al., 1999). These and similar studies have shown that hydrothermal fluids can redistribute the PGE from a primary magmatic deposit. But it has also become known that Pt and Pd can be transported in the surficial weathering environment as well (e.g. Azaroual et al., 2001; Cabral et al., 2007).

In the surficial environment, rocks are weathered and soil formation takes place (e.g. Robb, 2005). Dissolution of minerals, hydrolysis of metals and oxidation-reduction reactions cause metallic enrichment in soils. Soil formation is an intrinsic part of the surficial environment. Laterites are very thick tropical soils which result from intense weathering over millions of years; they are generally rich in kaolinitic clay as well as Fe- and Al-oxides. Laterites which form over ultramafic rocks can concentrate Ni, Mn, Au, Cu and the PGE within the soil profile (ibid.). Pt is usually found to be concentrated just above the coarse saprolite, which is defined as the horizon where 20% of the weatherable minerals have been altered, (Robb, 2005; Traoré et al., 2006) while Pd is more evenly spread throughout the soil profile (Traoré, 2006). This is because the palladium-chloride and –hydroxide complexes that transport Pd in solu-

tion are stable over a great range of conditions in the surficial zone, whereas the analogous platinum complexes are stable under more limited conditions (Robb, 2005; Cabral et al., 2007). If oxygen fugacity remains high, Pt will be precipitated from oxide complexes at pH values below 1 and higher than 8, while Pd will likely remain in solution (Cabral et al., 2007).

Dissolution and redistribution of Pt and Pd is not limited to laterites, and can occur in thinner soils as well, such as the oxidized portion of the Great Dyke of Zimbabwe, where similar processes to those in lateritic soils occur, such as greater mobilization of Pd relative to Pt and enrichment of Pt in the remaining soil (Oberthür et al., 2003). In these environments, Pd and Pt are more likely to be transported as hydroxide rather than chloride complexes due to groundwater being neutral or alkaline rather than acidic (Robb, 2015).

Another feature of the surficial zone is the presence of humic acid. This is defined as the portion of soil organic matter—resulting from decomposition of plants and animals—which can be dissolved in aqueous sodium hydroxide and precipitated by acidifying the resulting solution (Haworth, 1971). Humic substances are ubiquitous in soils and in natural waters, and they are capable of forming soluble and insoluble complexes with metals (Schnitzer, 1978). Different types of these humic substances may be found in soils; therefore, the exact results of any experiment involving “humic acid” will depend on the origin of the humic substance. Laboratory-produced humic acid is considered to be a chemical average of these substances. Humic acid interacts with Pd and Pt in the weathering environment, possibly forming complexes that keep these elements in solution, or transporting them by means of adsorption (Wood, 1990; 1996; et al., 1994). A detailed review of these sources may be found in Chapter 4. The interaction between PGE and humic acid in the surficial environment, although clearly of great importance, remains poorly constrained.

1.3. Aims of the project

The project seeks to answer the following questions by means of experimentation and geo-chemical analysis:

1. Can Pt and Pd be mobilized from PGE-rich minerals into solution by humic acids? This can be answered by comparing experiments conducted under the same conditions between humic acids and pure water.
2. Are there significant differences in PGE mobilization between different PGE minerals, and can these differences be applied to naturally occurring ore deposits? To answer this, different PGE-rich minerals can be used in similar experiments. Natural chromitite from the Thaba Mine can also be subjected to the same experimental process.
3. How can the results from this study be applied to natural ore-forming processes and the formation of soils from PGE deposits? This is discussed after results from the above experiments have been obtained.

2. Materials and methods

2.1. Starting materials

Humic acids

Two types of synthetic humic acid were available for the experiments. Firstly, a standard humic acid powder (HAP) from Alfa Aesar (lot no. R07A015) with a chemical formula of $C_9H_9NO_6$ was used. Secondly, a humic acid sodium salt powder (HASS) (also from Alfa Aesar, lot no. R07A015) with a chemical formula of $C_9H_8Na_2O_4$ was used. HASS is also counted as part of the humic substances; it was applied to the early experiments to assess any differences in Pd and Pt behavior compared to HAP. Both of these powders were dissolved in water to make solutions of known concentration for the experiments described in the section below. HASS and HAP both were used for early experiments, (see section below) but after establishing that both yielded similar results in these experiments, only HAP was used to set up the later experiments.

For the early short-term experiments, HAP and HASS were both diluted to form solutions of 0.1 M (mol/l). By weight rather than molecular mass, both of these solutions had a concentration of about 22.6 g/l, equivalent to 22.6 ‰, or 22 600 ppm. For the subsequent long-term experiments, much lower concentrations of HAP were used (0.1, 1 and 10 mg/l). In the final experiments, two concentrations of HAP were used—10 and 1 000 mg/l (1 g/l). Differences in the appearance of the humic acid solution could be seen between the different concentrations used (Figure 2.1). At a concentration of 10 mg/l, the humic acid solution becomes golden-colored; at concentrations below this, the solution is transparent. The brown color increases in intensity with the strength of the solution, becoming very thick and dark brown to black in color at a concentration of 22.6 g/l.

Figure 2.1: (a): HAP at concentrations of 10, 1 and 0.1 mg/l, used for long-term experiment. (b): HASS at a concentration of about 22.6 g/l.

For the short-term experiments using 22.6 g/l of humic acid, the pH of the solution was fixed at 3 for the HAP solution and 3.5 for the HASS solution. It was thought that lower pH might promote PGE mobility. After this was found to present experimental complications, (see Chapter 3) the pH of all subsequent solutions for both the long-term and the final solutions was not fixed or altered in any other way. The pH of these solutions was measured and the value was found to vary between 7 and 8 for the lower concentrations, (0.1-10 mg/l) while the stronger solutions had a pH of about 10 for all solutions.

Substrates

Four synthetic Pt-Pd minerals as well as chromite concentrate and tailings material from the Thaba Mine were used as solid substrate in the solution experiments. The chromite concentrate sample MNR60 and a sample of chromite tailings material were provided by the Thaba Mine. The chromite concentrate was characterized by large (up to 1 mm in diameter) chromite crystals and the lack of remaining silicate minerals. The tailings sample was characterized by chromite crystals in a matrix of silicate minerals. The tailings sample, being heterogeneous in grain size, was crushed to a grain size of <200 µm. The chromite concentrate MNR60 was used in the experiments in its original coarse-grained form, but was also crushed to a size of <100 µm to create two size fractions. Further details on these substrates may be found in Chapter 5.

The synthetic minerals used in this study had the chemical formulae of PtS_2, PdS, PdTe and $PdTe_2$. PtS_2 and PdS were acquired in powder form from American Elements, Merelex Cor-

poration, USA, whilst PdTe and $PdTe_2$ were synthesized from Pd and Te at the Leibniz University of Hannover using the evacuated tube method of Vymazalová et. al. (2005) which was itself modified from the method described earlier by Kullerud (1971). Further details on the properties of the synthetic substrates may be found in Chapter 4.

2.2. Laboratory setup

Overview

A graphical overview of all experiments done may be found in Table 2.1, including a description of the duration of each experiment along with the substrates and concentrations of humic acid solutions used.

Table 2.1: Overview of solution experiments.

Short-term experiments (continuously rotated)		
Duration	*Substrate*	*Reagent*
1 hour	MNR60	H_2O
		HASS (22.6 g/l; pH 3.5)
		HAP (22.6 g/l; pH 3)
	MNR60 (<100 µm)	H_2O
		HASS (22.6 g/l; pH 3.5)
		HAP (22.6 g/l; pH 3)
	PtS_2	H_2O
		HASS (22.6 g/l; pH 3.5)
		HAP (22.6 g/l; pH 3)
	PdS	H_2O
		HASS (22.6 g/l; pH 3.5)
		HAP (22.6 g/l; pH 3)
	PdTe	H_2O
		HASS (22.6 g/l; pH 3.5)
		HAP (22.6 g/l; pH 3)
	$PdTe_2$	H_2O
		HASS (22.6 g/l; pH 3.5)

		HAP (22.6 g/l; pH 3)
20 hours	MNR60	H_2O
		HASS (22.6 g/l; pH 3.5)
		HAP (22.6 g/l; pH 3)
	MNR60 (<100 µm)	H_2O
		HASS (22.6 g/l; pH 3.5)
		HAP (22.6 g/l; pH 3)
	PtS_2	H_2O
		HASS (22.6 g/l; pH 3.5)
		HAP (22.6 g/l; pH 3)
	PdS	H_2O
		HASS (22.6 g/l; pH 3.5)
		HAP (22.6 g/l; pH 3)
	PdTe	H_2O
		HASS (22.6 g/l; pH 3.5)
		HAP (22.6 g/l; pH 3)
	$PdTe_2$	H_2O
		HASS (22.6 g/l; pH 3.5)
		HAP (22.6 g/l; pH 3)
100 hours	MNR60	H_2O
		HASS (22.6 g/l; pH 3.5)
		HAP (22.6 g/l; pH 3)
	MNR60 (<100 µm)	H_2O
		HASS (22.6 g/l; pH 3.5)
		HAP (22.6 g/l; pH 3)
	PtS_2	H_2O
		HASS (22.6 g/l; pH 3.5)
		HAP (22.6 g/l; pH 3)
	PdS	H_2O
		HASS (22.6 g/l; pH 3.5)
		HAP (22.6 g/l; pH 3)
	PdTe	H_2O
		HASS (22.6 g/l; pH 3.5)
		HAP (22.6 g/l; pH 3)
	$PdTe_2$	H_2O

		HASS (22.6 g/l; pH 3.5)
		HAP (22.6 g/l; pH 3)
Long-term experiments: Total reaction time of 308 days		
Reagent	*Substrate*	
HAP (0.1 mg/l)	MNR60	
	MNR60 (<100 µm)	
	PtS_2	
	PdS	
	PdTe	
	$PdTe_2$	
HAP (1 mg/l)	MNR60	
	MNR60 (<100 µm)	
	PtS_2	
	PdS	
	PdTe	
	$PdTe_2$	
HAP (10 mg/l)	MNR60	
	MNR60 (<100 µm)	
	PtS_2	
	PdS	
	PdTe	
	$PdTe_2$	
H_2O	MNR60	
	PtS_2	
	$PdTe_2$	
Final experiments: Total reaction time of 49 days		
Reagent	*Substrate*	
HAP (10 mg/l)	Tailings	
HAP (1 g/l)	MNR60 (<100 µm)	
	PtS_2	
	PdS	
	Tailings	

Short-term (time-series) experiments

The initial experiments were designed to mimic natural weathering processes on three levels. First, exposure to water in the natural environment; second, leaching of the weathered material by humic-acid sodium salts, and third, reaction of the further weathered material with humic acid present in soils. Three time-series were planned for these experiments; a series of 1 hour, of 20 hours (1 day) and of 100 hours (1 week). The chromite concentrate, both unaltered and crushed to <100 µm, was used as substrate, as were the four synthetic PGE powders described above. Each substrate (0.5 g of chromite concentrate and 0.25 g of synthetic powder) was placed in a Corning CentriStar™ sample tube and covered with 5 ml of water. The tubes were then placed in a sample shaker and continuously rotated for the total experimental time. The experiment was rotated in order to simulate a longer reaction time, as the motion might cause any reactions to proceed faster than a stationary environment. After the end of the experimental time, each tube was centrifuged in a Sigma laboratory centrifuge at a speed of 5 000 rpm for about 30 minutes. The solution in each tube was siphoned off with a laboratory pipette and set aside for storage and analysis. For analysis, a 1 ml aliquot of this solution was taken and prepared (see below). The remaining solid material in each tube was briefly washed with water before adding 5 ml of 22.6 g/l HASS to the tube. The entire experimental process was repeated using HASS, and after that using the 22.6 g/l solution of HAP. Alongside each experimental time-series, a blank sample containing only water and humic acid solution (with no solid substrate) was subjected to exactly the same treatment as the samples and later analyzed with them. Two identical experiments were carried out for each substrate and time period; (see Table 2.1) in this way, the reproducibility of these type of experiments was tested.

Long-term and final experiments

The same 6 substrates (chromite concentrate, crushed chromite concentrate, PtS_2, PdS, PdTe and $PdTe_2$) were used to set up the long-term experiment, which was a stationary experiment

that ran for a total of 308 days. Each substrate was placed in a Savillex® teflon beaker of 240 ml, and then covered with 200 ml of each of the diluted HAP solutions (0.1, 1, and 10 mg/l). Five grams of chromite concentrate were used, 4 g of crushed chromite concentrate, and 0.03 g of each synthetic powder. As a control, three substrates (2 g chromite concentrate, and 0.01 g of PtS_2 and $PdTe_2$) were covered with H_2O in a 60 ml Savillex® teflon beaker and treated the same as the experimental solutions. The beakers were only moved gently when aliquots were taken, at preselected intervals during the experiment. Five aliquots were taken in total; for details of the timing, see Chapters 4 and 5. The beakers were stored away from sunlight to prevent photolytic decay of humic acid (e.g., Strome and Miller, 1978).

The final experiment was set up specifically to test the reaction of certain substrates (crushed chromite concentrate, PdS and PtS_2) with higher concentrations of humic acid, as well to establish the behavior of Pd and Pt in the chromite tailings sample received from Thaba Mine. Thus, the chromite tailings sample was reacted with two concentrations of humic acid powder solution, (10 and 1 000 mg/l) while the other three substrates were only reacted with the 1 000 mg/l humic acid powder solution. Further details on the setup and rationale of this experiment may be found in Chapter 5.

Sample preparation for ICP-MS

The aliquots of solution obtained from the various experiments were all analyzed by sector-field inductively coupled plasma mass spectrometry (SF-ICP-MS) at the Leibniz University in Hannover. To prepare for analysis using the machine, each aliquot was placed in a 60 ml Savillex® teflon beaker and allowed to react with 5 ml H_2O_2 (30%, Suprapure, Merck, Germany) which had been diluted to about 10%. Each beaker was set open on a hot plate in the laboratory and allowed to evaporate overnight at 90 °C. Various residues were obtained after the first evaporation; higher concentrations of humic acid produced a yellow or orange residue, while lower concentrations (<10 mg/l) yielded pale yellow or white residues. This resi-

due was then reacted with 5 ml concentrated aqua regia overnight at a temperature of 80 °C on the same hot plate, with the beakers closed. The beakers were then opened and the remaining solution allowed to evaporate. This yielded a paler residue which could be dissolved in 1 ml 1 M HNO_3 and stored. For analysis, this dissolved sample was further diluted in a 3% HNO_3 solution with 5 µg/l Rh added as an internal standard.

2.3. Analysis of solutions

All aliquots taken of the above described solutions were analyzed with a Thermo-Scientific Element-XR fast scanning-sector field-inductively coupled plasma mass spectrometer at the Institute of Mineralogy, University of Hannover. The technique of ICP-MS has many applications for earth science, and can be used to analyze elemental concentrations of metals dissolved in a solution of weak HNO_3. The sample solution is introduced into the machine by means of an analytical nebulizer, which converts the solution liquid into an aerosol. This aerosol is then caught up in the inductively coupled plasma, which consists of a heated plasma of ionized argon. This plasma ionizes the elements present in the sample so that they can be sent to the mass analyzer, which separates and the ions according to their atomic mass, after which the constituent elements can be classified (Downard, 2004).

The advantage of sector-field mass spectrometry (SF-ICP-MS) is that it can be used to quickly and accurately classify large numbers of samples. Care must be taken, however, to dilute samples in solution so as not to cause excessive matrix effects (Köllensperger et al., 2000; Bencs et al., 2003). Like all forms of mass spectrometry, this method is also subject to elemental interferences caused by the presence of oxygen; therefore, care must be taken to adjust instrument parameters so as to keep oxide formation below 5% in each analytical run (Thomas, 2002). The interferences relevant to analysis of Pd and Pt are those caused by the formation of Y–, Zr–, and Hf oxide complexes. Because all three of these elements were found to be present in the experimental solutions, (by analysis of blank samples of HAP and HASS)

all Pd and Pt data used have been reviewed to remove the contribution of the interfering compounds. With each analytical run, solutions of all three of these elements at concentrations of ~10 and ~1 µg/l were also analyzed, in order to determine the magnitude of interferences on Pd and Pt isotopes. The contribution of Hf oxides was found to be below ~0.1% of the total of each Pt isotope value measured, but interferences caused by Y and Zr were much higher. After calculating the contribution of these interferences for each Pd isotope, the ratio of each Pd isotope to the other isotopes was checked; if these agreed with the natural abundance of Pd isotopes given by Berglund & Wieser, (2011) they were accepted for use in the results. More specific information on the types of interferences experienced in this study and the solutions to this challenge, as well as details on the conditions of analysis, may be found in the Methods sections of Chapters 4 and 5. With each sample run, random duplicate samples were also included, to test the reproducibility of the analytical method. The approximate detection limit of Pt using this method is 0.005 µg/l, and for Pd it is 0.01 µg/l.

3. Short-term PGE mobility experiments at low pH

3.1. Results

The analyses of the short-term experiments, with a total of 100 hours of reaction, are shown in Figures 3.1–4. The data upon which these figures were based may be found in Table 8.1 of the Appendix. In each experimental run, a duplicate sample containing exactly the same substrate and reagent was made; these are indicated in the figures as 'II.' This was done in order to assess the variability of the experimental results. The average experimental error was calculated for each element (Pd, Pt, Te, Cr) and is indicated by means of error bars in the figures. The total error for Pd and Cr was ~20%, while the total error for Pt and Te was ~10%. These values include all possible sources of error, including isotopic calculations, machine error and errors introduced during sample dilution for analysis.

Fig. 3.1 depicts the results of analysis of the solutions resulting from reaction with palladium telluride (PdTe). Palladium was mobilized in much lower amounts than tellurium, and the trends in Fig. 3.1a indicate that with a longer reaction time, (100 hours) Pd was less mobile, compared to a reaction time of only 20 hours. Pd reached a maximum of ~20 µg/l in one of the H_2O solutions, after 20 hours of reaction. The maximum value of Pd in any of the humic acid solutions was ~25 µg/l, also after 20 hours of reaction. The majority of Pd values are below ~10 µg/l, with little clear difference between the trends for pure water and those for the humic acids (HASS and HAP).

Tellurium was mobilized from PdTe at a maximum of just under 1 400 µg/l (Fig. 3.1b). There is a clear difference to be seen in Fig. 3.1b between the water and humic acid solutions. The water solutions mobilized Te after 1 hour, at values of ~800–1 200 µg/l, and after 20 hours, the concentration of both water samples was ~1 300–1 400 µg/l. After 100 hours of reaction,

the values of Te in solution were approximately the same as those obtained after 20 hours. It seems likely that these two experiments obtained a steady state, reaching the maximum dissolved value of Te after 20 hours.

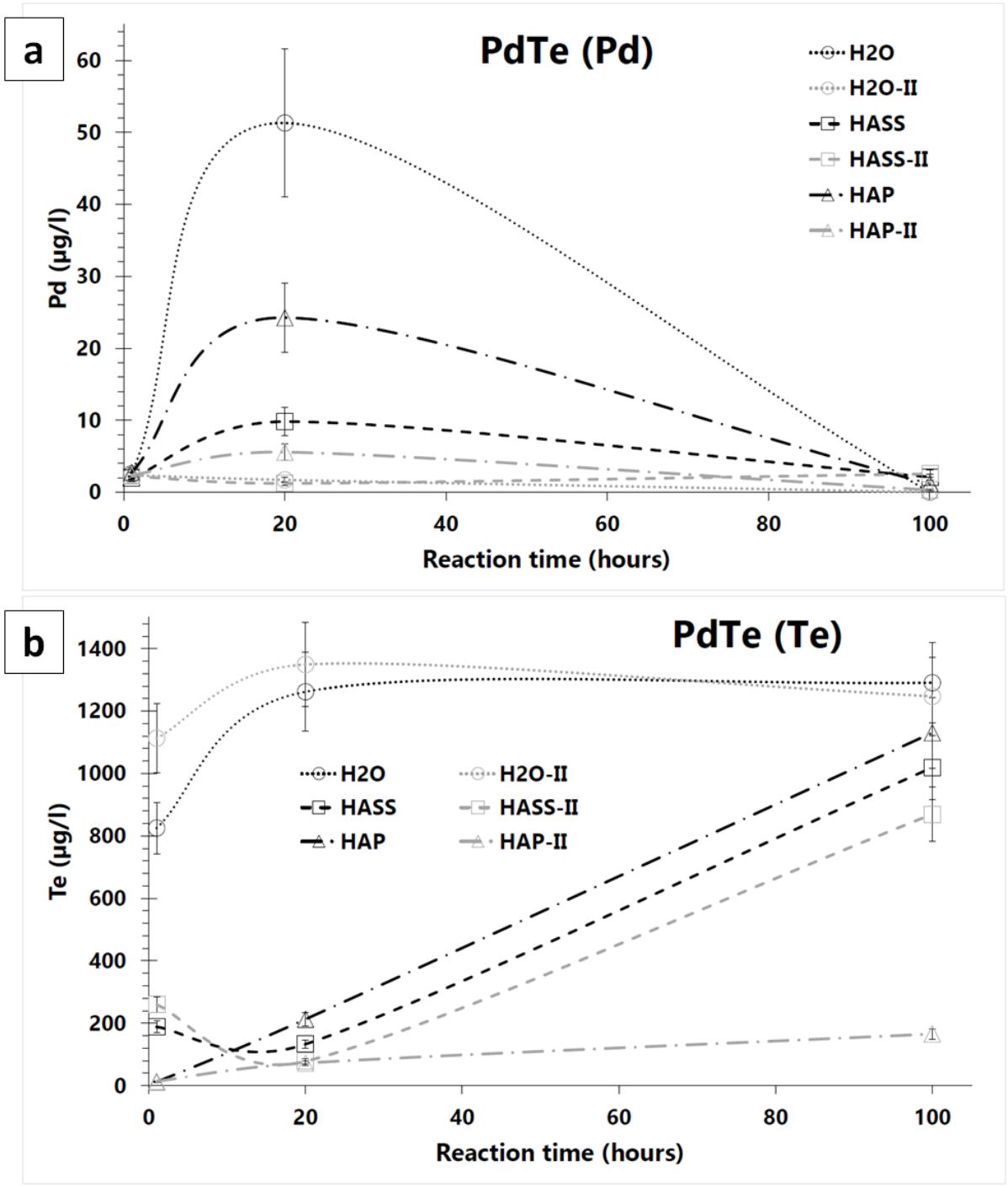

Figure 3.1: (a): Pd and (b): Te in solution, as mobilized from PdTe.

The humic acid solutions, however, all show a general increase in Te with time. The range of values is high, from ~150–1 200 µg/l. The values after 1 hour and after 20 hours of reaction do not exceed 300 µg/l. Three of the four humic acid solutions have values of Te between ~650 and ~1 200 µg/l after 100 hours of reaction. The last solution (HAP-II) shows generally lower values of Te, not exceeding ~100 µg/l.

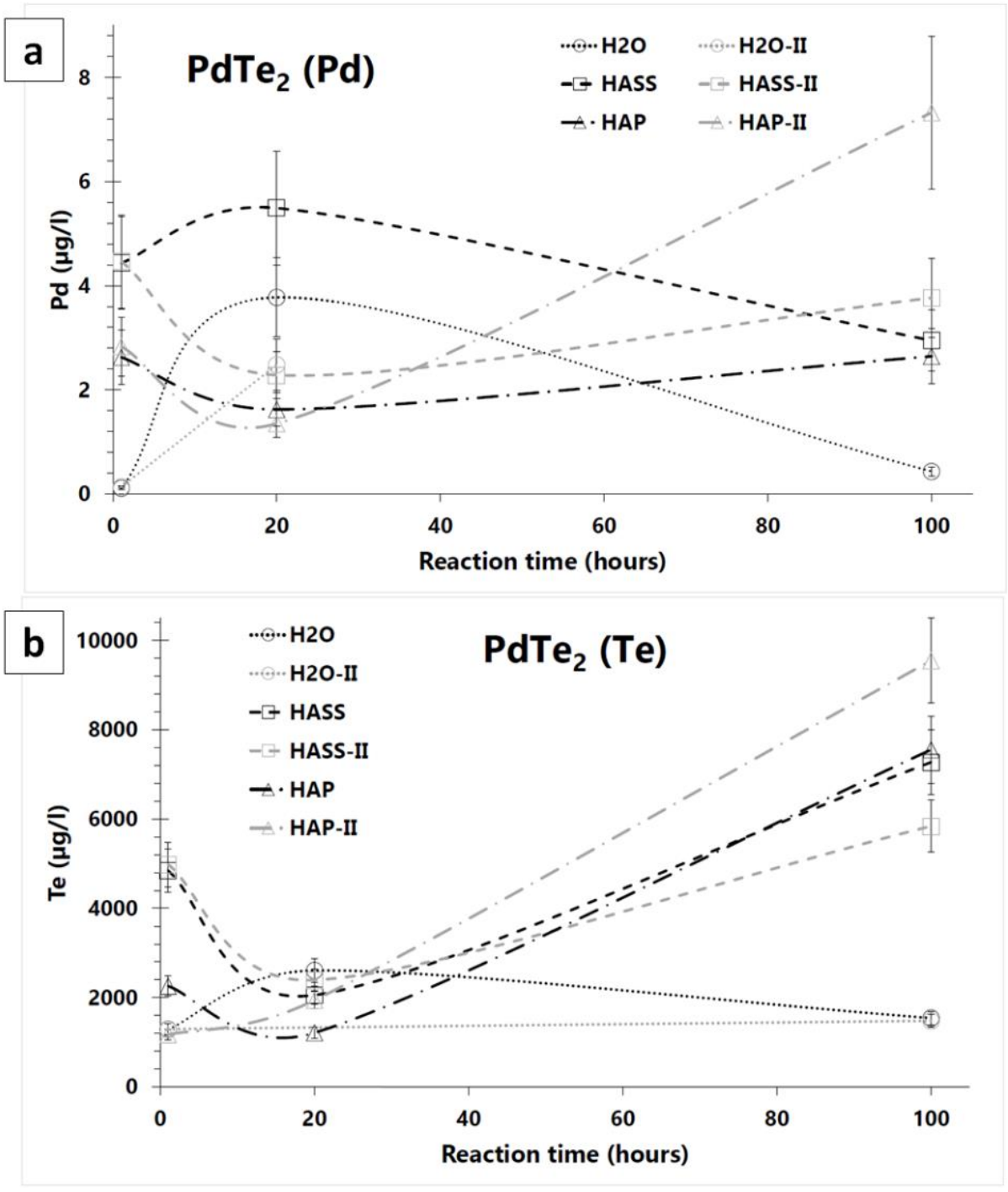

Figure 3.2: (a): Pd and (b): Te in solution, as mobilized from $PdTe_2$.

The results for the solutions that were exposed to $PdTe_2$ are shown in Fig. 3.2. Mobilization of Pd was very low, (Fig. 3.2a) and did not exceed ~8 µg/l in any of the analyzed solutions. Although the concentration of Pd was lowest in the H_2O solution (~0.2 µg/l) after 100 hours of reaction compared to the humic acid solutions, no other clear differences could be seen with regard to the humic acids. Including error, Pd varies from ~0.6 to ~8.4 µg/l in the humic acids.

The amount of Te mobilized from $PdTe_2$ was higher than that mobilized from PdTe (Fig. 3.2b). The amount of Te mobilized in H_2O was slightly higher than that from PdTe (~1 800–2 200 µg/l versus 1 300–1 400 µg/l from PdTe). The humic acids initially mobilized more Te compared to water after 1 hour, (~2 000–6 000 µg/l) but then the values of Te dropped and were equivalent to those mobilized by water after 20 hours of reaction (~1 800–2 400 µg/l). After 100 hours of reaction, however, the values of Te in all the humic acid solutions rose to ~5 000–10 000 µg/l.

In Fig. 3.3, Pd mobilized from PdS and Pt mobilized from PtS_2 are shown. Less than 500 µg/l of both Pd and Pt was mobilized in all solutions after 1 hour of reaction. However, there is a clear difference in trends between H_2O and humic acid solutions to be seen after 20 hours. The water solutions show a very sharp increase in both Pd (~1 500–3 500 µg/l) and Pt (~1 800–3 000 µg/l). All the humic acid solutions only increase in Pd and Pt slightly compared to water, with most values remaining under 500 µg/l. After 100 hours of reaction, Pd in water drops back down to ~500 µg/l, while slightly increasing, decreasing or remaining more or less the same in the humic acids. Pt, however, shows high variation in H_2O after 100 hours, with one sample showing ~1 500 µg/l Pt and the other ~6 500 µg/l. While the possibility remains that the higher value may be an outlier caused by sampling error, these values and the trends shown by Pd and Pt are discussed below. Pt steadily increases in the humic acid solutions after 100 hours of reaction, reaching a maximum value of ~1 300 µg/l.

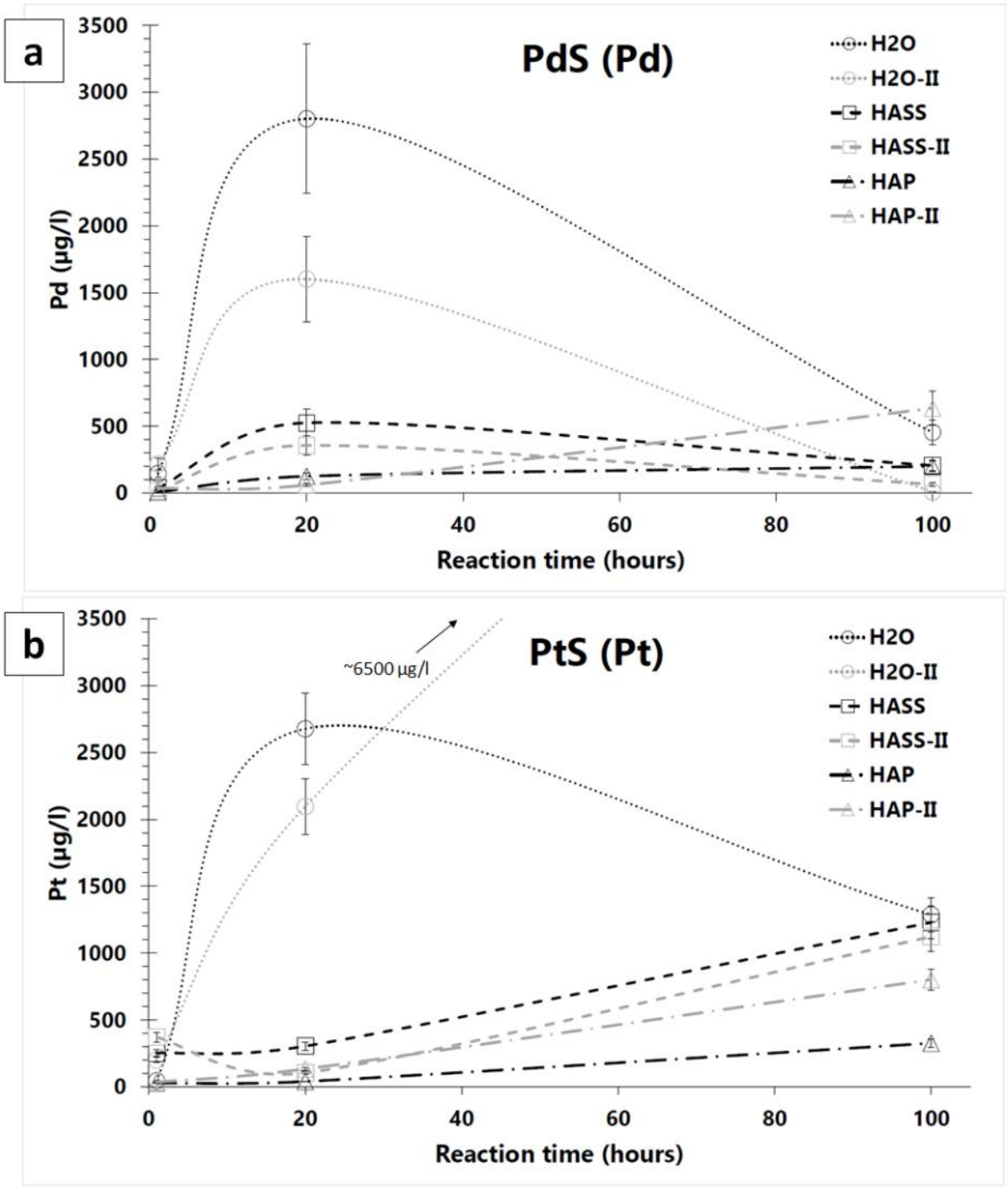

Figure 3.3: (a): Pd as mobilized from PdS and (b): Pt as mobilized from PtS_2.

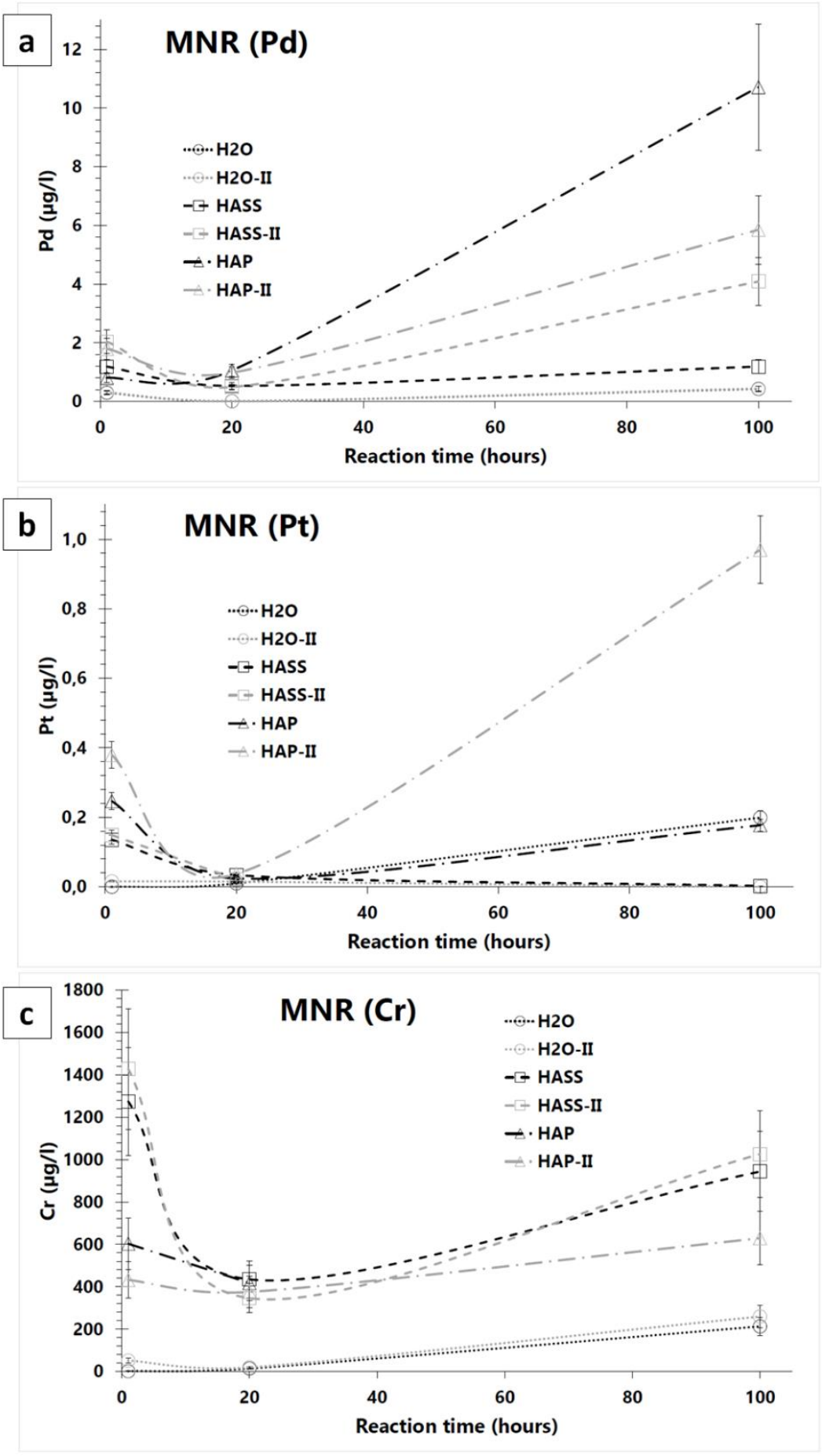

Figure 3.4: (a): Pd, (b) Pt, and (c) Cr, as mobilized from the chromitite concentrate sample.

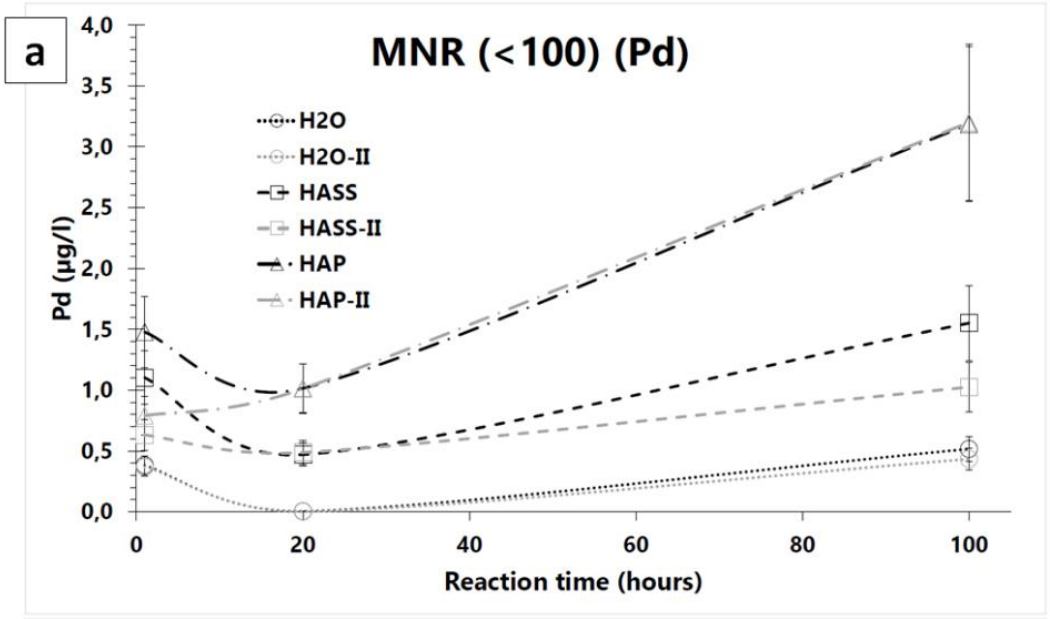

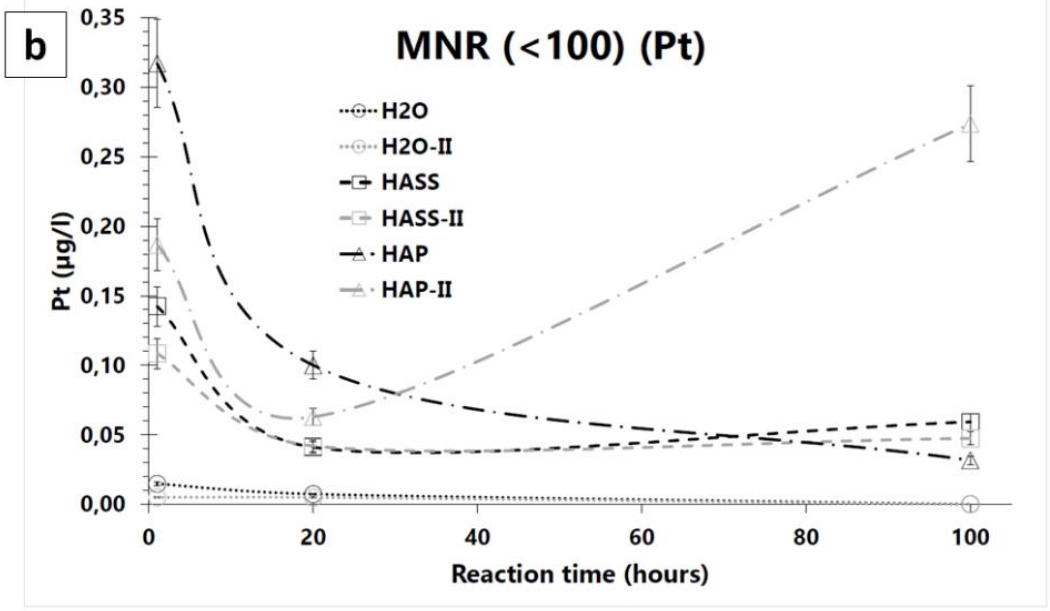

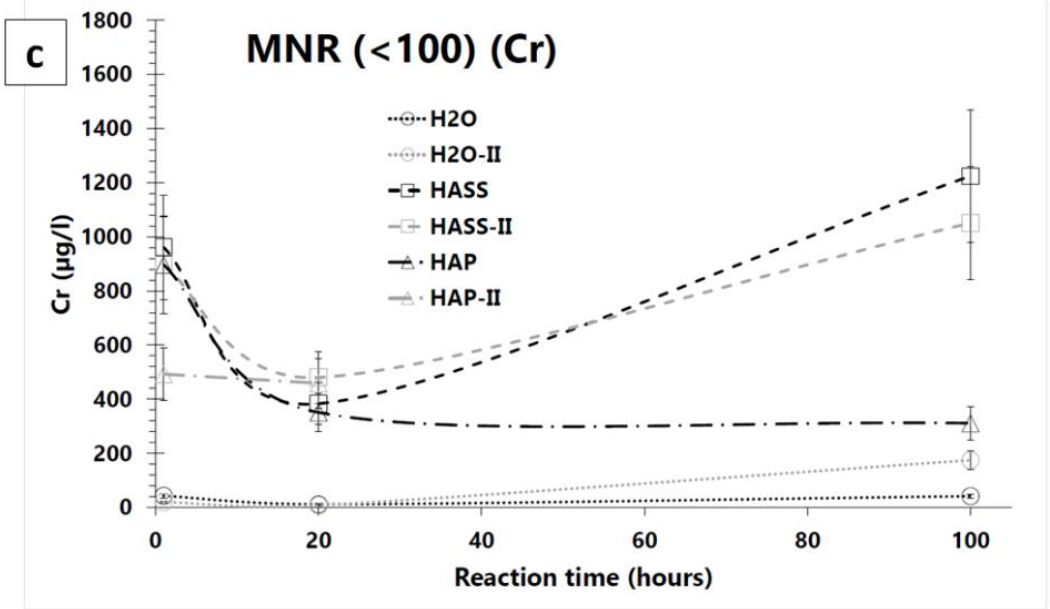

Figure 3.5:(a): Pd, (b) Pt, and (c) Cr, as mobilized from the crushed chromitite concentrate sample.

Fig. 3.4 shows the values of Pd, Pt and Cr as analyzed from the solutions that were exposed to the uncrushed chromitite concentrate sample (MNR). Pt and Pd both generally show an increase with time, (Fig. 3.4a–b) but Pd reaches a maximum value of ~12 µg/l in solution, whereas Pt reaches a maximum of ~1 µg/l. There is no clear difference between the trends for H_2O, HASS or HAP for Pt, while Pd appears to show three distinct trends: a slowly increasing trend for water, reaching a maximum of about 0.1 µg/l after 100 hours; a faster increasing but more variable trend for HASS, reaching ~0.2–4 µg/l after 100 hours of reaction; and a trend increasing still faster, but also quite variable, for HAP, with maximum values of ~4.2–12.2 µg/l Pd in solution after 100 hours.

Chromium also shows a distinct difference in trends of water compared to humic acid solution (Fig. 3.4c). While Cr slowly increases to a maximum of ~200 µg/l after 100 hours of reaction in water, it is quickly mobilized (after 1 hour) in humic acid, (up to ~1 700 µg/l) but the values of Cr are lower or much the same after 20 hours of reaction (~400 µg/l). After 100 hours of reaction, however, Cr values are higher (~400–1 200 µg/l).

Figure 3.5 shows the amount of Pd, Pt and Cr mobilized from the crushed chromitite sample. The trends here are very similar to those seen in the uncrushed chromitite (Fig. 3.4). Palladium reaches a lower maximum value, (~4 µg/l) (Fig. 3.5a) but the same three distinct trends are seen for H_2O, HASS and HAP. The HAP solutions mobilize ~0.7–1.5 µg/l Pd after 1 hour, but after 20 hours only ~1 µg/l Pd remains. After 100 hours, however, a value of ~3 µg/l Pd is seen in both samples. HASS mobilizes similar amounts of Pd after 1 hour, (~0.6–1.2 µg/l) and is left with only ~0.5 µg/l Pd after 20 hours. About 0.7 to 1.4 µg/l Pd is seen in these solutions after 100 hours.

Platinum reaches a maximum of just under 3.5 µg/l in all solutions, (Fig. 3.5b) this amount similar to the majority of the solutions seen in Fig. 3.4b. There is a clear difference here, however, between the humic acid solutions and H_2O, which mobilizes less than 0.02 µg/l Pt.

A difference between the H_2O and humic acid solutions is again seen with regard to Cr, (Fig. 3.5c) where the H_2O trend is almost identical to that seen in Fig. 3.4c. The same amount of Cr is generally mobilized from the crushed chromitite concentrate compared to the uncrushed concentrate, with Cr values after 100 hours of reaction ranging from ~380 to ~1 400 µg/l.

3.2. Discussion

The results of these solutions with regard to the palladium tellurides indicate that Te has a much higher affinity for being leached out of the palladium telluride molecule than Pd does. Unsurprisingly, Te is also more likely to be mobilized from $PdTe_2$ than PdTe. The amount of Te mobilized by the humic acids approached the total amount of Te mobilized by water with PdTe, but exceeded it when it came to $PdTe_2$. In water, a steady state appears to have been reached with regard to Te after 20 hours; in the humic acids, Te is still increasing after 100 hours of reaction. This indicates that the humic acids may be capable of mobilizing still greater amounts of Te, but that a longer reaction time is needed for this to occur. Longer reaction times with Te and diluted amounts of humic acid are discussed in Chapter 4.

Despite higher Pd values after 20 hours of reaction with PdTe, Pd does not appear to be significantly mobilized from any of the six solutions containing palladium telluride after 100 hours of reaction. The results after 20 hours are likely an indication that the system needs more time to reach a steady state; after 100 hours, it is more likely to have reached a steady state. It seems that Pd shows a clear preference to remain in the mineral structure rather than be mobilized into the fluid phase, especially when the original Pd:Te ratio is lower (i.e. in $PdTe_2$). There is no distinction in Pd mobility between the humic acids and water; in fact, the trends for H_2O almost fully enclose the humic acid trends in Fig. 3.1a. It is possible, given that HASS and HAP in this same figure have more Pd than H_2O at the last aliquot, that the presence of humic acid causes solution/ precipitation reactions to slow down, as the mobilization of Te is slowed down in Fig. 3.1b and 3.2b. The highest amount of Pd from PdTe is mo-

bilized by HAP, (~2.5 µg/l) but the duplicate sample of HAP mobilized only 0.3 µg/l Pd by the end, indicating that the mobilization of Pd is highly variable. With the short-term experiments as well as subsequent experiments, reproducibility of the analytical method was tested by analyzing the same sample several times; in this way it has been ensured that the variable results obtained on parallel experimental runs are not due to analytical error. As described in Chapter 2, each solution was also centrifuged before taking an aliquot for analysis, and care was taken to exclude any remaining substrate. Therefore the likeliest explanation for the high variability seen in the duplicate experiments is probably due to an inherent variation, possibly because these experiments have not reached chemical equilibrium in the time they were allowed to react; the results of only certain solutions suggest that they may have reached a steady state.

With regard to the sulfide powders, it must be taken into account that the sulfide molecule has likely undergone hydrolysis (this is confirmed in Chapter 4 below). This process involves the oxidation of sulfur and the production of sulfurous acid in solution (see Chapter 4). Because of the presence of free H^+ ions resulting from this process, the initial pH of the solutions involved may be lowered.

According to the trends seen in Fig. 3.3 for Pd and Pt, one hour does not appear to be enough for significant hydrolysis to take place, but after 20 hours, an extreme change is seen in the amount of Pd and Pt mobilized by H_2O. There may be several reasons for the high amounts of Pd and Pt going into solution: breakdown of the sulfide molecule will result in free Pd and Pt, unbound by the sulfide molecule, and with this happening, Pd and Pt can be transported as hydroxide complexes (Mountain & Wood, 1988; Cabral et al., 2007). The PtS_2 (disulphide) used in these experiments is probably more likely to break down in the presence of water than PdS, given that the usual form of platinum and palladium sulfide in geological deposits is monosulfide (PtS, PdS) (e.g. Verryn & Merkle, 1994). The associated probable lowering of

pH promotes Pt mobility, explaining why there is little difference seen in the amounts of Pd and Pt mobilized by water in Fig. 3.3. After 100 hours of reaction with water, however, Pd is seen to be much lower (<500 µg/l) while Pt still shows high values (~1 500 µg/l and above). These amounts are extremely variable and indicate that the system is very far from attaining a steady state with respect to dissolved Pd and Pt, but it can be speculated that hydrolysis of the platinum bisulfide (PtS_2) is still ongoing, using up all the "excess" sulfur, while with the PdS molecule, hydrolysis may be more limited. Precipitation of Pd may take place, presumably as PdS, palladium metal, or palladium oxy-hydroxide (evidence for Pd-oxide minerals occurring in nature is discussed in sources such as Oberthür et al., 2003, Cabral et al., 2008, and Locmelis et al., 2010). Another possibility is that Pt is being simultaneously mobilized by bisulfide complexes, as discussed by Mountain & Wood, (1988) although these type of complexes are thought to significantly mobilize Pt and Pd only at much higher temperatures (close to 300 °C) (ibid.).

Chlorine becomes an important element in these solutions when it is considered that the pH of both humic acid solutions was fixed using small concentrations of HCl. Mountain & Wood (1988) suggested that chloride complexes for both Pd and Pt were important at temperatures as low as 25 °C, if pH was lower than 4 for Pd and 3 for Pt. In later studies, the exact type of complex formed and the conditions under which they became predominant were constrained. Sassani & Shock (1998) concluded that palladium chloride complexes at low hydrothermal temperatures might be less stable than platinum chloride complexes at the same conditions, and Bazarkina et al. (2014) concluded that Pd-chloride complexes could only be predominant in sulfide-free oxidizing conditions.

Regarding the trends for Pd and Pt in the humic acid solutions of Fig. 3.3, Pt appears to be more mobile than Pd. After 100 hours of reaction, Pd shows a maximum value of ~700 µg/l in the humic acid solutions, while Pt is seen to be on the increase compared to the previous time

point in all the humic acid solutions, with the final value of Pt being ~300–1 300 µg/l. The high mobility of Pt in these experiments is unexpected, given the general paradigm of Pt being less mobile than Pd, (see Chapters 1 & 4) but it may be explained by the presence of chlorine and presumed formation of platinum chloride complexes. It may be that, due to the low pH of these solutions, that chloride (or mixed chloride-hydroxide) complexes are the dominant species mobilizing Pt, not the organometallic complex expected from the humic acids. Given that Pd displays a lesser affinity for such complexes, this may explain the slightly lesser amounts of Pd in solution. It could also be that Pd is even preferentially mobilized by means of an organic complex. A comparison of these findings with the other data of this project may be found in Chapter 6, where further conclusions on these experiments are made. The complication of possible multiple species mobilizing Pd and Pt in these solutions was a reason why no pH fixing was carried out in subsequent experiments.

After consideration of the sulfide samples, the most striking feature of the trends for the chromitite samples is the difference in Pd and Pt mobility. Pd is about 10 times higher in solution than Pt for the samples of both whole and crushed chromitite. Since the composition of the solutions was no different, the difference seen must be due to composition of the sample. Since sulfide was not present in large amounts, no hydrolysis-driven change in conditions could take place. This indicates that the mobilization of Pd and Pt in the sulfide samples must have been driven by breakdown of the sulfide molecule and associated lowering of pH.

In the chromitites, Cr showed an affinity for the humic acids over water. There was no difference between the results for whole and uncrushed chromitite. Pt and Pd were actually higher in the solutions with whole chromitite compared to those with crushed chromitite; it may be that the process of crushing caused loss of some PGM because of their small size. Both Pd and Pt display a slight affinity for the humic acids over water. Although the maximum values of Pt in Fig. 3.4 and 3.5 were both obtained from the HAP solution, Pt did not display a clear

preference for either HAP or HASS. Palladium, however, appears to have an affinity for HAP over HASS, with the final values for HAP being higher than those for HASS in Fig. 3.4 and 3.5. Oppermann et al. (2017) found that Pt had an affinity for fulvic acid over humic acid in natural soils of the Bushveld Complex, whereas Pd showed no preference between fulvic and humic acid. Wood et al. (1994) also noted that Pd showed preferences for some organic ligands over others. Our results also suggest that the organic molecule involved must be important to the mobilization of Pd and Pt.

3.3. Conclusion

Because of the presence of chlorine in these solutions, the results obtained may be a composite of different ligands capable of transporting Pd and Pt: organic complexes, oxy-hydroxide complexes (from water) and chloride complexes. The humic acids involved may have had an effect on Pd and Pt mobility, but this cannot be confirmed. These experiments do show that an inherent variability is to be expected from the humic acid solutions used in this study; the elements involved show variation across a large range of values depending on both the solution and the substrate involved. Although these solutions appear to be capable of mobilizing Pd and Pt, (as well as Te) their mobility cannot be definitively quantified.

4. Long-term PGE mobility experiments on synthetic material (sulfides and tellurides)

This chapter is published as:

Kotzé, E., Schuth, S., Goldmann, S., Winkler, B., Botcharnikov, R. E. & Holtz, F. (2019). The mobility of palladium and platinum in the presence of humic acids: an experimental study. Chemical Geology 514: 65–78. https://doi.org/10.1016/j.chemgeo.2019.03.028.

4.1. Introduction

The economically important platinum group elements (PGE) are extracted from primary magmatic deposits, as well as hydrothermal (secondary) deposits. Other deposit types, such as Kupferschiefer-related deposits (e.g. Oszczepalski et al., 2002) and PGE placers (e.g. Grayson et al., 2000; Johan, 2006), are of lesser economic importance. The primary magmatic PGE are deposited mainly as sulfides, tellurides/ bismuthotellurides, alloys, and arsenides, or in solid solution in base metal sulfides (e.g. Augé & Maurizot, 1995; Daltry & Wilson, 1997; Andersen et al., 1998; Ballhaus & Sylvester, 2000; Andrews & Brenan, 2002; Cawthorn et al., 2002; Oberthür et al., 2003; Holwell & McDonald, 2007; Godel & Barnes, 2008; Locmelis et al., 2010; Dare et al., 2011; Oberthür et al., 2013; Junge et al., 2014; Oberthür et al., 2016). Hydrothermal or "late-magmatic" remobilization by high-temperature fluids containing sulfide or chloride complexes can lead to PGE enrichment in the form of minerals similar to primary magmatic assemblages (e.g. McCallum et al., 1976; Schiffries, 1982; Ballhaus & Stumpfl, 1985; Boudreau & McCallum, 1992; Cawthorn et al., 2002; Andersen et al., 2006; Bazarkina et al., 2014), as well as secondary PGE assemblages which may contain selenides (e.g. palladseite, $Pd_{17}Se_{15}$), antimonides (e.g. the antimony-rich endmember of insizwaite, $Pt(Bi,Se)_2$ and naldrettite, Pd_2Sb), stannides (e.g. rustenburgite, $(Pt, Pd)_3Sn$), native Pt and Pd (Cousins, 1966; Tarkian & Stumpfl, 1975; Kinloch, 1982; Oberthür et al., 2004; Melcher et al., 2005;

Johan, 2006) and lead-rich minerals such as plumbopalladinite (Pd_3Pb_2) (Kinloch, 1982; Melcher et al., 2005).

In addition to the mobilization of PGE by high-temperature fluids below the Earth's surface, the PGE can also be remobilized under near-surface weathering conditions. Studies of lateritic deposits (e.g. Bowles, 1986; Traoré et al., 2006; Ndjigui & Bilong, 2010; Aiglsperger et al., 2015; Bowles et al., 2017), as well as oxidized magmatic ores (e.g. Augé & Maurizot, 1995; Garuti & Zaccarini, 1997; Oberthür et al., 2003; Locmelis et al., 2010), show that processes occurring at or near the surface can influence the distribution of the PGE, in some cases producing substantial changes of the PGE distribution of the weathered bedrock (Oberthür et al., 2003), as well of the soils and laterites which form associated with such deposits (Cousins & Kinloch, 1976; Traoré et al., 2006; Oppermann et al., 2017). In such weathered deposits, the PGE may occur in weathered primary minerals, as new PGM formed by the weathering process, or in the products of weathering such as oxides, hydroxides and phyllosilicates (Augé & Maurizot, 1995; Evans & Spratt, 2000; Oberthür et al., 2003; Melcher et al., 2005; Locmelis et al., 2010; Aiglsperger et al., 2015; Bowles et al., 2017).

The behavior of the PGE in the weathering environment is a multi-faceted field of study, but few studies have quantitatively investigated the role of organic matter, which is ubiquitous in natural soils, on PGE mobility under supergene conditions. Studies such as Azaroual et al. (2001) and Van Middlesworth & Wood (1999) demonstrated that under laboratory conditions, Pt and Pd can be mobilized by hydroxylated complexes as well as low-pH chloride complexes. Studies such as Turner et al. (2006) demonstrated that Pt and Pd can enter the weathering environment and be transported by means of adsorption, to particulates found in river water, with Pd having more potential for long-range transport in the environment than Pt. Palladium also reacts faster with organic substances than Pt (Wood, 1996) and was found to be mobilized more easily in tropical soils compared to Pt by Traoré et al. (2006), hence changing the

ratio of platinum to palladium from the primary rock to the topsoil. Palladium and platinum were also found to follow independent trends in weathering profiles, as suggested by Oberthür et al. (2003), Locmelis et al. (2010), and Bowles et al. (2017), with Pt/Pd in the studied soils varying greatly; for example, at the Great Dyke this ratio changes from 1.4-1.7 in the pristine ore to around 2.5 in the oxidized ore (Oberthür et al., 2003), and in the Freetown lateritic PGE deposits in Sierra Leone, the same ratio increases fivefold from the source rocks to the overlying soil (Bowles et al., 1994). Platinum oxides as well as adsorbed Pd and Pt on clay and oxide minerals were found in these studies, and the findings were concluded to be consistent with the transport of Pt and Pd in solution, with Pt being less mobile than Pd. Similar results were found in studies of non-lateritic soils overlying the Great Dyke, Zimbabwe (Locmelis et al., 2010; Oberthür et al., 2003; 2013), and the Bushveld Complex (Oppermann et al., 2017). Fuchs & Rose (1974) showed that Pd is more mobile in the weathering environment due to complexation over a wide range of pH and Eh values, while the mobility of Pt is restricted to certain conditions, such as a very low (i.e. acidic) pH. The conditions of Pt mobility were further investigated by Cabral et al. (2007), who showed that Pd is mobile over a wide pH range at oxidizing conditions, whereas for Pt, the pH needs to be under 1 or over 8 for Pt to be mobilized.

The experiments of Wood (1990, 1996), and Wood et al. (1994) demonstrated that organic compounds such as fulvic acid, oxalate, and acetate chelates are capable of complexing Pt and Pd in the weathering environment and thus mobilizing them. Natural soils contain many different organic components, one of the most important being humus (decomposed biological matter), of which the soluble, precipitable portion is known as humic acid (Haworth, 1971). Humic substances make up the majority of organic material in the surficial environment (Wood, 1996), and humic acid can be expected to influence the mobility of PGE under supergene conditions by means of chemical processes (complexation in solution) or by physico-

chemical processes, such as adsorption of PGE ions by humate complexes (Wood, 1996; Turner et al., 2006).

Bowles et al. (1994, 1995) obtained elevated values in solution of both Pt and Pd during experimentation which involved subjecting Pt foil, Pd foil, and synthetic PtS to 393 days of reaction with both humic and fulvic acids. Humic acid was shown to mobilize both Pt and Pd more efficiently than fulvic acid (~37 µg/l Pt in HA vs. ~20 µg/l Pt in fulvic acid; ~8 µg/l Pd in HA vs. ~6 µg/l Pd in fulvic acid). Pt was mobilized from both pure Pt foil and PtS. These results were interpreted to represent a two-stage process which occurred with respect to Pt and Pd, with these elements being initially taken into solution, and then undergoing reduction by the organic compounds, leading to Pd and Pt precipitation. The humic substances therefore represent an important aspect of our understanding of PGE interaction with the natural environment. Oppermann et al. (2017) measured the concentration of Pt and Pd in humic and fulvic acids from the soil profiles overlying the PGE-mineralized chromite reefs of the Bushveld Igneous Complex (BIC), and found that Pt was present in concentrations of up to 0.04 µg/l (equivalent to parts per billion) in humic acid, whereas Pd was present in much higher concentrations (1-3 µg/l). This further illustrates the different behavior between Pt and Pd in the supergene environment.

In the following study, we present the results of a laboratory study using synthetic humic acids and platinum-group minerals (PGM). Selected powders (platinum and palladium sulfides; palladium tellurides) were allowed to react with different concentrations of humic acid over a period of 306 to 308 days. Aliquots of solution were taken in various time intervals up to 306-308 days and analyzed for Pt, Pd, and Te. In addition, selected solution experiments with water instead of humic acid were made for comparison and control. Our results demonstrate that the humic acids are indeed efficient mobilizing agents for both Pt and Pd, depending on the PGM composition.

4.2. Materials and methods

4.2.1. Pt-Pd minerals and production of synthetic phases

Pd and Pt sulfide

To represent the Pt and Pd minerals of unweathered, primary PGE deposits, we chose to use sulfide and telluride minerals as substrates for the solution experiments. Palladium-platinum sulfides form a solid-solution mineral series known as the braggite series (Tarkian, 1987). They often contain minor amounts of nickel and can be described using a ternary diagram with the end-members PtS, PdS, and NiS (Tarkian, 1987). The solid solution series of Pd-Pt sulfide comprises three minerals: cooperite (PtS), vysotskite (PdS), and braggite ((Pd,Pt)S) (Tarkian, 1987; Verryn & Merkle, 1994). A discussion of the varied compositional attributes of these minerals may be found in these references, but for this study, the end-members PdS and PtS were deemed the most relevant.

We acquired Pt and Pd sulfides in powder form from American Elements, Merelex Corporation, USA. Platinum sulfide was obtained as Pt(IV) sulfide (i.e. PtS_2) powder (lot no. 2641593747-404). It was certified as 99.95% pure on metals basis. Palladium sulfide was obtained as Pd(II) sulfide (PdS) powder (lot no. 3421593447-416) with a certified degree of purity of 99.9% on metals basis. The type of impurities present in the PtS_2 was not given, but PdS could contain impurities in the form of many metals, the principal ones being Pt, Ag, and Na (American Elements, 2015). The maximum possible amount of Pt present in PdS was given to be 15 ppm. The same amount of Ru was also present in PdS.

Before the start of the leaching experiments, the sulfide powders were mounted and investigated with a JEOL JSM-6390 scanning electron microscope (SEM) at the University of Hannover. The machine was operated at an accelerating voltage of 30 kV, and a working distance of 20 mm. All images were produced by secondary electrons (SEI). Both powders were com-

posed of fine-grained material, with grain sizes less than 100 µm, and had a tendency to clump together (Figures 4.1a and b).

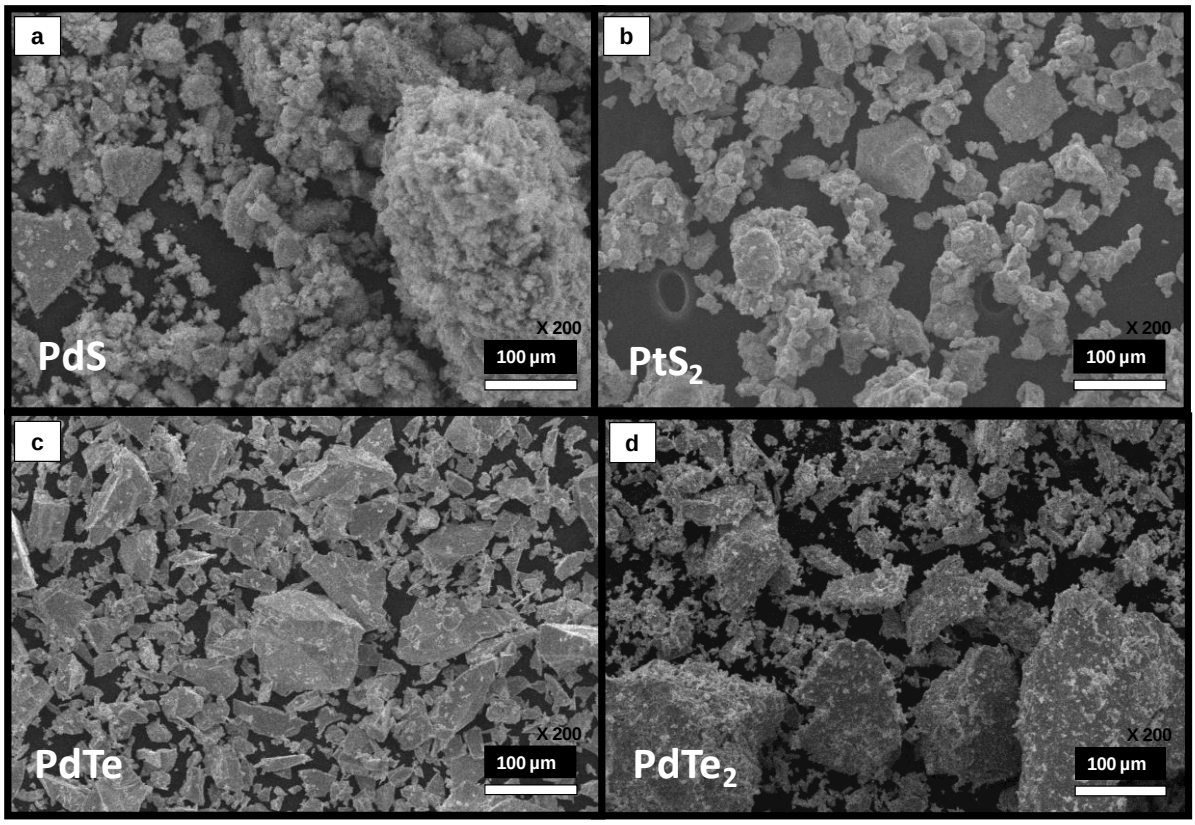

Figure 4.1: Synthetic powders used for solution experiments, imaged by SEI (secondary electrons). (a): PdS. (b): PtS_2. (c): PdTe. (d): $PdTe_2$.

Palladium tellurides

Palladium and platinum telluride minerals comprise an important and varied group in the characterization of PGE ores. For our purposes, only palladium tellurides were synthesized. Multiple ratios of Pd to Te may exist in natural minerals (Vymazalová et al., 2005; Shackleton et al., 2007). Pd-Pt-Te minerals tend to accommodate Bi in their structure as well, thus forming the group of PGE-bismuthotelluride minerals (e.g. Shackleton et al., 2007). Palladium bismuthotellurides can be described by a Pd-Te-Bi ternary diagram in which the compositional ranges of the minerals kotulskite (Pd(Te,Bi)) and merenskyite ((Pd,Pt)$(Te,Bi)_2$) form semi-linear trends (Tarkian, 1987; Shackleton et al., 2007). The PdTe-rich end members of

kotulskite and merenskyite have the ideal stoichiometric compositions of PdTe and $PdTe_2$, respectively (Tarkian, 1987).

Powders of PdTe and $PdTe_2$ were synthesized at the Institute of Mineralogy, Leibniz Universität Hannover, Germany. We used the evacuated tube method of Vymazalová et al. (2005), which was modified from the method described earlier by Kullerud (1971). Tellurium (Alfa Aesar, lot no. F29X179) and Pd (Alfa Aesar, lot no. A23Y050) were used as starting materials at a certified purity of 99.99% on a metal basis. The grains of Te and Pd powder passed sieve mesh sizes of 30 µm and 60 µm, respectively. The metals were mixed in stoichiometric proportions to form PdTe (ideal weight: 0.24 g Te; 0.20 g Pd) and $PdTe_2$ (ideal weight: 0.48 g Te; 0.20 g Pd).

The mixed Pd and Te powders were placed in a quartz ampule which was then welded shut whilst connected to a vacuum pump. The ampule was then placed in a 1 atmosphere Carbolite Gero furnace and heated to 1150°C at a rate of 20°C/min, held there for 30 minutes, then cooled down to 350°C over a period of 60 hours, and finally cooled slowly to ambient temperature at a rate of 10°C/min. Both PdTe and $PdTe_2$ were synthesized in parallel in different tubes in the same furnace. After cooling to room temperature, the ampules were carefully opened, and the homogeneity of the telluride button was tested by subjecting it to microprobe analyses employing a Bruker Quantax SEM-EDS system with an accelerating voltage of 25 kV, and a working distance of 9 mm, at the Bundesanstalt für Geowissenschaften und Rohstoffe (BGR) in Hannover. The button was then crushed with an agate mortar to a powder passing a mesh of 100 µm. The hardness of both resulting Pd tellurides discouraged finer crushing with the agate mortar. Investigation of the morphologic textures and surface characteristics of the powders was carried out in the same way as with the sulfide powders above, with a JEOL-6390 at the University of Hannover, using the same instrumental parameters (Figures 4.1c and d).

4.2.2. Experimental approach and sample preparation

Although laterite-hosted PGE occurrences are clearly of significance, at least two of the most important primary PGE deposits, the BIC and the Great Dyke, occur in areas where the environment is not favorable for the formation of lateritic soils. We conducted this study with special reference to the BIC and so attempted to simulate in a simplified approach the representative supergene weathering environment typical of near-surface PGE ores in this particular area. The soils of the BIC studied by Oppermann et al. (2017), (western limb of the BIC, near the town of Thabazimbi) developed in a semi-arid zone. They resemble vertisols known for the area (Ahmad, 1996; Dudal, 1963), with a simple A-C soil horizon profile, which is locally separated by a transitional horizon labeled as AC because of gravel from the weathered bed rock (C horizon) being embedded in the top soil (A horizon). The concentration of humic acid in the soil samples are between 0.003 and 0.46 g/kg for all samples, with the samples of the C and AC horizons containing less than 0.03 g/kg (Oppermann et al., 2017).

The experiments performed in this study involve low concentrations (solutions of 0.1, 1, and 10 mg/l, respectively) of humic acid (HA), and an experimental reaction time of about one year. The experiments are considered to be particularly relevant for environmental conditions prevailing in the BIC since they were planned following the results of Oppermann et al. (2017) so that humic acid concentrations employed in the experiments could match those of the natural setting. Using the HA concentrations determined by Oppermann et al. (2017) as a rough guide, the experiments were set up to last for 306-308 days, with sample aliquots of solution being taken at planned intervals. The exact duration of each experiment can be found in Table 8.2 of the Appendix. Three experimental series of HA solutions were set up in parallel, and selected solutions containing pure water (18.2 MΩ grade, Millipore Mill-Q system, Germany) were used as a control. Synthetic humic acid powder (Alfa Aesar, lot no. R07A015) was dissolved in pure water to yield concentrations of 0.1, 1, and 10 mg/l HA, re-

spectively. Approximately 0.035 g of each PGM powder (PdTe, $PdTe_2$, PdS, PtS_2) was added to a Savillex® teflon beaker of 240 ml, and were covered by 200 ml of HA solution. All solutions were kept at ambient temperature and only carefully moved when sampling. This was intended to simulate a natural, undisturbed soil weathering system and to avoid abrasion. The solutions were stored away from sunlight to prevent the decay of humic acid by photolysis (e.g., Strome and Miller, 1978). The pH of the solutions was not adjusted or buffered to a certain level. The pH of all solutions was measured with a Mettler Toledo FG2 pH meter, which was calibrated using two buffer solutions (EMD Millipore Corp., Certipur®) before measurements were taken. The pH values of all starting HA solutions were in the range 7-8. Five aliquots of 4 ml each were taken during the course of the experiment, after 5-7, 63-65, 89-91, 148-150, and 306-308 days. The exact timing of each aliquot for each solution can be found in Table 8.2 of the Appendix. Aliquots were taken more frequently in the earlier stages, as it was expected that the reactions might initially take place more rapidly due to an initial disequilibrium between solid and leaching solution. As a control experiment, 0.1 g of $PdTe_2$ and of PtS_2 were placed separately in containers with 50 ml of pure water and sampled on the same schedule as the HA solutions, with aliquots of 1 ml taken on each sampling day.

Different steps were involved in the preparation of the samples before analysis. Initially, the aliquot of solution was placed in a Savillex® Teflon beaker to which 5 ml H_2O_2, (30%, Suprapure, Merck, Germany), having been diluted to 10%, were added. The open beaker was then allowed to evaporate overnight upon a hot plate set to 90 °C. The residue after evaporation was subjected to a further treatment with 5 ml of aqua regia at 80 °C overnight in the closed beakers before being opened to evaporate. This yielded a white residue which was then dissolved in 1 ml of 1 M HNO_3. This solution was further diluted in 3% HNO_3 + 5 µg/l Rh for analyses via ICP-MS (see below). All employed acids were purified by distillation of pro analysis grade (high-purity grade; commercially available) acid at sub-boiling conditions.

After the end of the experiment, the solutions were drained from the beakers and the remaining solid material was dried at about 50°C on a hot plate in Savillex® beakers until all moisture had evaporated. These residues were first investigated for changes in surface morphology at the University of Hannover, using the same machine (JEOL) and exactly the same instrumental parameters as described before. Images were obtained by SEI and are presented below. Afterwards, the residues were investigated as grain mounts at the BGR in Hannover, with the same instrument (Bruker Quantax) as described above. Surface changes were observed, and the material was analyzed to determine if compositional changes had taken place. High-resolution images were obtained with the backscatter detector (BSE). Qualitative Energy-dispersive X-ray spectroscopy (EDX) measurements were carried out on the experimental residues to determine the ratio of major elements (Pd, S, Pt, Te). The accelerating voltage of the SEM remained at 25 kV during these measurements. No noticeable interferences were recorded on the analyzed elements.

4.2.3. Analysis of solutions by mass spectrometry

All solutions sampled from the experiments described above were analyzed using the Thermo-Scientific Element-XR fast scanning-sector field-ICP-MS (inductively coupled plasma mass spectrometer) at the Institute of Mineralogy, University of Hannover. All elements were analyzed in low-resolution mode. Custom calibration solutions were prepared from ICP-MS stock laboratory solutions of 1000 mg/l from Alfa Aesar, Germany. Three calibration solutions were prepared with concentrations of 0.1 µg/l, 1 µg/l, and 10 µg/l, respectively, of the elements Ru, Pd, Pt, Rh, Ir, Te, and Cr in a matrix of 3% HNO_3 prepared from pure water and distilled ~15 M HNO_3. A 1000 mg/l Rh solution (EMD Millipore Corp., Certipur®) was used to prepare an internal standard solution of 5 µg/l Rh. The three standard solutions were used to set up a calibration method for sample analyses.

The measurements were carried out via an automated system (SC-2DX autosampler, Elemental Scientific, Germany), connected to a PFA nebulizer that introduced the sample aerosol at a rate of ca. 100 µL/min into a double-pass quartz glass spray chamber (Scott design, Thermo-Scientific). A jet-type sampler cone and x-type skimmer cone made of Ni (Thermo-Scientific) were installed to improve signal intensity and to obtain accurate results in the concentration range of 0.01-10 µg/l. Random duplicate sample analyses were included to assess accuracy and precision of measurements in each sample run. Each sample was measured at least three times to calculate average concentrations and to determine the reproducibility of the analyses.

Analysis of an 1 M HA solution (the same HA powder used for all experiments) revealed detectable amounts of Y, Zr, and Hf, which are presumably present as trace elements in the starting HA powder. Yttrium and zirconium can be present as mass interferences on Pd isotopes due to formation of Y and Zr oxides in the argon plasma (e.g. $^{89}Y^{16}O$, $^{90}Zr^{16}O$), and Hf causes interferences on the signal of Pt isotopes for the same reason. Of the six stable Pd isotopes, ^{102}Pd and ^{104}Pd were not considered for calculation of concentration due to possible trace amounts of Ru in the Pt and Pd sulfides. On mass ^{105}Pd, the oxide $^{89}Y^{16}O^{+}$ may occur during analyses and on mass $^{106}Pd^{+}$, $^{89}Y^{17}O^{+}$ may also be present (but in a lesser amount because the natural abundance of ^{17}O is only 0.04%; Berglund & Wieser, 2011). Furthermore, $^{90}Zr^{16}O^{+}$ also may appear on the signal of $^{106}Pd^{+}$. For the signal of $^{108}Pd^{+}$, only $^{92}Zr^{16}O^{+}$ has a potentially significant high abundance. Strontium, Mo, and Cd are also known to form oxide complexes that interfere with the latter three Pd isotopes, but these elements were not found in the humic acid solution. Because of their highest relative abundance, ^{105}Pd (22.3 %), ^{106}Pd (27.3 %), and ^{108}Pd (26.5 %) were measured in order to calculate the Pd concentration in the solutions.

For platinum isotope analyses, the signal of $^{194}Pt^{+}$ is interfered by the complex $^{178}Hf^{16}O^{+}$, and similarly, $^{195}Pt^{+}$ is affected by the presence of $^{179}Hf^{16}O^{+}$ (see e.g., Köllensperger et al., 2000; Thomas, 2002; Bencs et al., 2003, and Meisel et al., 2003, for details regarding the effect of oxide formation during Pd and Pt analyses employing ICP-MS). In order to correct for Y, Zr, and Hf oxide interferences, solutions containing these elements at concentrations of 1 µg/l and 10 µg/l (prepared from Certipur® 1000 mg/l Y, Zr, and Hf solutions, respectively), but free of Pd and Pt were analyzed along with the samples in each analytical run.

The signals measured for each concentration of Y, Zr, and Hf and those on the masses 105, 106, 108, 194, and 195, respectively, were used to calculate the formation rate of the relevant elemental oxides. This "oxide contribution" to each isotope was then subtracted from the total signal intensity of each Pd and Pt isotope. These numbers were verified by comparing natural isotopic abundance ratios to the measured and oxide-corrected isotope ratios. The elemental concentrations were then calculated from the oxide-corrected isotope signals. For Pt, the measured Pt isotope ratio agreed perfectly with the natural ratio of $^{194}Pt/^{195}Pt$ as given by Berglund & Wieser (2011). For Pd, however, disturbances in the ratios were observed with at least one isotope pair on almost all samples. By means of calculating every ratio for each possible pair of isotopes the disturbed isotope signal was then not further considered for calculation of the Pd concentration. Instead, the concentration of Pd was determined by using the other isotopes after confirming that their ratio matched the natural ratios as given by Berglund & Wieser (2011). There was unfortunately no pattern visible for our Pd analyses (i.e. a mass that was dominantly prone to interferences by oxide). One explanation is a minor presence of organic complexes in some samples that were not fully removed prior to analyses and that may have produced compounds that interfered with the signals of one of the three measured Pd isotopes. A summary of the isotopes used, calculated concentrations of elements, and the standard deviation of analyses may be found in Table 8.2 of the Appendix.

4.3. Results

4.3.1. Surface effects on residual phases after reaction

The post-experimental residues are shown in Figures 4.2-4.4. In experiments that employed PdS and PtS_2, the surface morphologies of both sulfide minerals changed in a rather subtle way (Fig. 4.2). Rounded aggregates can be seen in Figure 4.2d-f. Compared to the original material, the residues show a smoother surface. Also visible are features from the drying process, e.g. Figure 4.2g and 4.2h both show particles that resemble dried clay minerals because of small cracks.

The SEM analyses of the experimental residues showed an increase in the metal content of the sulfides compared to the starting material. The residues of the experiments originally containing PdS appear to consist of a mixture of PdS and Pd_2S. In the 10 mg/l HA and 1 mg/l HA residues, a composition close to Pd_3S was also found. The residues of experiments conducted with PtS_2 were composed of a homogeneous residue with Pt and S in equal proportions, hence suggesting a formation of PtS. Examples of SEM spectra are shown in Figures 8.1 and 8.2 in the Appendix.

Figure 4.3 and 4.4 show post-experimental residues of PdTe and $PdTe_2$, respectively. Both telluride residues feature a well-developed formation of new crystal phases which were not present in the starting material (see Fig. 4.1c and d). These new crystal phases are close to idiomorphic, and differ in size and distribution depending on the substrate and leaching solution used during the experiments. The idiomorphic crystals appear to have overgrown the original grains of telluride, and the remaining surfaces of the telluride grains of the starting material appear to be heavily corroded. High-resolution BSE images and SEM analyses show that these new phases are tellurium oxides that have grown both on the surface of the residual telluride grains, as well as over microcracks in the original material (Fig. 4.3a, b).

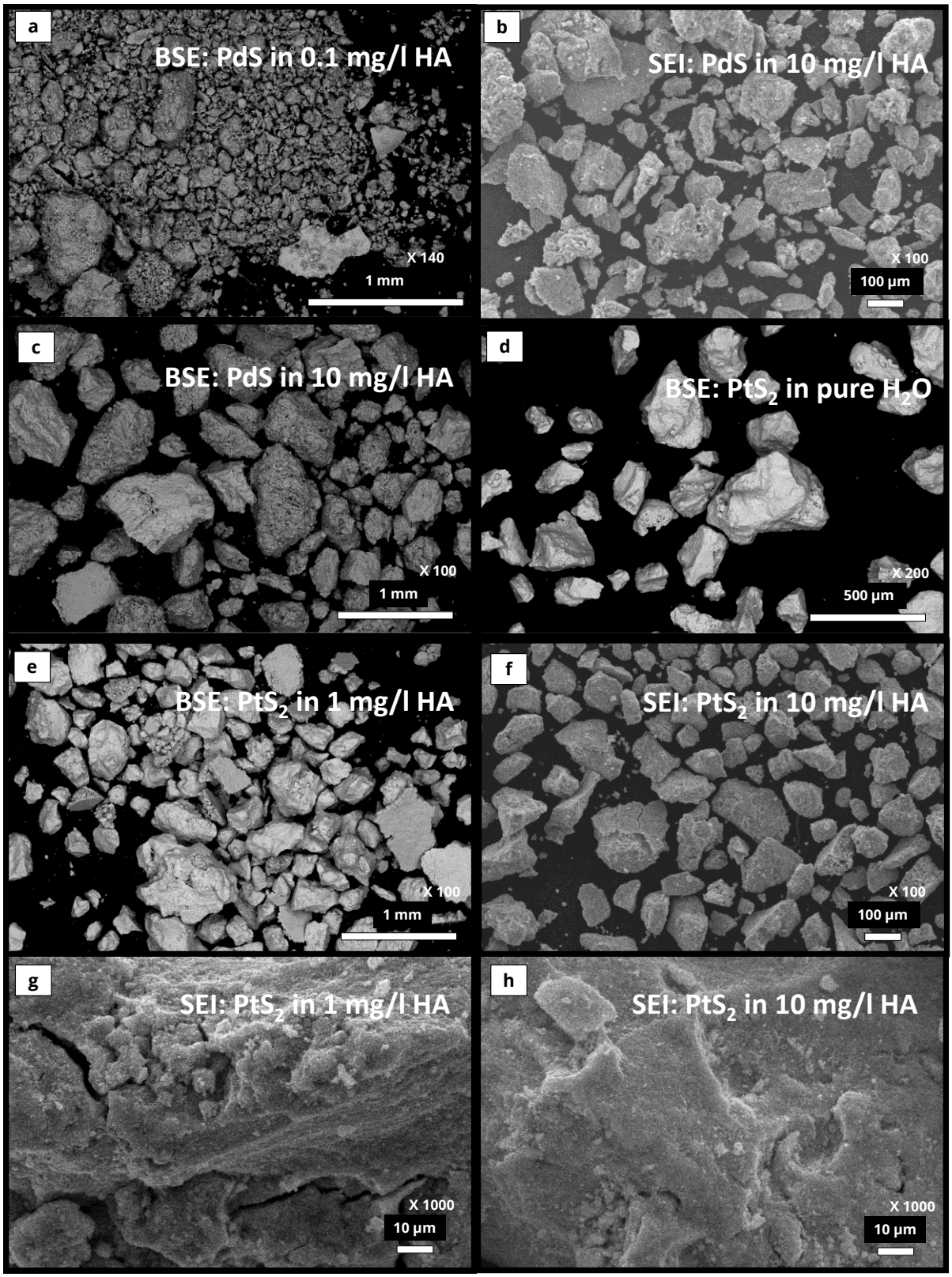

Figure 4.2: Residues after about 308 days: sulfides. (a): BSE image of Pd sulfide after reaction with 0.1 mg/l HA. (b): SEI image of Pd sulfide after reaction with 10 mg/l HA. (c): BSE image of Pd sulfide after reaction with 10 mg/l HA. (d): BSE image of Pt sulfide after reaction with H2O. (e): BSE image of Pt sulfide after reaction with 1 mg/l HA. (f): SEI image of Pt sulfide after reaction with 10 mg/l HA. (g): Higher-magnification SEI image of Pt sulfide after reaction with 0.1 mg/l HA. (h): Higher-magnification SEI image of Pt sulfide after reaction with 10 mg/l HA.

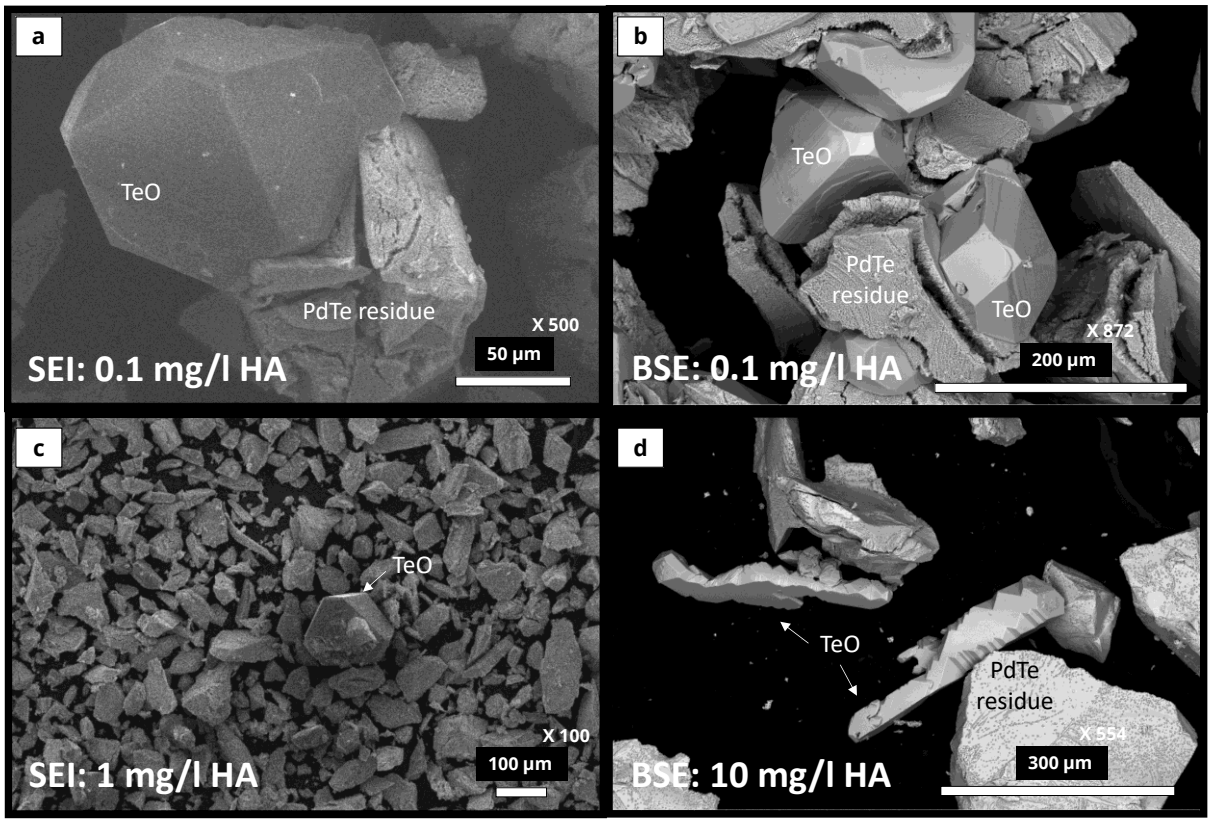

Figure 4.3: PdTe residues after about 308 days, showing newly formed tellurium oxides. (a): SEI image of idiomorphic crystal of tellurium oxide upon residual matrix of altered PdTe, after reaction with 0.1 mg/l HA. (b): High-resolution BSE image of tellurium oxide crystals upon altered PdTe, after reaction with 0.1 mg/l HA. (c): SEI image of large euhedral grain of tellurium oxide, formed after reaction with 1 mg/l HA. (d): BSE image of angular tellurium oxide crystals beside residual PdTe after reaction with 10 mg/l HA.

Qualitative SEM analyses revealed that these new crystals consisted of tellurium oxide, with only minor to trace amounts of Pd (about 0.01–0.1 wt%) (see Fig. 8.3 of the Appendix for analysis). The grain surfaces of the residual Pd tellurides showed a significant increase in Pd/Te when compared to Pd/Te of the starting material. While the original materials consisted of stoichiometric PdTe and $PdTe_2$, respectively, after the experiment this ratio changed to 70-75 atom-% Pd and 25-30 atom-% Te. Notably both PdTe and $PdTe_2$ residues showed the same Pd-Te distribution, i.e. a strong enrichment of Pd that likely occurred in situ. An example of Te oxide as well as post-experimental Pd-Te analysis is shown in Figure 8.3 of the Appendix.

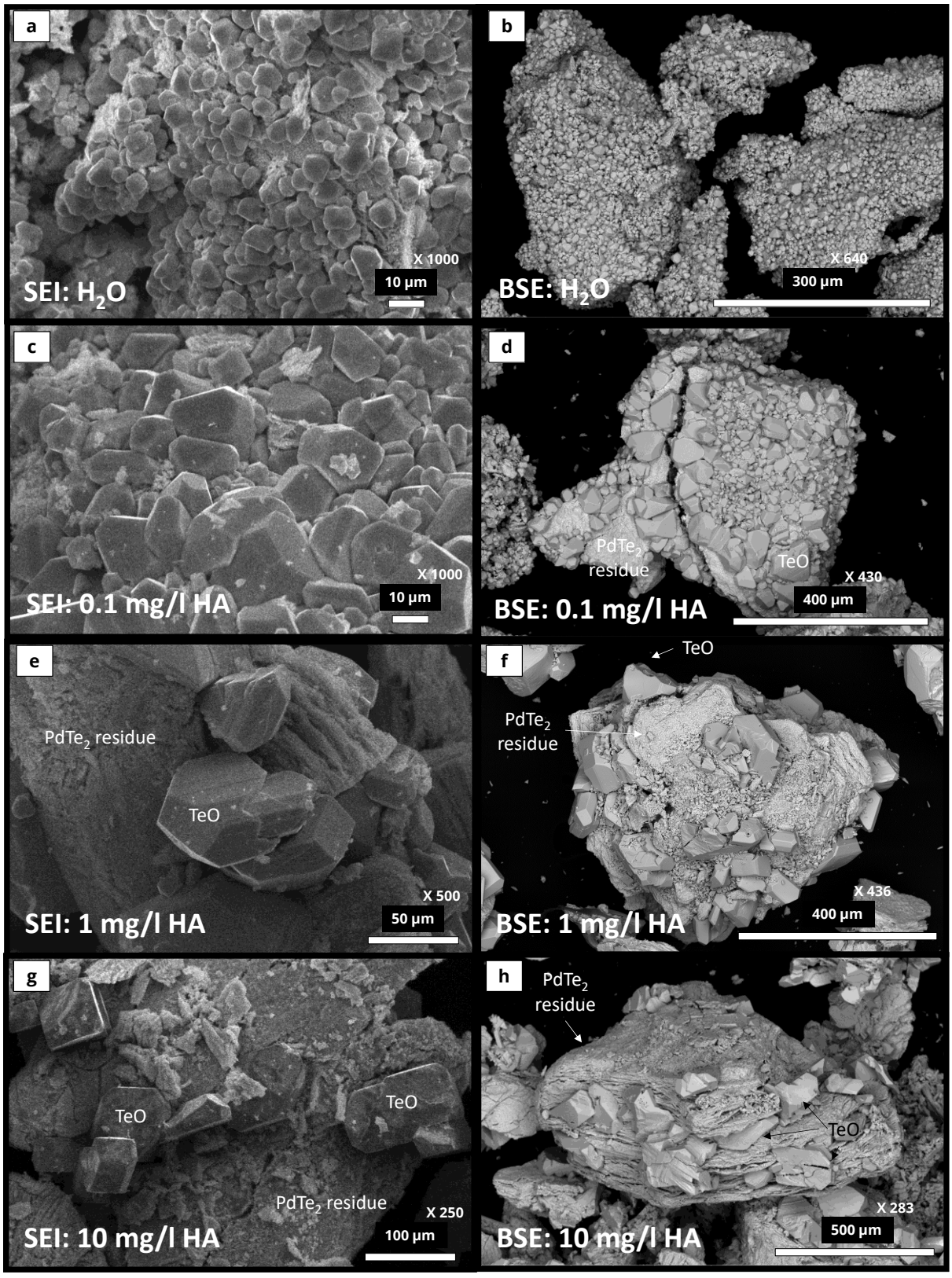

Figure 4.4: $PdTe_2$ residues after about 308 days. (a): SEI image of tellurium oxide crystals encrusting original grains of $PdTe_2$ after reaction with H_2O. (b): BSE image of grains encrusted with tellurium oxide crystals after reaction with H_2O. (c): SEI image of slightly larger tellurium oxide crystals after reaction of $PdTe_2$ with 0.1 mg/l HA. (d): BSE image of residual grain with crystals of tellurium oxide after reaction with 0.1 mg/l HA. (e): SEI image of tellurium oxide crystals upon a matrix of altered $PdTe_2$ after reaction with 1 mg/l HA. (f): BSE image of residual grain with larger tellurium oxide crystals after reaction with 1 mg/l HA. (g): SEI image of idiomorphic tellurium oxide crystals upon $PdTe_2$ after reaction with 10 mg/l HA. (h): BSE image of tellurium oxide crystals overgrowing cracks of original $PdTe_2$ after reaction with 10 mg/l HA.

The amount and distribution of the newly formed Te oxides appear to be dependent on the concentration of humic acid. In the control solution without HA (Figure 4.4a and 4.4b, only done with $PdTe_2$), many crystals smaller than 10 µm encrust and wholly cover the original grains of telluride. In those solutions leaching both telluride types (PdTe and $PdTe_2$) with HA=0.1 mg/l, the individual Te oxide crystals are larger with sizes of up to about 200 µm, and the residual Pd-telluride grains are not completely covered (Figure 4.4c and 4.4d). The residues from solutions that contained HA=1 mg/l (Figure 4.4e & f) and HA=10 mg/l (Figure 4.4g and 4.4h) have even larger individual Te oxide crystals, but they are more sparsely distributed. In the PdTe residue in particular, individual Te oxide crystals were less abundant and they tended to occur as discrete phases (Fig. 4.3d), or in small dispersed clusters (Fig. 4.3b).

4.3.2. Solution measurements

Palladium and platinum sulfide

Figure 4.5 shows concentrations of Pd and Pt in solutions as a function of time for the experiments containing PdS (4.5a) and PtS (4.5b). All figures of solution measurements include the analytical uncertainty given as one standard deviation from the analyzed value. The solutions containing PdS (Fig. 4.5a) revealed peaks of Pd mobilization between around 40-170 µg/l, which is at least ten times more mobilized Pd compared to the experiments employing PdTe and $PdTe_2$ (see below). All three leaching solutions in contact with PdS featured a concentration of about 20 µg/l Pd after 5 days. The 0.1 and 1 mg/l HA solutions continued to show very similar Pd concentrations in each aliquot thereafter, both gradually increasing towards the end of the experiment. The final value for the 0.1 mg/l HA solution was just under 50 µg/l, and for the 1 mg/l HA solution, approximately 40 µg/l Pd (the final aliquot was taken at 306 days). The 10 mg/l HA solution increased in Pd to about 35 µg/l Pd at 63 days, and then continued to increase until it reached a maximum value of about 170 µg/l Pd at 306 days.

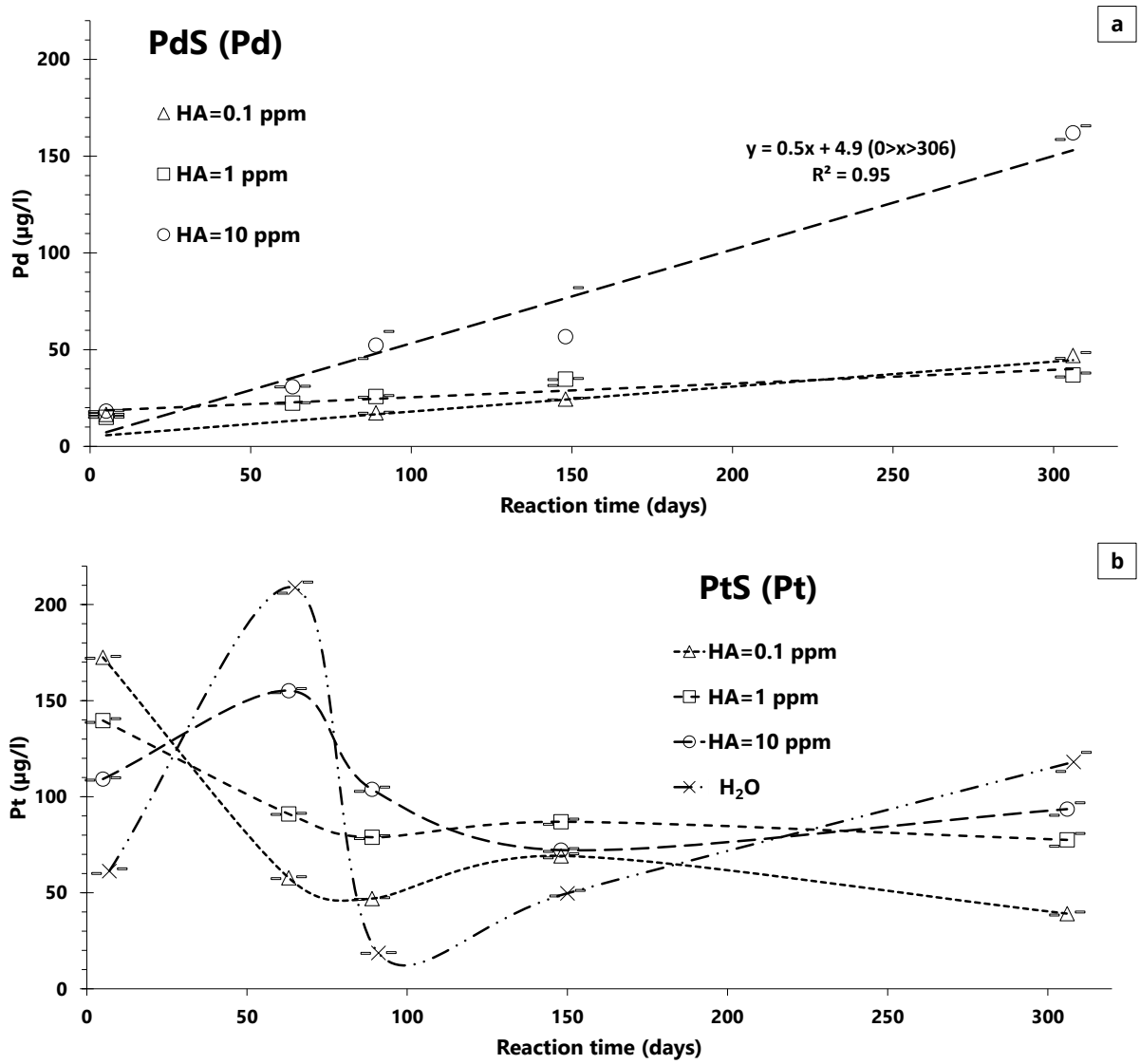

Figure 4.5: Pd (a) and Pt (b) contents measured during the duration of long-term experiments containing PdS and PtS, including analytical error parameters. The error bars to either side of each analysis indicate one standard deviation for vertical error only; they are offset for clarity of results.

The Pd measured in the aliquots of this solution fits, within analytical uncertainty, a straight line drawn from the starting value at 5 days to the last value at 306 days, indicating that Pd increases in a roughly linear fashion in this solution. The trendline for the 10 mg/l solution appearing in Fig. 5a has the equation y = 0.5x + 4.9, (0>x>306) where x = time in days, and y = concentration of Pd in µg/l. The r^2 value of our linear regression for this line is 0.95.

The solutions containing PtS displayed a complex evolution of the Pt concentration from one aliquot to the next (Fig. 4.5b). After 5 days, all four solutions (including the H_2O control solu-

tion) already mobilized Pt comparable to the amounts of Pd in the final stages (see Fig. 4.7). The highest Pt mobilization was observed in the 0.1 mg/l HA solution, with ~170 µg/l Pt, and a comparable Pt concentration was measured for the 1 mg/l HA solution with ~140 µg/l Pt. A slightly lower concentration was found for the 10 mg/l HA solution with ~110 µg/l Pt. Platinum mobilization by pure H_2O was lowest with 60 µg/l Pt.

After 63 days, the Pt concentration in the 10 mg/l HA solution increased to ~155 µg/l, and in pure H_2O by almost a factor of 4 to about 220 µg/l. In contrast to this increase in Pt, the Pt concentration in the 1 mg/l and 0.1 mg/l HA solutions decreased at this time to around 90 µg/l and 60 µg/l, respectively.

After 89 days of leaching, all four solutions showed a decrease in Pt concentration. The 0.1 and 1 mg/l HA solutions had the least decrease, with Pt concentrations of 45 µg/l and 80 µg/l, respectively. The Pt concentration in the 10 mg/l HA solution dropped to ~110 µg/l, whilst Pt in pure H_2O fell drastically with time, to only ~20 µg/l, i.e. a tenfold decrease compared to the previous aliquot.

The Pt concentrations in all four solutions remained low after 148 days and varied between 50 and 90 µg/l. The 1 mg/l HA solution had the highest Pt concentration of about 90 µg/l Pt, and the 0.1 and 10 mg/l HA solutions had both slightly lower Pt concentrations scattering near 70 µg/l. Pure H_2O, however, revealed a slight increase in mobilized Pt to about 50 µg/l Pt, i.e. an increase by 100 % compared to the previous aliquot.

In the last aliquot taken at 306 days, Pt in the 0.1 mg/l HA solution continued to decrease to a final value of ~40 µg/l. In the 1 mg/l HA solution, Pt also decreased, to ~75 µg/l. For the 10 mg/l HA solution, a slight increase of the Pt concentration to ~90 µg/l was observed. The increase of dissolved Pt in pure H_2O continued, reaching a final concentration of ~120 µg/l Pt, again a doubling of the concentration when compared to the previous aliquot.

Palladium tellurides

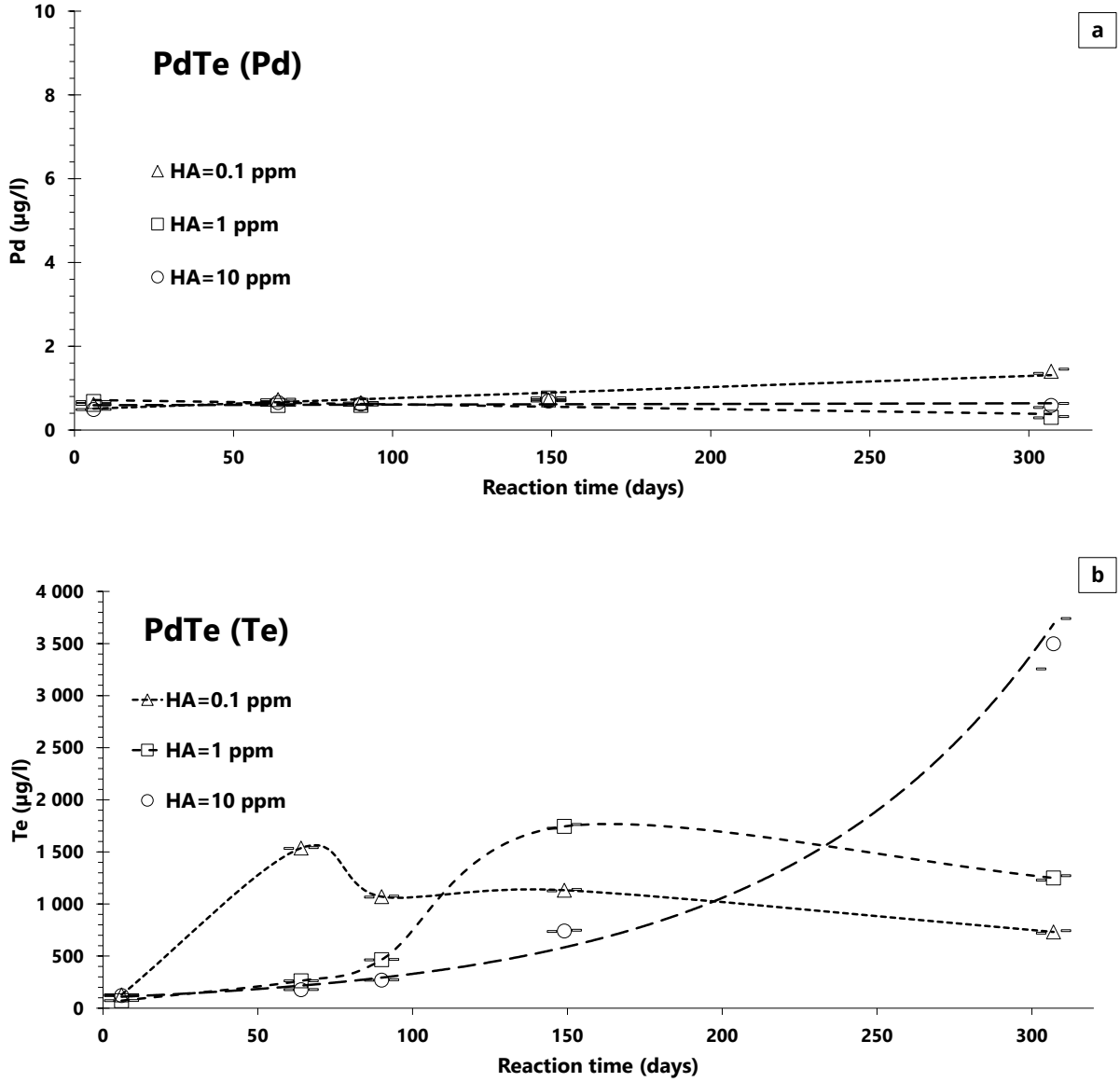

Figure 4.6: Pd (a) and Te (b) contents measured during the duration of long-term experiments containing PdTe, including analytical error parameters. The error bars to either side of each analysis indicate one standard deviation for vertical error only; they are offset for clarity of results.

Figures 4.6 and 4.7 show concentrations of Pd and Te in solutions as a function of time for the experiments containing PdTe and $PdTe_2$, respectively.

For PdTe, no more than 1.8 µg/l Pd was mobilized in any of the samples (Fig. 4.6a). There was less than 1 µg/l difference between the values of 0.1 mg/l HA, 1 mg/l HA, and 10 mg/l HA solutions in the last sample (taken at 307 days).

Compared to Pd, Te was mobilized by several orders of magnitude (Fig. 4.6b), with a maximum concentration of ~3 500 µg/l measured in the aliquot of 10 mg/l HA taken at the end of the experiment. The final aliquot of 1 mg/l HA was lower in its dissolved Te content at ~1 200 µg/l, and the last aliquot of 0.1 mg/l HA was even lower in Te, yielding ~700 µg/l. Both 0.1 and 1 mg/l HA solutions reached their maximum Te concentration before the final aliquot at the end of the experiment was taken. For 0.1 mg/l HA the highest concentration of Te (~1 500 µg/l) occurred at 64 days. For 1 mg/l HA, however, the highest concentration of Te, about 1 700 µg/l, occurred at 149 days. The Te concentrations in both of these HA solutions steadily increased, reaching their maxima, after which the concentrations of dissolved Te decreased (see Fig. 6b). By the end of the experiment, the concentration of Te was more than halved for the 0.1 mg/l HA solution, while for the 1 mg/l HA, the amount of Te in solution decreased by about 40%. The lower values that occurred after the peak concentrations indicate that the solutions did not reach a steady state. For the 10 mg/l HA solution, the Te concentrations steadily rose until the end of the experiment. The increase of Te followed a curved, exponential pattern rather than a linear one. Since Te was still being mobilized by the end of the experiment, this solution also did not attain a steady state.

The $PdTe_2$ solutions mobilized more Pd compared to the PdTe solutions (Fig. 4.7a), with maximum values of about 3 µg/l Pd for 0.1 mg/l HA, 4.2 µg/l Pd for 1 mg/l HA and 1.9 µg/l Pd for 10 mg/l HA. Although the lower two HA concentrations showed a slight rise in dissolved Pd after an initial rise and fall, the maximum Pd concentration attained was ~4.2 µg/l for the 1 mg/l solution, and ~3 µg/l for the 0.1 mg/l solution. An experiment employing pure H_2O was conducted for $PdTe_2$, and may be seen alongside the HA solutions in Fig. 4.7. In this solution, the concentration of Pd gradually increased from about 2.5 µg/l at 65 days, up to about 9 µg/l at 308 days. From 150 days onward, the concentration of Pd in H_2O was higher than in all three HA solutions. The humic acids appeared to have an inhibiting effect on Pd mobilization in this case.

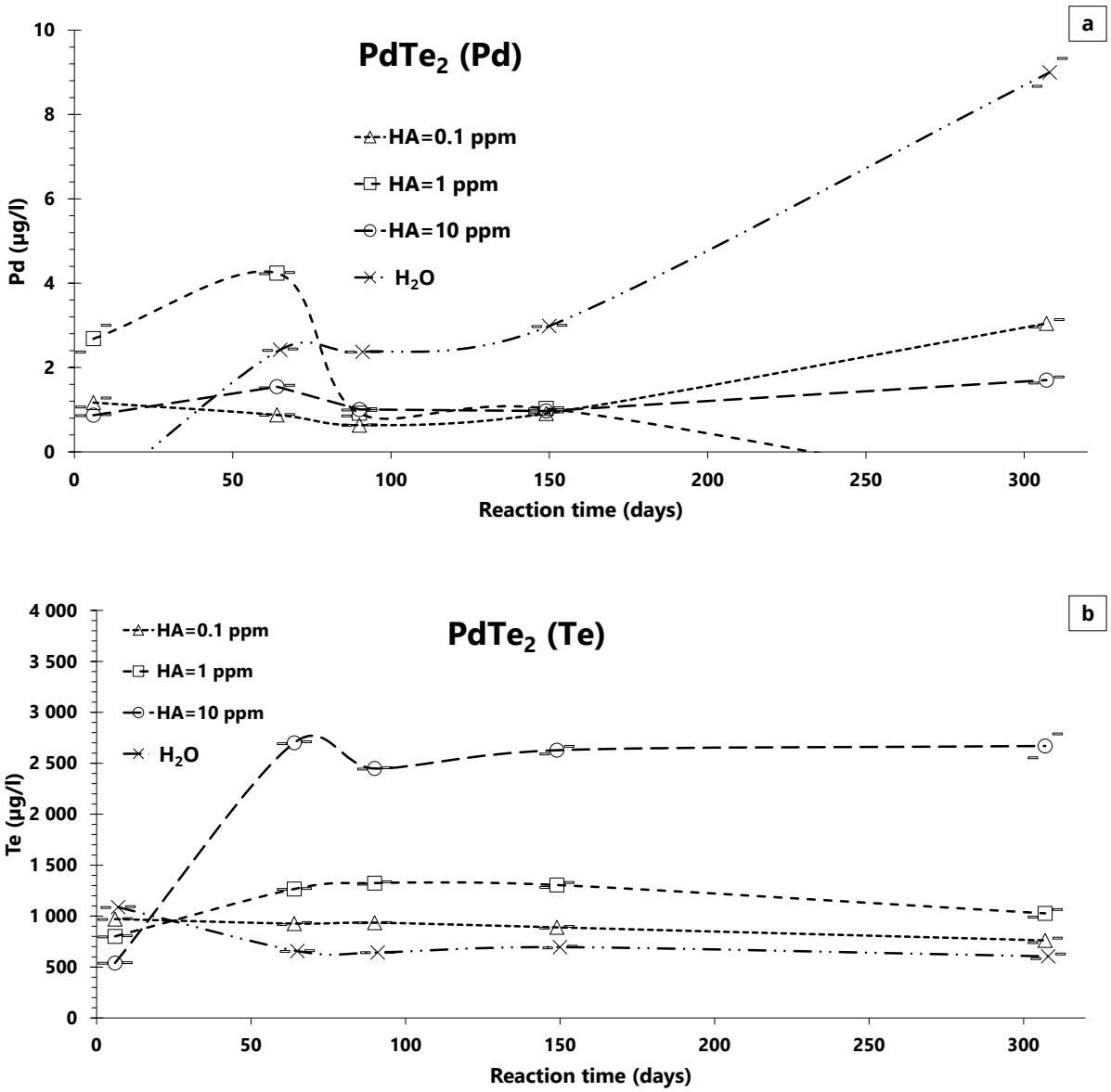

Figure 4.7: Pd (a) and Te (b) contents measured during the duration of long-term experiments containing $PdTe_2$, including analytical error parameters. The error bars to either side of each analysis indicate vertical error only; they are offset for clarity of results.

Similar to the PdTe solutions, Te was mobilized by almost three orders of magnitude when compared to Pd in the $PdTe_2$ solutions (Fig. 4.7b). The 10 mg/l HA solution started out at 6 days with the lowest Te concentration of ~500 µg/l and rose to a constant value of around 2 500 µg/l for all the subsequent aliquots, which was also the highest Te concentration compared to all leaching solutions employing Pd tellurides. Since there was no change in Te values, this solution might have reached a steady state with respect to Te concentration. The 1 mg/l HA solution yielded ~800 µg/l Te after 6 days, and Te increased to about 1 300 µg/l for

the next three aliquots, but the Te concentration decreased to just over 1 000 µg/l in the last aliquot (307 days). The 0.1 mg/l HA solution was marked by about 1 000 µg/l Te after 6 days, which was the highest starting value for the three HA solutions. The next three aliquots showed similar Te concentrations of just under 1 000 µg/l, with Te decreasing to about 700 µg/l at the end of the experiment. The H_2O control solution also had a Te concentration of ~1 000 µg/l at 7 days, i.e. higher than the humic acid solutions at 6 days, but the amount of dissolved Te subsequently decreased to about 600 µg/l Te in the following aliquots, and continued to decrease until the experiment's end. The ongoing trend of decreasing Te in the previously described three solutions suggests that a steady state did not exist in these solutions yet.

Results of pH measurements

At the beginning of the experiment, pH values for all humic acid solutions were between 7 and 8. No change in pH of the solution of the telluride-containing solutions was noted when the experiment was terminated. The control sample with H_2O had a pH of 6.8. The pH value of the 0.1 mg/l HA solutions was 7.8, of the 1 mg/l HA solutions it was 7.2, and of the 10 mg/l HA solutions the pH was 7.7. For details, see Table 8.3 of the Appendix.

The sulfide solutions, however, showed a very clear acidification after the end of the experiment (see Table 8.3 of the Appendix). The pH of solutions that contained PtS_2 was also consistently lower than that of their equivalent solutions containing PdS. The value for the H_2O-control solution containing PtS_2 was 3.4. For the 0.1 mg/l HA solutions, the PdS-containing solution showed a pH of 3.5, whilst in the PtS solution the pH was at 3.3. For the 1 mg/l HA solutions, the PdS-containing solution showed a pH of 3.7, and in the PtS solution the pH was 3.3. For the 10 mg/l HA solutions, the PdS-containing solution had a pH of 3.8, and the PtS solution had a slightly lower pH of 3.4.

4.4. Discussion

Our experiments yielded conflicting results. While Pd concentrations in the 10 mg/l HA solution containing PdS shows a linear trend with time, such a relationship was not seen for Pd in the telluride solutions, and the PtS solutions did not show any correlation of HA concentration to metal mobility. No clear pattern of one HA solution consistently reporting higher or lower concentrations of Pt is evident when compared to the other solutions. Also, the HA solutions do not mobilize more Pt than H_2O. In fact pure water mobilized more Pt than HA. It appears from the HA leaching experiments that after an initial peak in Pt concentration for each solution, the amount of dissolved Pt decreased in solution, only increasing again in the final stages of the experiment for H_2O and the 10 mg/l HA solution. Notably, for the 0.1 mg/l and 1 mg/l HA solutions, a peak of Pt mobilization was observed after 5 days, but for the 10 mg/l HA solution and also for pure H_2O, this peak of Pt mobilization appeared later, after 63 days. The lower concentrations of HA (0.1 and 1 mg/l) appear to speed up the mobilization of Pt, hence reaching the Pt peak concentration earlier when compared to water or high HA concentrations.

The lower pH of the sulfide solutions when compared to the telluride solutions, which showed unchanged pH, is interpreted to be related to the formation of sulfurous acid by reaction of the S-containing compounds with water (e.g. Binnewies et al., 2004). The small amount of humic acid present does not appear to have inhibited this process, which begins with the oxidation of sulfur to SO_2, which is then dissolved in the aqueous phase present in all our experiments. The reaction may be represented by the following chemical reaction:

$$SO_{2\,(g)} + H_2O \longrightarrow H^+_{(aq)} + HSO_3^-{}_{(aq)}$$

This solution may be referred to as sulfurous acid (Binnewies et al., 2004). In the presence of an excess of water, the following reaction takes place:

$SO_{2\ (g)} + 2H_2O \longrightarrow SO_4^{-2}{}_{(aq)} + 4H^+{}_{(aq)} + 2e^-$

The presence of free H^+ ions causes lowering of the pH of the solution, which may then be related to formation of sulfuric acid (H_2SO_4).

Pd vs Pt in sulfide

The relative mobility of Pd over Pt in natural systems is well known (e.g. Oberthür et al., 2003; Traoré et al., 2006; Turner et al., 2006; Cabral et al., 2007). Our findings agree with a higher Pd mobility over Pt, here in HA solutions rather than in water, because Pd continued to increase in the solutions leaching a solid PdS phase, while in the solutions attacking solid PtS_2, the amount of dissolved Pt decreased in the solution after an early Pt maximum. This reflects the range of conditions over which dissolved Pd species are stable when compared to Pt. Palladium is mobile over a wide range of pH and Eh (i.e. redox) conditions, including typical conditions during weathering (Cabral et al., 2007). In comparison, Pt is only mobile under supergene conditions when the pH is high (>8) or very low (<1) (Cabral et al., 2007). Considering that the pH of the sulfide solutions changes from values of 7 to 8 down to about 3.5 during the course of the experiment, the variations of the Pt concentrations throughout the experiments may be explained by a changing pH. At the beginning of the experiments, the pH values were close to 8, thereby supporting Pt mobilization from the Pt sulfide into solution. Therefore, initial dissolved Pt concentrations were similar to those of dissolved Pd in the PdS solutions (compare Fig. 4.7a and b). But after a certain period of time, which depended on the strength of HA in the solutions (see Fig. 4.5b) the hydrolysis of sulfur took place as described above. This caused the pH to lower and dissolved Pt species to become unstable as a result. Pt was most likely precipitated, as described by Oberthür et al. (2003) and Locmelis et al. (2010). Bowles et al. (2018) inferred the coexistence of the Pt-hydroxide complexes $Pt^{2+}(H_2O)_2(OH)_2$ and $Pt^{4+}(H_2O)_2(OH)_4$ along with humic substances in the soils above the Freetown Layered Intrusion (Sierra Leone). These complexes may have occurred in our solu-

tions as well, influencing not only the pattern of Pt mobilization seen in Fig. 4.5b, but also the structure of the humic acids themselves. The absence of Pt oxide/hydroxide phases in the dried residues may be explained with reference to Cabral et al. (2008), who describe the process of formation of Pt alloys in soils: hydrous Pt oxide minerals form by oxidation of the original minerals, but deoxygenation / dehydration of these oxides leads to formation of native Pt and alloys (typically with Fe or Cu) with characteristic desiccation structures. If this same process occurred in our experiments (which may be possible when observing the surface morphology shown in Fig. 4.2g and h), Pt (or Pd) oxides may have been transformed into native Pt (or Pd) during the drying process. Notably, if the pH in the sulfide solutions had continued to decrease further close to pH ~1 or even less, conditions might have become favorable for Pt mobilization once more (Cabral et al., 2007; Azaroual et al., 2001), but humic acid would no longer have been soluble and would have precipitated at pH <3 (Haworth, 1971), causing all Pt possibly adsorbed / complexed with it to precipitate as well (Wood, 1996; Turner, et al., 2006).

In a natural environment, a relative enrichment of Pt in soils closer to the bedrock has been observed, whereas Pd which is typically more widely distributed in the soil profile (Traoré et al., 2006; Oppermann et al., 2017). The experiments presented in this paper, however, represent a closed system, from which no elements can be lost to the environment. Consequently, in the duration of the experiment, one would expect a slow increase of dissolved Pd. Of the three concentrations of humic acid used, the 10 mg/l HA solution has been the most efficient in mobilizing Pd from PdS, showing a threefold increase of the dissolved Pd concentration compared to the other two solutions. This suggests that the abundance of humic acid is an important parameter for Pd mobilization. Turner et al. (2006) concluded that Pt and Pd were likely to form complexes with suspended organic matter present in particulate matter transported by rivers when brought into a relatively undisturbed environment, but that Pd was more likely than Pt to leave the organo-metallic complex and dissolve into water when

brought into a faster-flowing area of water (like a river). The adsorption of Pd by organic complexes initially took place at a faster rate than Pt adsorption. However, Pd gradually became desorbed in the presence of fresh water due to the process of redistribution between adsorption sites on the organic particles (Turner et al., 2006). This implies that our experiments are able to keep Pd in solution only because they are undisturbed and are not subject to a new influx of water. If we assume that Pd is forming an organic complex with HA, it seems that a greater amount of available organic ligands results in more Pd being adsorbed, but when a maximum is reached, Pd will precipitate, possibly as Pd oxide/hydroxide as described by e.g. Oberthür et al. (2003), Cabral et al. (2008), and Locmelis et al. (2010). Palladium does not appear to have reached this maximum dissolved concentration in any of our PdS experiments, since Pd was increasing in all three HA solutions, at a slower rate in the 0.1 and 1 mg/l HA solutions (see the flatter slopes of the lines given in Fig. 4.5a). However, in the Pd-telluride experiments, Te seems to have followed this pattern of behavior, since Te oxides are found that may have been formed by precipitation of Te oxide, after Te reached a maximum in each solution (see Figs. 4.6 and 4.7).

Platinum does not immediately decrease in solution once the pH begins to decrease; it only does so gradually as seen in Fig. 4.5b. Wood (1996) suggests that humate complexes could keep Pt and Pd in solution, effectively slowing down precipitation of native Pt or Pt oxides where the conditions change to become unfavorable to Pt mobilization. Pt has a great affinity for organic complexes, as discussed by Turner et al. (2006), supporting the idea that the presence of HA may have slowed down the precipitation reaction of Pt in our experiments.

With reference to how much of the original Pd and Pt is actually taken into solution, the total mass of Pd in the PdS powder for the 10 mg/l HA experiment is 25 000 µg. The total mass of Pt in PtS_2 for the 0.1 mg/l HA experiment is also 25 000 µg. Taking the final value of Pd in solution (162.08 µg/l), we find that 29.82 µg Pd has actually been mobilized, making up 0.12

% of the total mass of Pd. If we take the value of Pt in solution from the first aliquot (where it is at its highest for the HA solutions), we find that 31.75 µg of Pt has been mobilized, making up 0.13 % of the total mass of Pt. It can therefore be assumed that Pd and Pt largely remain in the residual minerals, which is consistent with our observations that the metal:sulfur ratio increases in the experimental residues, from PdS to Pd_2S and from PtS_2 to PtS.

According to the equation we obtained from the 10 mg/l HA solution with PdS, the amount of Pd increases by about 0.5 µg/l every day between 5 and 306 days. The y-axis cutoff is calculated as 4.9 µg/l. A likely explanation for this is that during the first 5 days of reaction, the mobilization of Pd happens much faster than during the rest of the experiment. This would be in agreement to Turner et al. (2006), who concluded that the initial reaction between Pd and organic complexes happens rapidly as Pd is quickly adsorbed onto the organic particles. This offers an explanation of why in our experiments Pd is rapidly taken into solution in the first 5 days, rising to a value of about 18 µg/l.

Platinum-palladium sulfides are often found as part of an oxidized ore assemblage (as PdS or PtS) while bismuthotellurides in primary deposits are quicker to disintegrate (e.g. Locmelis et al., 2010; Melcher et al., 2005; Oberthür et al., 2003; 2013). These authors and also Cabral et al. (2007; 2008) and Traoré et al. (2006) describe the formation of various weathering rims on detrital PGM grains, often formed by selective leaching of certain metals like Ag and Pd, hence leading to an enrichment of less mobile metals such as Pt on these weathering rims. In our qualitative analyses of experimental residues, it is impossible to distinguish whether we are measuring a new phase (PtS), or whether in fact we are measuring desiccated Pt-oxide/hydroxide plus the original PtS_2. Given that only a very small percentage of Pt was taken into solution, we can expect that the contribution from precipitated Pt phases was very low. From our results, we cannot prove nor disprove the presence of possible metal-rich weathering rims on our sulfide mineral grains.

Palladium tellurides and their significance to the natural weathering environment

In the residual, i.e. "weathered", grains of both PdTe and $PdTe_2$ in our experiments, the Pd content became enriched to three times the Te content. The amount of Te leached from Pd ditelluride directly correlates with the humic acid concentration as seen in Fig. 4.7b. For Pd monotelluride, the highest maxima in the 0.1 and 1 mg/l HA solutions are seen before Te decreases. To get an idea of how much Te was dissolved at this point, a simple mass balance was calculated. The mass of Te in the original powder was 17 000 µg. Calculating the mass of Te in solution in the 0.1 mg/l HA experiment at 64 days, we find that 301.32 µg Te was mobilized. This works out to be about 1.77 % of the total mass of Te present. If we take the amount of Te mobilized in the 10 mg/l HA solution with $PdTe_2$ after 64 days, we see that 529.4 µg Te was in solution at that point, which equals 2.3 % of the total mass of Te (which was, in total, 23 000 µg in the solid phase). A loss in the order of 1-2 % Te cannot explain the drastic reduction in the Te:Pd ratio observed in the experimental residues, which is 1:3 (from 1:1 for PdTe and 2:1 for $PdTe_2$). Therefore, the missing Te must be present in the newly formed Te oxide phase. Tellurium monoxide (as suggested by qualitative SEM analysis of the Te oxide crystals) does not occur in nature; only TeO_2 (tellurite, or its dimorph, paratellurite) is known (Switzer & Swanson, 1960). These rare minerals can be found in native telluride seams (ibd.). A possible reason why TeO_2 is not seen in our experiments is because Te exists in our palladium minerals as an anion. The Te species in the new crystals must be Te^{2+} to combine with oxygen, indicating that oxidation of Te had already taken place, but under the aqueous conditions of the experiment, it appears that Te was not oxidized to Te^{4+} yet, which is presumably required for tellurite or paratellurite to form.

The formation of the Te oxide crystals provides a possible answer to why Te begins to decrease towards the end of the PdTe experiments: if Te oxide crystals are actively forming, they will withdraw Te from solution. The $PdTe_2$ residues are almost completely encrusted

with Te oxide crystals as seen in Fig. 4.4a-d, and it is possible that the formation of these crystals prevent further leaching of Te from the residues, keeping Te in solution at a relatively stable concentration. If Te is still being released from the $PdTe_2$ grains, Te oxide may be forming simply by oxidation of the released Te at the same rate at which it is being released.

For the 10 mg/l HA solution with PdTe, fewer Te oxide crystals were observed compared to the other PdTe residues (see Fig. 4.3d). This also happens to be the only solution where Te is still increasing in solution; there seems to be an interplay between palladium telluride, Te oxide and the possible Te-organometallic complex by which humic acid mobilizes Te. In this case Te is not decreasing in solution and is therefore not widely precipitated as Te oxide.

With reference to natural Pd telluride minerals, an unnamed phase described by Kweiyang Institute of Geochemistry (1974) matches the composition of our residues (Pd_3Te) exactly. However, no other occurrences of this mineral are known. Compositionally, the ratio of our residues is also close to that of keithconnite ($Pd_{20}Te_7$), a mineral found in PGE-bearing layered complexes, notably the Stillwater Complex (Cabri et al., 1979) but also in the BIC (Melcher et al., 2005). Another mineral of similar composition, telargpalite ($(Pd,Ag)_3(Te,Bi)$) is found in the mafic PGE-nickel deposits of Noril'sk, Russia (Sluzhenikin & Mokhov, 2015), but it is usually defined by the presence of silver along with palladium. Melcher et al. (2005) describe keithconnite as occurring as inclusions along with the closely related kotulskite (Pd(Te, Bi)), inside altered Pt-Fe alloy found as detrital minerals in the alluvial sediments of rivers draining the area of the eastern BIC. In our experiments, the conditions to form keithconnite may not be favorable; however, an enrichment of Pd is seen relative to Te, which is seen in natural deposits when the minerals kotulskite and merenskyite (see also Section 2), which are relatively common in primary magmatic PGE deposits, undergo weathering at the earth's surface. These experiments can be said to represent an early phase of weathering during which all mineral phases may not be stable; therefore, we may not be seeing the final

product of natural weathering of these minerals, but rather an intermediate, metastable phase. "Pd_3Te" may simply be a dissolution relict and not a crystal phase.

Under surficial weathering conditions, PGE-bismuthotelluride minerals tend to be destroyed, while sulfides are more stable (e.g. Locmelis et al., 2010; Oberthür et al., 2003; 2013). These authors describe relict PGE sulfides in the oxidized Main Sulfide Zone of Zimbabwe's Great Dyke and categorize bismuthotellurides as being rare in the oxidized portion, although they are abundant in the pristine ore. Cooperite and braggite, both Pd-Pt sulfides, form up to 11% of the pristine ore and 33% of the oxidized ore according to Locmelis et al. (2010), whilst the bismuthotellurides only form 3.3% of the oxidized PGE assemblage, despite forming 71% of the pristine ore. Being mobile in the surface environment, Te would disperse into the environment under natural conditions; no Te oxide has been described in the oxidized portions of the Great Dyke or the BIC. The observed Te oxide crystals are only preserved in this study because of the artificial, closed system that existed in our experiments.

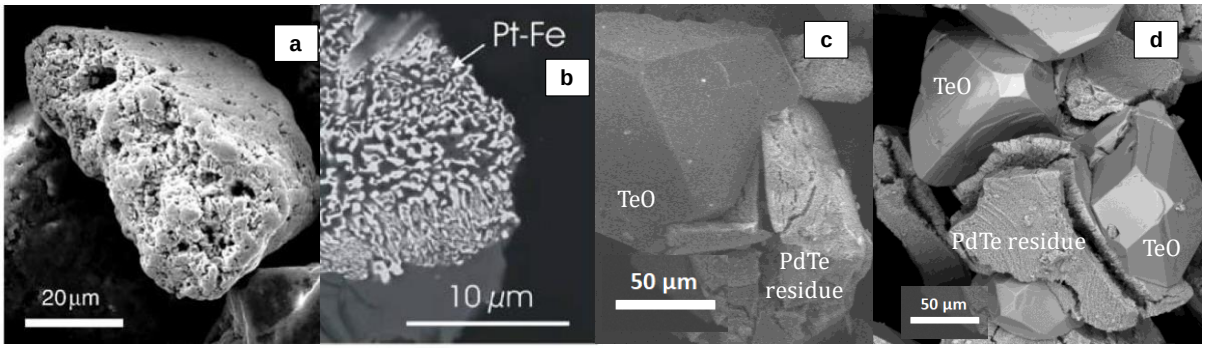

Figure 4.8: Comparison of experimental residues with weathering products of the natural environment. (a): Weathered PGM, from Traoré et al. (2006), likely a deeply weathered alloy of Pt and Fe. (b): Relict Pt-Fe phase, from Locmelis et al. (2010). (c) and (d): Residual palladium telluride with tellurium oxide crystals, from this study.

The telluride crystals in these experiments show indications of chemical leaching (as seen in Figures 4.3 and 4.4), with pitted and cracked surfaces. Optically, these residues (Figure 4.8c-d) are similar to weathered PGM grains found in soil horizons (Fig. 4.8a-b). This suggests that these features might form by the same mechanism that operates during weathering and soil

formation. Humic acids must play a role during this process, given that a relatively low concentration of HA (10 mg/l) can increase the leaching of Te out of the primary mineral and therefore increase the weathering rate in the natural environment. Comparison with mineral surfaces from the oxidized Main Sulfide Zone, as seen in Locmelis et al. (2010) (Fig. 4.8b), shows a slightly different kind of surface, with the relict mineral appearing spongy rather than pitted. This may indicate a slightly different weathering mechanism; the mineral is intergrown with Fe hydroxide. The grain in Fig. 4.8a is from a lateritic soil in New Caledonia, whilst the grain in Fig. 8b is from a soil environment in Zimbabwe, similar to the vertisols of the BIC. Given the aqueous environment to which the grains in Fig. 4.8c-d was subjected, it is not altogether surprising that it shows more similarity to the weathered products found in soils from a tropical region such as that in New Caledonia.

These experiments represent a first step into understanding the interaction between PGE and humic acid by using only a small selection of possible PGE minerals. In natural PGE minerals with a more diverse set of elements being present (e.g., also As, Fe, and Bi), we might expect to see different, but related effects when such phases are exposed to humic acids. For example, with PGE arsenide minerals, As is well known to be taken up by humic substances, and this relationship depends strongly on pH, with sorption dropping off strongly at pH >7 (Thanabalasingam & Pickering, 1986; Warwick et al., 2005). Since the experiments from this paper started with a pH of between 7 and 8, there may be a preference for HA to leach PGE over As, creating a situation completely different from our tellurides. With alloys such as isoferroplatinum, $((Pt, Pd)_3(Fe, Cu))$ we would expect Fe to be oxidized, forming Fe-oxide/hydroxides, which may lead to mobilization of Pd and possibly Pt by humic compounds. However, as discussed in this paper, Pt (and Pd) can be precipitated as oxide/hydroxide minerals which, in turn, subsequently may form native Pt (and Pd) or alloys (Cabral et al., 2008). Keeping this in mind, there may be very little change to these alloys in the presence of humic acid.

4.5. Conclusion

The humic acid solutions in this study show weathering effects that are different from those of pure water alone. There is no simple relationship between PGE mobility and humic acids; their interaction, as represented by synthetic PdS, PtS_2, PdTe and $PdTe_2$, depends on factors such as mineral type (sulfide versus telluride), concentration and pH of the humic acid solution itself, and the reaction time. Some of our results can be considered to approximate the "humic acid" factor involved in the natural weathering of PGEs. It is likely that humic acids play an important role in PGE mineral weathering processes by changing the rate of reaction, or enhancing mobility of elements such as Pd and Te.

Pd and Pt showed different behavior even where the mineral type (sulfide) was analogous. After 306 days, the experiments never reached an equilibrium value of Pd dissolution in humic acid solutions. Pt, however, underwent initial dissolution in both humic acid solutions and water, followed by a stage of precipitation, the timing of which depended on the concentration of humic acid. The behavior of Pt was therefore governed not only by its mobility with respect to water, but also by the presence of humic acid in solution. This confirms that during surficial weathering processes, the PGE can be influenced by natural humic substances present in soil solution.

5. Mobility of Pt and Pd from chromitite (long-term and final experiments)

This chapter is to be submitted for publication in a peer-reviewed journal, in a modified form, as:

Kotzé, E., Schuth, S., Goldmann, S. & Holtz, F. *The influence of humic acids on the weathering of PGE in chromitite: a study of ore-grade chromite concentrate and chromite-poor tailings.*

5.1. Introduction

Chromitite, defined as a rock made up of 90% or more chromite (ideal formula: FeCr2O4) or magnesiochromite (ideal formula: MgCr2O4), is a particular feature of layered igneous complexes such as the Bushveld Igneous Complex (BIC) and is often considered as an important marker for associated minerals containing platinum group elements, (PGE) which comprise the six elements Pt, Pd, Ru, Rh, Os and Ir. In the Bushveld complex, the UG-2 chromitite layer is currently,the largest depository of PGE-bearing minerals. The chromitite is mined extensively and comprises at least a third of current mineable PGE targets in South Africa (Cawthorn, 1999). Some of the other chromitite seams of the BIC are actively mined for their chromium content; in the past, the LG-3, -4 and -6 were the most attractive targets (Hatton & Von Gruenewaldt, 1985), but more recent operations such as Cronimet's Thaba Mine exploit the MG chromitite layers as well (Oppermann et al., 2017). These chromium-rich layers contain minor deposits of PGE, (e.g. Cawthorn, 1999; Naldrett et al., 2011) which may be beneficiated from the waste plant, or left to join the drainage. Other worldwide occurrences of chromitite include parts of the Great Dyke, Zimbabwe, (e.g. Wilson, 1982) the various chromitites of the ultramafic complexes of the Ural Mountains, (e.g. Garuti et al., 2012) the podiform chromitites of Ortaca, Turkey, (e.g. Uysal et al., 2005) the cyclic chromite-rich layers of

the Stillwater Complex, (e.g. Page et al., 1976) the Kemi stratiform chromitite deposit in Finland, (e.g. Alapieti et al., 1989) and others.

Since the BIC contains up to 14 laterally continuous chromitite layers enriched in PGE compared to their host rocks, (Kinnaird, et al., 2002) these layers are a logical example to consider when studying the fate of PGE during weathering. The distribution of the six PGE within the chromitite layers themselves shows differences according to the position of the chromitite within the stratigraphy, as well as within the layer itself according to element. In the lowermost chromitite layers, which comprise the so-called Lower Group (LG) chromitites, the platinum subgroup PGE (PPGE – Pt, Pd and Rh) tend to be present in similar concentrations to the iridium subgroup PGE (IPGE – Ir, Os and Ru), with the IPGE sometimes present in concentrations higher than the PPGE, especially in the lowermost three chromitites (LG-1 to -4) (Barnes & Maier, 2002). Scoon & Teigler (1994) found the average Pd/Ir ratio in these four layers to be about 0.5, and the overall PPGE/IPGE ratio to be 0.3. But moving up in the stratigraphy, at about the level of the LG-5, (Barnes & Maier, 2002; Naldrett et al., 2011) the PPGE begin to increase relative to the IPGE, and sulfide minerals begin to appear, with which PPGE-containing minerals are invariably associated (e.g. Von Gruenewaldt & Merkle, 1995; Naldrett et al., 2011). Scoon & Teigler (1994) found the Pd/Ir ratio in the LG-5 to be about 3, and the overall PPGE/IPGE ratio in this layer was found to be ~1.9. The PPGE show a steady increase relative to the IPGE up until the UG-2, which contains the highest levels of PGE in all the chromitite layers, and generally the highest amount of sulfide minerals as well (e.g. Teigler & Eales, 1993; Von Gruenewaldt & Merkle, 1995; Barnes & Maier, 2002; Cawthorn et al., 2002; Naldrett et al., 2011). The average Pd/Ir ratio of the UG-2 is at about 10 (Barnes & Maier, 2002), and the overall PPGE/IPGE as ~4.5.

The theories that have been put forward with regard to the formation of these chromitite layers are numerous, and a full discussion is outside the scope of this paper (see e.g. Kinnaird et

al., 2002; Mondal & Mathez, 2002; Cawthorn, 2007; Voordouw et al., 2009 & Naldrett et al., 2011 for discussion on the viability of different formation theories). An explanation of how the PGE became enriched in these chromitite layers was put forward by Tredoux et al. (1995), who showed that the siderophilic nature of the PGE, particularly the IPGE, might lead to formation of metallic PGE "clusters" stabilized by ligands such as S, As, Sb and Te within a magma. This would lead to early PGE minerals (PGM) being co-precipitated along with chromite, and thus in the early chromitite layers, PGM are associated strongly with chromite-rich layers, there is no difference between IPGE and PPGE distribution, and PGM could occur in layers which are rich or poor in sulphide (Tredoux et al., 1995). Helmy et al. (2013) showed experimentally that Pt and As combined to form nanoparticles before sulfur saturation occurred in an Fe-(Cu)-sulphide melt, supporting the previously discussed model and implying that partitioning of noble metals between melts of different composition (such as sulfide vs. silicate) might not be governed by the properties of the metal itself, but by the properties of the nano-clusters consisting of both Pt and As.

However, studies have shown that the PGM formation in the BIC chromitites cannot be explained by just one mechanism (e.g. Von Gruenewaldt & Merkle, 1995; Barnes & Maier, 2002; Cawthorn et al., 2002; Gain, 1985; Barnes & Maier, 2002; Naldrett et al., 2011), but that it is rather a result of a combination of factors, including the above discussed "cluster model" as well as previously proposed models involving the formation of an immiscible sulfide fraction from an ultrabasic magma which scavenges the remaining PGE, eventually producing PGM that are generally associated with base sulfide minerals.

Weathering of chromitite

Most chromitite layers of the BIC outcrop or occur near the surface, exposing them to weathering (Figure 5.1). Chromite is known to be strongly resistant to chemical weathering (e.g. Garnier et al., 2008) and in many instances can be found as identifiable residual chromitite

layers in strongly weathered soil horizons (Fig. 5.1f). Mg-rich chromite (magnesiochromite) may be found to be serpentinized, (e.g. Garuti & Zaccarini, 1997) and particularly in komatiites, may be altered to chromian magnetite, with which it is isomorphous, or to "ferritchromit," iron-rich chromite (Barnes & Roeder, 2001). However, these changes are usually considered to be the result of metamorphism, and may not involve surface weathering.

Observations from soil chromites carried out by Garnier et al. (2008) revealed that Cr(III) may be slowly dissolved from chromite during weathering, releasing Cr into the environment; however, other Cr-bearing minerals probably provide Cr to soils at a faster rate. Since the PGM of the Bushveld Complex are typically present in chromitite as discrete minerals and not in solid solution with chromite, (e.g. Tredoux et al., 1995; Naldrett et al., 2011) the PGE could be removed from chromitite without the chromite crystal having to dissolve, e.g. after the chromitite host rock has been fractured during mechanical weathering. Since Pt and Pd are not bound by chromite crystals, their weathering would depend on the stability and rate of dissolution of the mineral they were associated with (typical examples include Pt–Pd sulfide as well as arsenide and telluride).

The possibility of humic acids being capable of mobilizing the PGE has been put forward by many authors (e.g. Bowles, 1995; Wood, 1996; Oppermann et al., 2017). Kotzé et al. (2019) showed that under laboratory conditions, low concentrations (0.1-10 mg/l, dissolved in water) of synthetic humic acid can mobilize palladium and platinum, with Pd increasing steadily in solution. Platinum displayed a more complex evolution in these experiments, being mobile under more restricted conditions compared to Pd.

In this study, the possible influence of humic acids during the weathering of PGE-containing chromitites is presented. Three types of samples are considered: chromite crystals, crushed chromite crystals, and waste tailings supposed to be enriched in PGE. Solution experiments with different concentrations of synthetic humic acid were carried out on these three sub-

strates, and our results show that the humic acids are indeed involved in the process of weathering chromite and liberating PGE, which may then be released into the natural environment to form oxidized PGE deposits.

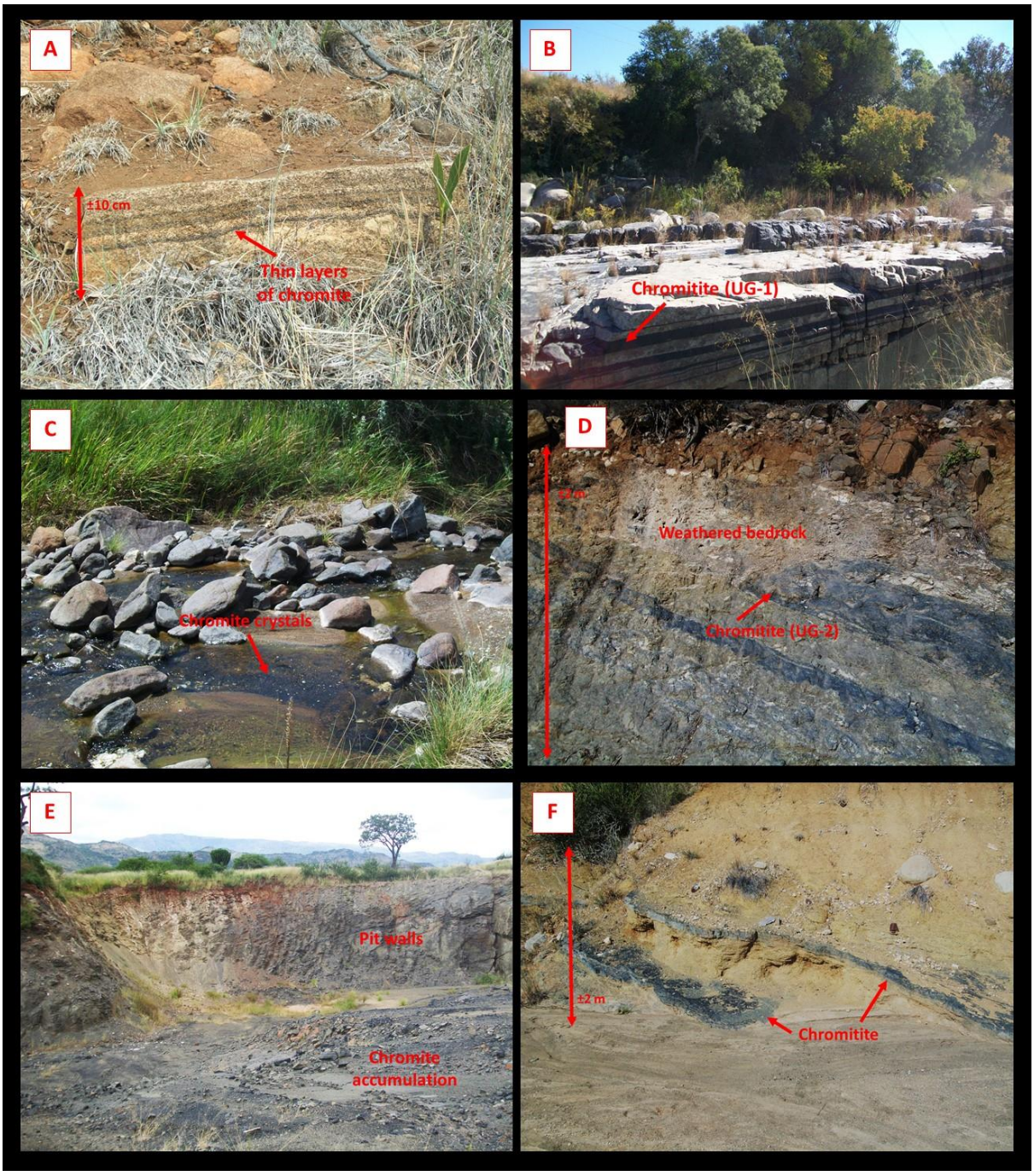

Figure 5.1: Weathering of the Bushveld chromitites, South Africa (all pictures taken at sites of the eastern outcrop of the BIC near Burgersfort, Limpopo Province). (a): Chunks of mechanically weathered rock are exposed on slopes. (b): The outcrop of UG-1 chromitite at the Dwars River Monument: here the rocks have been worn away to create a river channel, and the chromitites are exposed to further weathering. (c): Chromite crystals are eroded from their original position in the bedrock and transported by rivers, where they accumulate in low-energy areas. (d):A roadcut at a mining site shows the UG-2 chromitite layer, which is overlain by a zone of deeply weathered bedrock beneath the thin topsoil. (e): In an abandoned open-pit chromium mine, the pit walls are eroded and chromite accumulates inside the pit under the influence of gravity, where it

becomes part of the soil or may be carried away by flowing water. (f): Despite wholesale bedrock alteration and soil formation, chromitite layers still remain identifiable, resistant to chemical weathering.

5.2. Materials and methods

5.2.1. Material from the Thaba Mine

The Thaba Chromium Mine is located near the town of Thabazimbi in the north of South Africa. It is placed so as to exploit the chromitite layers of the western lobe of the Bushveld Igneous Complex (BIC). The Lower Group (LG) and Middle Group (MG) chromitites of the BIC are well-developed here, and at Thaba Mine the LG-6 and its leader seam LG-6a, as well as the MG-1 to -4 and -4a, are mined for chromium (Oppermann et al., 2017). The PGE are a possible source of extra revenue here, as the chromitite layers are apt to contain low concentrations (<1 mg/kg) of total PGE.

A sample of the high-grade chromite concentrate (named MNR-60) was obtained at Thaba and by Cronimet SA for the first experiments of this study. This concentrate consists of close to 100% chromite, with less than 1% other minerals present. Possible non-chromite minerals from the natural chromitite layers are silicates such as olivine, pyroxene, plagioclase and muscovite, as well as platinum-group element minerals (PGM) and base metal sulfides (BMS). The diameter of the chromite crystals in this concentrate is about 0.5-1 mm. The unaltered concentrate was used in the experiments, along with a portion of the concentrate which was crushed using an agate mortar to <100 µm.

After the first experiments were completed, a sample of chromitite tailings from the Thaba Mine was obtained. Since the first experiments with the chromite concentrate yielded little data, (see Results section for details) a second experiment was set up using stronger concentrations of humic acid (see below). For the second experiment, both the chromite concentrate MNR-60 as well as a sample of chromite tailings at Thaba Mine was available. The tailings

sample consists of waste material that is discarded after concentration of the high-grade chromite; thus, a mixture of chromite and associated silicate minerals. The grain size of the material is variable, but it was crushed to a grain size of <200 µm for our experiments.

In the third experiment described in this study, synthetic PdS and PtS_2 were also used as substrates, in order to illustrate what the effect of stronger concentrations of humic acid has on high-PGE content minerals. These were both obtained in powder form from American Elements, Merelex Corporation, USA. The PtS_2 (Pt(IV) sulfide) powder (lot no. 2641593747-404) was certified as 99.95% pure on metals basis. The PdS (Pd(II) sulfide) powder (lot no. 3421593447-416) had a certified degree of purity of 99.9% on metals basis, with the principal possible metallic impurities given as Pt, Ag, Ru and Na (American Elements, 2015). The maximum possible amount of Pt and Ru in the PdS powder was 15 mg/l (ibid.).

5.2.2. Experimental approach and sample preparation

Experiment 1 (longer)

The chromitites of the Thaba Mine have undergone oxidation in certain areas, forming a thin vertisol which is typical for the semi-arid conditions under which it formed (Ahmad, 1996; Dudal, 1963). Oppermann et al. (2017) noted that only A and C horizons are present in these soils, and that the concentration of humic acid was found to lie between 0.003-0.46 g/kg in all their analyzed samples. The first experiment of our study was designed to reflect these conditions, with relatively low concentrations of humic acid. The experiment was designed with the same conditions as those described in Kotzé et al. (2019). Three solutions of humic acid were prepared at concentrations of 0.1, 1 and 10 mg/l. Approximately 4 g of the original chromite concentrate (coarse-grained) as well as the crushed concentrate (fine-grained) were placed in 240 ml Savillex® teflon beakers, and covered by 240 ml of HA solution. The solutions were

kept at ambient temperature, and were only gently moved when sampling, to avoid abrasion and to help simulate a natural soil environment. Since humic acid can decay by photolysis, (e.g., Strome and Miller, 1978) the containers were stored away from sunlight. The starting pH of all HA solutions was 7-8, and the pH was not buffered or otherwise modified. Five aliquots of 4 ml each were taken during the course of the experiment, after 5-7, 63-65, 89-91, 148-150, and 306-308 days. In the initial stages of the experiment, aliquots were taken more frequently, since it was expected that reactions would take place more rapidly due to initial disequilibrium between the chromitite and solution. As a control experiment, 2 g of the original chromite concentrate was placed in a beaker with 50 ml pure water. This control reactor was sampled at the same frequency as the main experiment, and 1 ml of solution was taken for each aliquot.

Experiment 2 (shorter)

This experiment was set up to investigate the first stages of Experiment 1 in detail. For this experiment, a tailings sample was also available. Since the lack of PGE in the chromite concentrate could be due to PGM escaping into the tailings, it was proposed that the tailings material might be more successful in concentrating PGE when reacted with humic acid. For this reason, the chromite tailings sample, crushed to <200 µm, was reacted with two concentrations of humic acid (10 and 1000 mg/l).

Experiment 3 (synthetic material)

This experiment was set up in order to observe the effect of strong concentrations of humic acid on PGE minerals (PGM) without chromite. For this experiment, the PGM needed to be present in large amounts to determine if Pd and Pt could be mobilized by humic acid when they are present in excess.

The 10 mg/l HA solution was prepared using the same synthetic humic acid powder as previously described. 1 g of the crushed tailings sample was placed in a 60 ml Savillex® teflon beaker, and covered with 50 ml of 10 mg/l HA solution. Then, 1 g of the MNR chromite concentrate crushed to <100 µm, 1 g of the crushed tailings sample, 0.5 g PdS powder and 0.5 g PtS powder were each placed separately in 60 ml Savillex® teflon beakers. They were each covered with 50 ml 1000 mg/l HA solution, respectively.

This experiment was sampled at shorter intervals compared to the initial experiment, since it was assumed that stronger concentrations of humic acid would result in faster reactions. An aliquot of 1 ml was removed from each of the 5 beakers after 2, 9, 24 and 49 days.

Sample preparation

All samples from both experiments were prepared for analysis by ICP-MS (see below) using different steps. Initially, the aliquot of solution was placed in a Savillex® Teflon beaker to which 5 ml H_2O_2, (30%, Suprapure, Merck, Germany), having been diluted to 10%, was added. The open beaker was then allowed to evaporate overnight upon a hot plate set to 90 °C. The residue after evaporation was subjected to a further treatment with 5 ml of aqua regia at 80 °C overnight in the closed beakers before being opened to evaporate. This yielded a white residue which was then dissolved in 1 ml of 1 M HNO_3. This solution was further diluted in 3% HNO_3 + 5 µg/l Rh for analyses via ICP-MS (see below). All employed acids were purified by distillation of pro analysis grade acid at sub-boiling conditions.

Both of the above described experiments were drained after the last aliquot was taken, by removing the solution from the beakers. The solid residue of each beaker was dried at about 50°C on a hot plate in Savillex® beakers until all moisture had evaporated. These residues were then investigated for textural features and major compositional changes as grain mounts at the Bundesanstalt für Geowissenschaften und Rohstoffe (BGR) in Hannover, employing a

Bruker Quantax SEM-EDS system at a low vacuum with an accelerating voltage of 25 kV and a working distance of 12 mm. Qualitative compositional measurements of the remaining substrate were carried out using these conditions, in order to determine if any change in composition had taken place during the experiments. For the sulfide residues, Pt, Pd and S were analyzed and approximate Pd:S and Pt:S were determined. For chromitite (and tailings) residues, O, Mg, Al, Si, Ca, Ti, Cr and Fe were analyzed. The approximate ratio of Cr to total Fe was determined. Silicon and calcium contents were measured to ensure that the analyzed mineral was in fact chromite and not a silicate mineral (chromite can only contain trace to minor amounts of these elements, while they are major components of associated silicates).

5.2.3. Analysis of solutions by mass spectrometry

All solutions sampled from the experiments described above were analyzed using the Thermo-Scientific Element-XR fast scanning-sector field-ICP-MS (inductively coupled plasma mass spectrometer) at the Institute of Mineralogy, Hannover. All elements except for ^{52}Cr and ^{53}Cr were analyzed in low-resolution mode; because of known interferences with Ar species, Cr was analyzed in medium resolution, at which the Cr mass peaks could be distinguished from those of $^{36}Ar^{16}O$, $^{38}Ar^{14}N$ and $^{36}Ar^{16}O^{1}H$. Custom calibration solutions were prepared from ICP-MS stock laboratory solutions of 1000 mg/l from Alfa Aesar, Germany. Three calibration solutions were prepared with concentrations of 0.1 µg/l, 1 µg/l, and 10 µg/l, respectively, of the elements Ru, Pd, Pt, Rh, Ir, Te, and Cr in a matrix of 3% HNO_3 prepared from pure water and distilled ~15 M HNO_3. A 1000 mg/l Rh solution (Certipur®) was used to prepare an internal standard solution of 5 µg/l Rh. The three standard solutions were used to set up a calibration method for sample analyses.

The measurements were carried out via an automated system (SC-2DX autosampler, Elemental Scientific, Germany), connected to a teflon nebulizer that introduced the sample aerosol at a rate of ±100 µL/min into a double-pass quartz glass spray chamber (Scott design,

Thermo-Scientific). A jet-type sampler cone and x-type skimmer cone made of Ni (Thermo-Scientific) were installed to improve signal intensity and to obtain accurate results in the concentration range of 0.01-10 µg/l. Random duplicate sample analyses were included to assess accuracy and precision of measurements in each sample run. Each sample was measured at least three times to calculate average concentrations and to determine the reproducibility of the analyses.

The HA powder used for the above experiments contains detectable amounts of Y, Zr, and Hf (as determined by analysis of a blank sample containing only a solution of the humic acid powder). Yttrium and zirconium can also both be found as trace elements at variable absolute amounts in the rocks of the BIC, including chromitites (e.g. Cawthorn & McCarthy, 1985). These two elements can be present as mass interferences on Pd isotopes due to formation of Y and Zr oxides in the argon plasma (e.g. $^{89}Y^{16}O$, $^{90}Zr^{16}O$). Hafnium may cause interferences on the signal of Pt isotopes for the same reason. Strontium is found in slightly higher values as a trace element in BIC chromitites, but of the six stable Pd isotopes, ^{102}Pd and ^{104}Pd were not considered for calculation of concentration because of the likely presence of Ru in the starting chromitites, and the likeliest interference of Sr would be on ^{104}Pd (as $^{88}Sr^{16}O$) (Thomas, 2002). However, on mass ^{105}Pd, the oxide $^{89}Y^{16}O^+$ may occur during analyses, and on mass $^{106}Pd^+$, $^{89}Y^{17}O^+$ may also be present (but at a lower rate because the natural abundance of ^{17}O is only 0.04%). Furthermore, $^{90}Zr^{16}O^+$ also may appear on the signal of $^{106}Pd^+$. For the signal of $^{108}Pd^+$, only $^{92}Zr^{16}O^+$ has a potentially significant high abundance. Because of their highest relative abundance, ^{105}Pd (22.3 %), ^{106}Pd (27.3 %) and ^{108}Pd (26.5 %) were measured in order to calculate the Pd concentration in the solutions. The signal of $^{194}Pt^+$ is interfered by $^{178}Hf^{16}O^+$, and similarly, $^{195}Pt^+$ is affected by the presence of $^{179}Hf^{16}O^+$ (see e.g. Köllensperger et. al., 2000; Thomas, 2002; Bencs et. al., 2003, and Meisel et. al., 2003 for further details regarding the effect of oxide formation on Pd and Pt during ICP-MS analysis). In order to correct for the interferences caused by Y, Zr and Hf, solutions containing purely these ele-

ments at concentrations of 1 µg/l and 10 µg/l (prepared from Certipur® 1000 mg/l Y, Zr, and Hf solutions, respectively) were analyzed along with the samples in each analytical run. The signals measured for each concentration of Y, Zr, and Hf and those on the masses 105, 106, 108, 194, and 195, respectively, were used to calculate the formation rate of the relevant elemental oxides. This "oxide contribution" to each isotope was then subtracted from the total signal intensity of each Pd and Pt isotope. These numbers were verified by comparing natural isotopic abundance ratios (as given by Berglund & Wieser, 2011) to the measured and oxide corrected isotope ratios. The elemental concentrations were then calculated from the oxide-corrected isotope signals. It was found that the total contribution of Hf to Pt isotope signals was close to zero; however, the contribution of Y and Zr to the signals of ^{105}Pd, ^{106}Pd and ^{108}Pd was significant, especially regarding ^{106}Pd and ^{108}Pd, indicating a possible concentrated Zr contribution from chromite. After calculation and removal of the Y and Zr contribution to each of these isotopes, the isotopic ratios of ^{105}Pd, ^{106}Pd and ^{108}Pd agreed with the natural ratio.

5.3. Results

5.3.1. Experimental residues

Figure 5.2 shows experimental residues of selected chromitite material as well as PdS and PtS_2. Some chromite grains appear to have developed a partial coating of material that appears darker in BSE images. The composition of this coating could not be determined. No compositional changes were detected in the chromite grains subjected to qualitative analysis; the ratio of Cr to total Fe was ~1.5 on average both before and after the experiment. PdS also showed no compositional changes, while PtS_2 was changed to PtS. The tailings residues show unchanged chromites in a matrix of fine-grained material which consists of a mixture of silicate minerals, including primary silicate minerals associated with chromitite (pyroxene, plagio-

clase) as well as phyllosilicates and possible clay minerals generally associated with alteration of pyroxene and plagioclase.

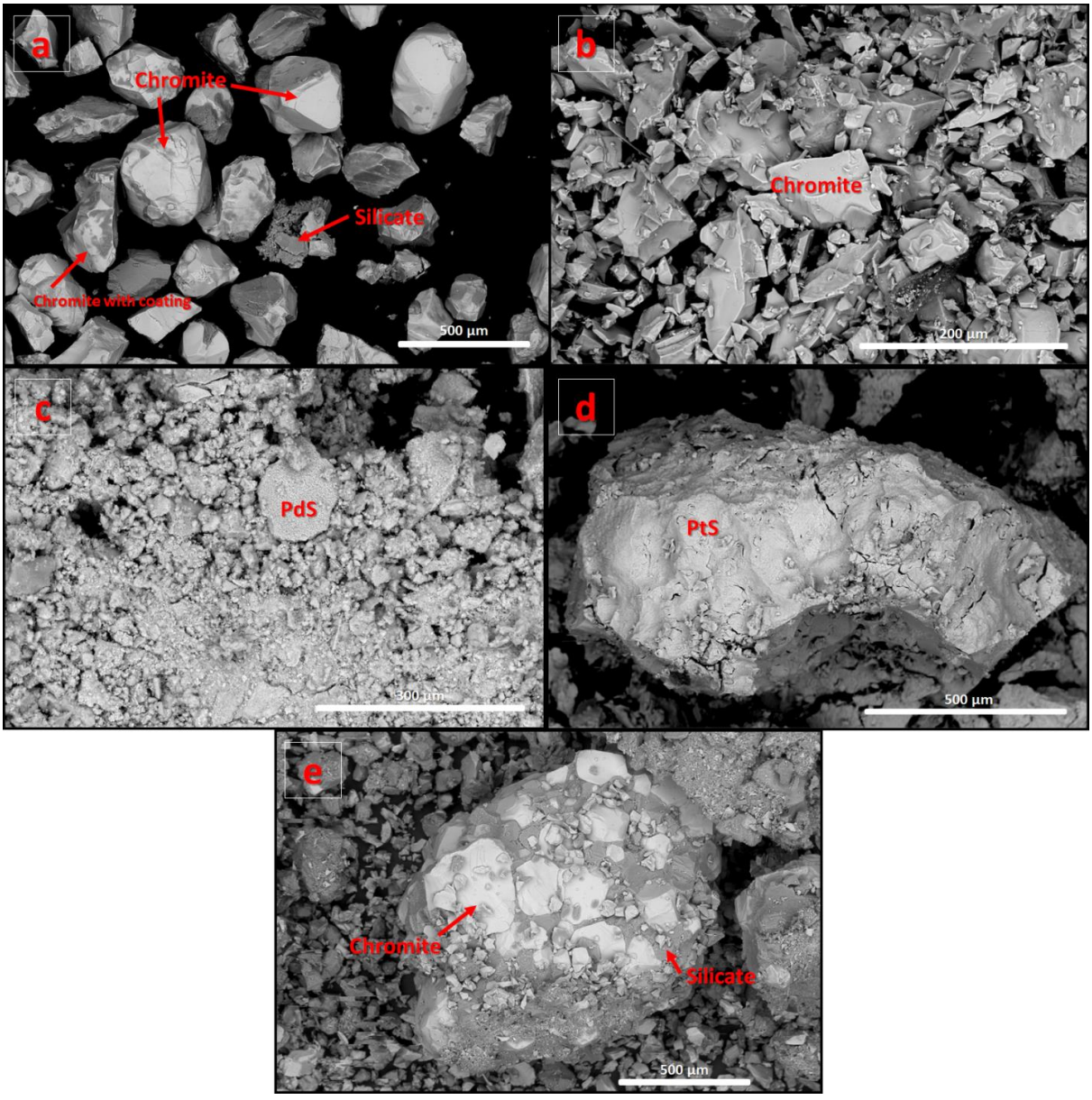

Figure 5.2: (a): Chromite concentrate after reaction with 10 mg/l HA. (b): Crushed chromite concentrate after reaction with 0.1 mg/l HA. (c): PdS after reaction with 1000 mg/l HA. (d): Platinum sulfide after reaction with 1000 mg/l HA. (e): Chromite tailings after reaction with 1000 mg/l HA. All pictures imaged with BSE.

5.3.2. Solutions

Experiment 1

The results of solution analyses for the initial, long-running experiments are shown in Figure 5.3 and 5.4. The data used to produce these figures are given in Table 8.4 of the Appendix. Figure 5.3a-d depict the results for the unaltered chromite concentrate. Figure 5.4a-c depict the results for the crushed chromite concentrate. In each figure, Pd and Pt values are compared with values obtained for Cr. An average analytical error of about 10% (as calculated using reported standard deviation plus the average error for the calculations described above) is depicted with error bars in each graph. The error bars are offset horizontally for the sake of readability.

Referring to the coarse chromite concentrate in the three HA solutions, (Fig. 5.3a-c) Cr behaves similarly in each solution. The total value of Cr dissolved by the end of the experiment is only slightly more than 10 µg/l. Cr rises slightly after about 70 days of reaction, after which it falls to a minimum of about 5 µg/l after about 150 days. In the final aliquot at about 310 days, Cr rises again, reaching its maximum value.

In the 0.1 mg/l HA solution, Pt and Pd both never rise above 1 µg/l. Pt falls from ~0.3 µg/l after about 5 days, to ~0.2 µg/l after about 310 days. Pd rises from ~0.01 µg/l after about 5 days, to ~0.36 after about 310 days. Both Pd and Pt fall slightly after about 70 days of reaction, only to rise in the next aliquot at ~90 days and fall again after ~150 days.

In the 1 mg/l HA solution, Pt is mobilized about 100x compared to Pd at the beginning of the experiment, (~5 days) and about 10 times by the end of the experiment (~310 days). Pt reaches a maximum of ~2 µg/l at about 50 days, after which it falls to a final value of ~0.8 µg/l. Pd rises from ~0.01 µg/l at about 5 days, falling in the next aliquot, to ~0.03 µg/l at about 90

days. It falls again at ~150 days, but rises to its maximum value of 0.1 µg/l after about 310 days.

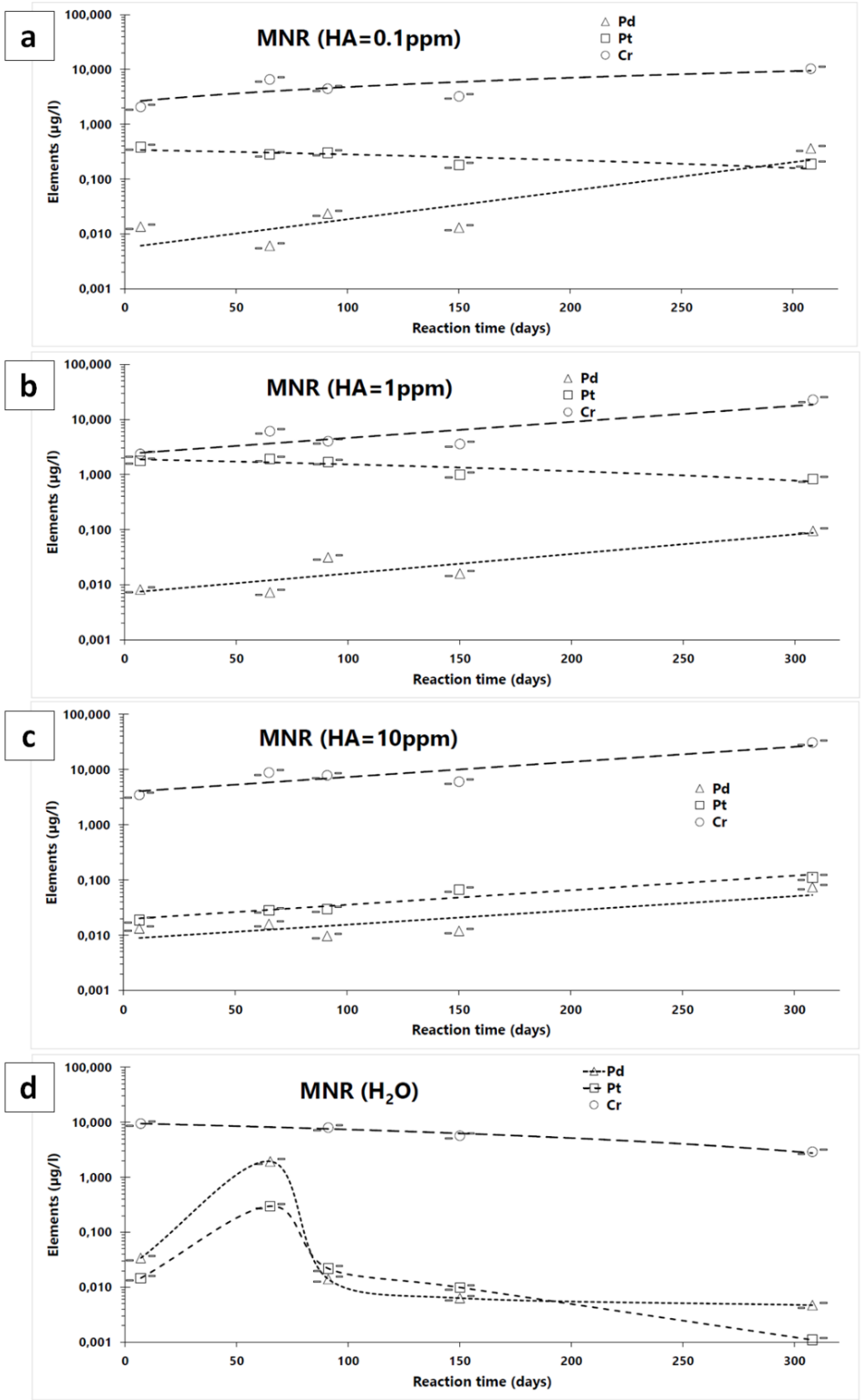

Figure 5.3: Solution results for uncrushed chromite concentrate.

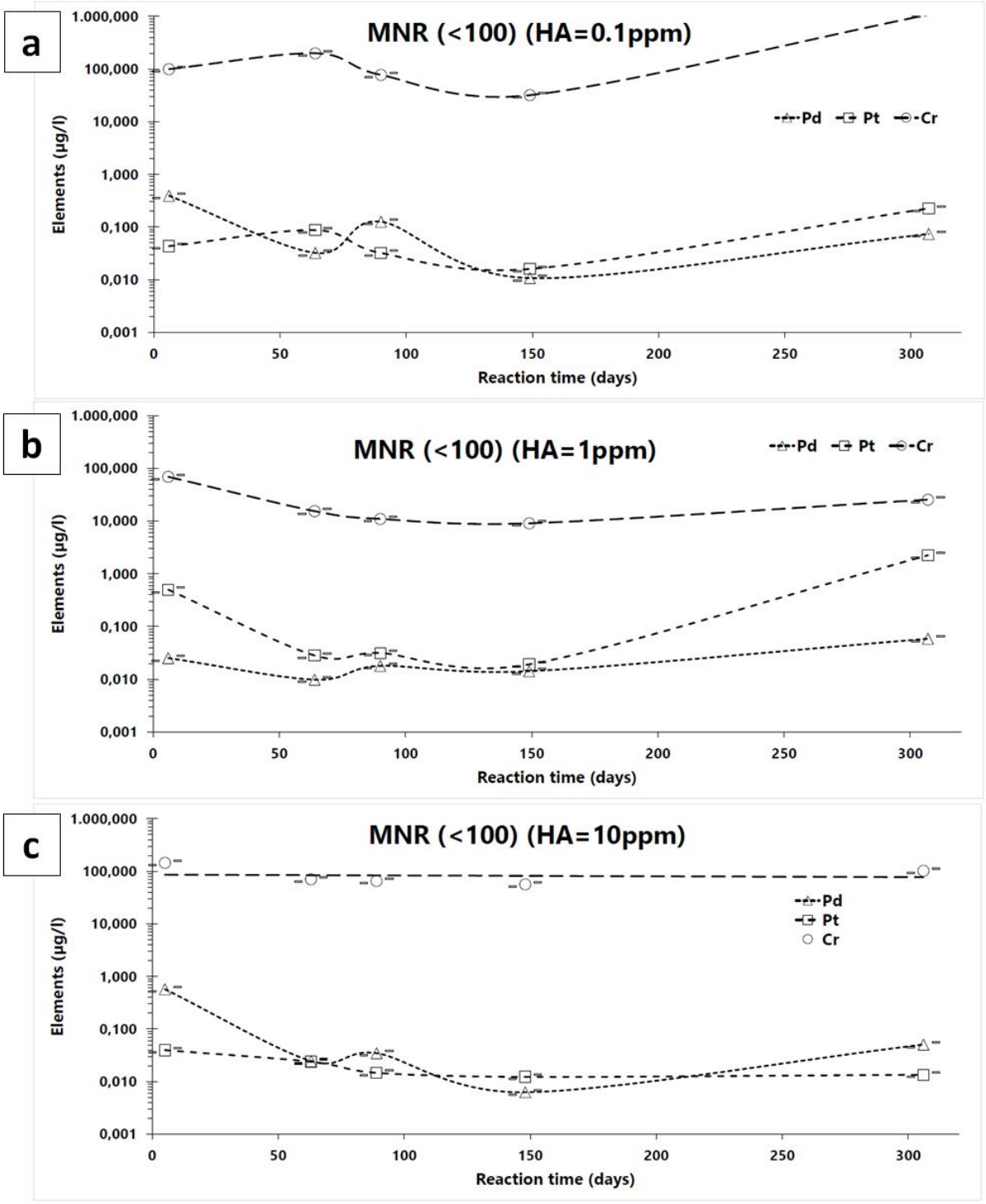

Figure 5.4: Solution results for crushed chromite concentrate.

In the 10 mg/l HA solution, both Pt and Pd constantly lie at or below 0.1 µg/l, but both elements show a gentle rise from ~0.02 µg/l at about 5 days, to ~0.1 µg/l at about 310 days.

In the control experiment with no HA, (only pure water) Cr decreases slightly from ~10 µg/l at about 5 days, to ~6 µg/l at about 310 days. Both Pt and Pd behave similarly, rising to a

maximum value of ~2 µg/l for Pd and ~0.3 µg/l for Pt at about 70 days, but falling sharply thereafter to values below 0.01 µg/l after 310 days.

Compared to the uncrushed chromite concentrate, Cr of the crushed chromite concentrate is taken into solution at values of about ten times higher (Fig. 5.4a-c). All three concentrations of humic acid solution show an initial high value of Cr of about 100 µg/l at ~5 days which decreases after ~70 days. In both the 1 and 10 mg/l HA solutions, Cr reaches a minimum at ~150 days (~9 µg/l for 1 mg/l HA, ~55 µg/l for 10 mg/l HA) and then increases after ~310 days (to ~26 µg/l for 1 mg/l HA, and ~100 µg/l for 10 mg/l HA). In the 0.1 HA solution, Cr also reaches its minimum value after ~150 days (~30 µg/l) but then increases by an order of magnitude (over 1000 µg/l) after ~310 days. Pt and Pd show very similar trends in all 3 solutions of humic acid, showing initial high values at ~5 days which then decrease in the next 3 aliquots only to increase again after ~310 days. Only Pt in the 1 mg/l HA solution shows a value higher than 1 µg/l after ~310 days.

Experiments 2 and 3

The results of solution analyses for the shorter, follow-up experiments are shown in Figure 5.5–7. The data on which these figures are based may be found in Table 8.5 of the Appendix. Figure 5.5 depicts results for the crushed chromite concentrate MNR60. Similarly to the longer-term experiments on the crushed concentrate, the Cr content in Fig. 5.5 remains more or less the same at ~100 µg/l. However, Pd and Pt both show an initial maximum value of ~5 µg/l after 2 days of reaction. This initial high value drops after 9 days of reaction, to ~0.7 µg/l for Pd and lower (~0.3 µg/l) for Pt. Pt increases again slowly for the rest of the experiment, reaching a value of ~0.5 µg/l after 49 days of reaction. Pd increases after 24 days and decreases again at 49 days, but is still higher than Pt (~2.5 µg/l) by the end of the experiment. The values obtained with 1000 mg/l HA, despite having a much shorter reaction time, are about an order of magnitude higher than those obtained with lower concentrations of humic acid.

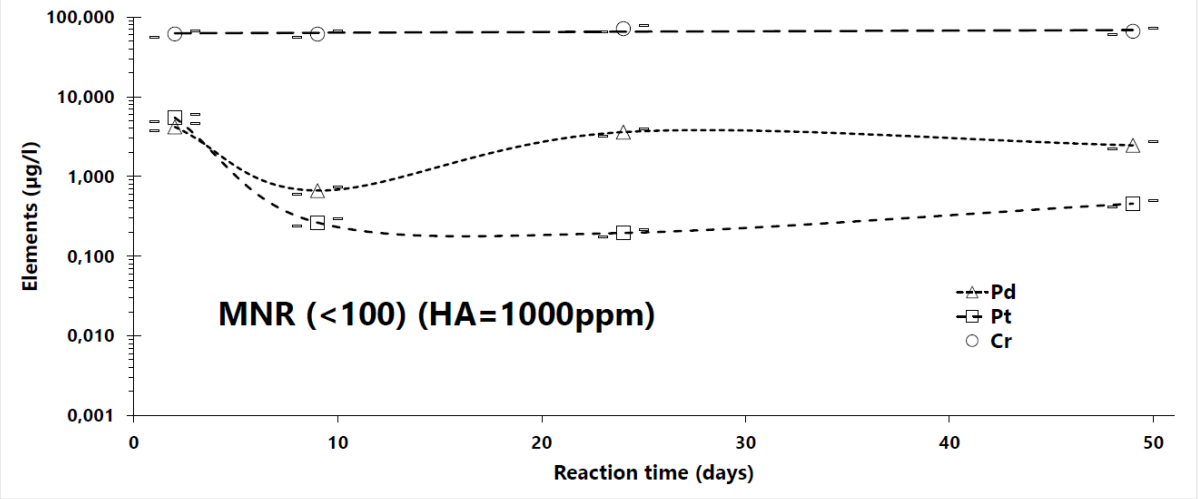

Figure 5.5: Results for crushed chromite concentrate after reaction with 1000 mg/l HA.

Figure 5.6 shows solution results for the chromite tailings material, after about 50 days of reaction with (a) 10 mg/l HA and (b) 1000 mg/l HA. In the 10 mg/l HA experiment, Cr is still increasing by the end of the experiment, reaching a final value of ~45 µg/l. In the 1000 mg/l HA experiment, Cr remains between 35-50 µg/l for the whole of the experiment. For the 10 mg/l HA experiment, Pt shows an initial high value of ~2 µg/l after 2 days of reaction, which then decreases to ~0.01 µg/l after 24 days. After 49 days, a slight increase of Pt is seen for a final value of ~0.06 µg/l. Pd reaches a similar maximum value of ~2 µg/l after 9 days of reaction, after which it drops (by less than Pt) to a value of ~0.3 µg/l after 49 days of reaction. In the 1000 mg/l HA experiment, Pt reaches a higher maximum value (~9 µg/l) after 9 days of reaction, after which Pt values drop off, reaching a minimum value of ~0.1 µg/l at the end of the experiment. Pd initially has a value of ~1.2 µg/l after 2 days of reaction, which increases to a maximum of ~2.2 µg/l after 24 days, and then decreases to ~0.5 µg/l after 49 days of reaction.

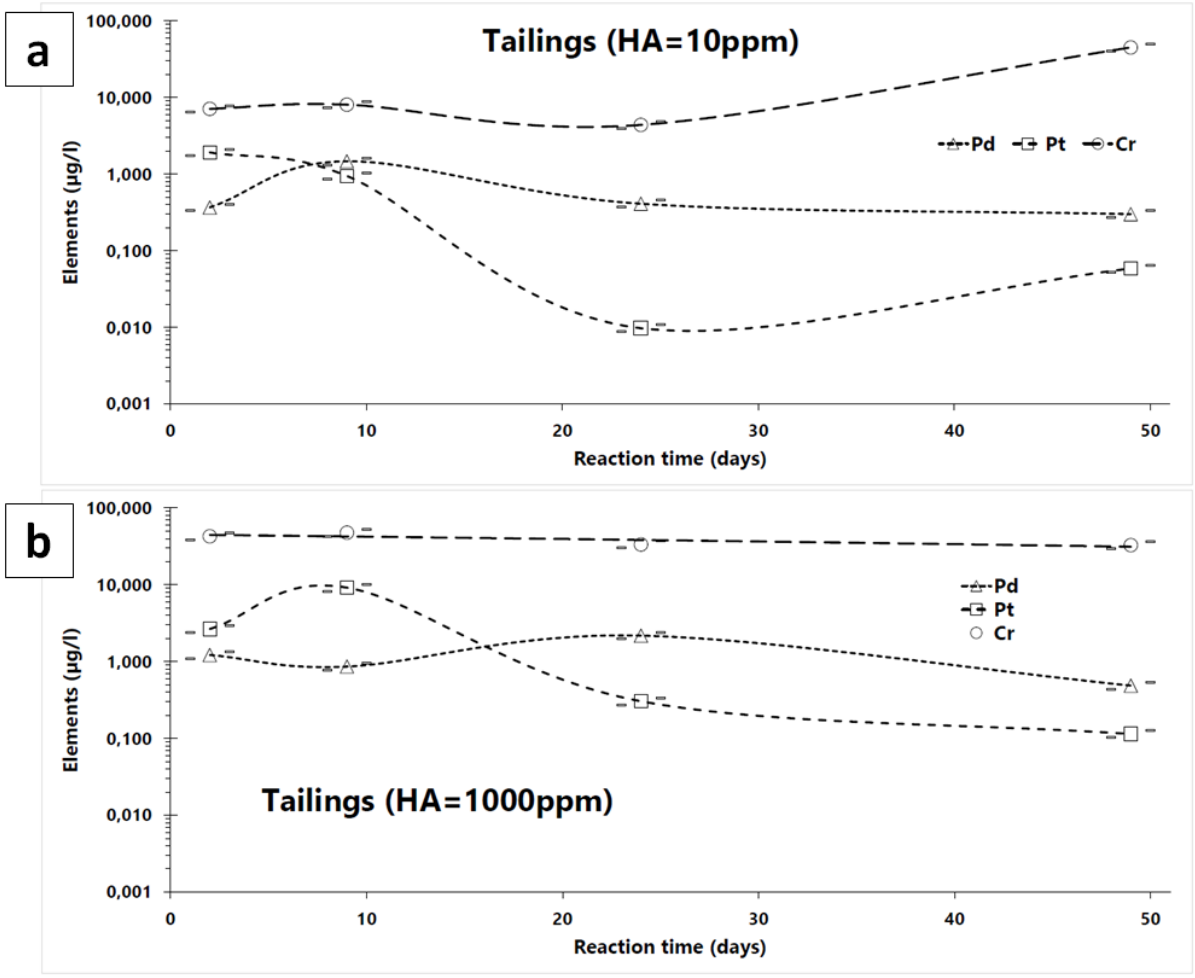

Figure 5.6: Solution results for tailings material after reaction with (a): 10 mg/l HA and (b): 1 000 mg/l HA.

Figure 5.7 shows the results of PdS and PtS after reaction with 1000 mg/l HA. It must be noted that the two solution series depicted in Fig. 5.7 were in different beakers, one containing only PtS and the other containing only PdS. Pt from PtS and Pd from PdS both show bell-shaped patterns across time, but in opposite directions. Pd is mobilized from PdS at an initial concentration of almost 15000 µg/l after 2 days of reaction, but drops down to only ~3000 µg/l after 24 days, after which it increases again to reach a final value of ~11000 µg/l after 49 days of reaction. Pt initially shows much lower levels compared to Pd and increases until the 24-day mark to a maximum of ~2000 µg/l, after which it decreases to ~900 µg/l after 49 days of reaction.

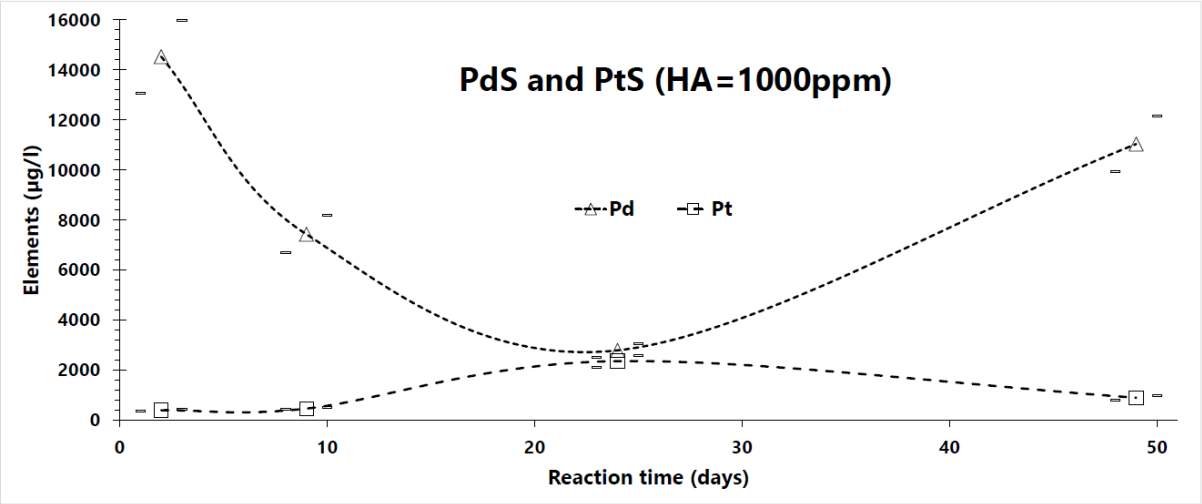

Figure 5.7: Solution results for PdS and PtS after reaction with 1 000 mg/l HA.

5.4. Discussion

As seen in Chapter 3, solutions of humic acid show a high amount of inherent variability of element mobilization, with mobilized Pd and Pt showing a wide range of possible values for identical solutions. This is especially to be expected in solutions with higher concentrations of humic acid (see the results of Chapter 3 compared to Chapter 4).

Mobilization of Pt and Pd from synthetic minerals

In the previous experiments with humic acid and synthetic PdS and PtS_2, (presented in Chapter 4) it was shown that humic acid in concentrations of 10 mg/l and below were sufficient to mobilize Pd and Pt. In Figure 5.8, the results of that study are compared with our results. Kotzé et al (2019) subjected the synthetic PGE powders to 320 days of reaction; only the trend for the first 50 days is shown in Fig. 5.8. It is clear that a higher concentration of humic acid causes Pt and Pd to be mobilized in greater amounts. Pd is about 100 times higher in our experiments compared to the lower concentrations of HA, while Pt is between 2 and 10 times higher. Platinum mobility is clearer lower than that of palladium.

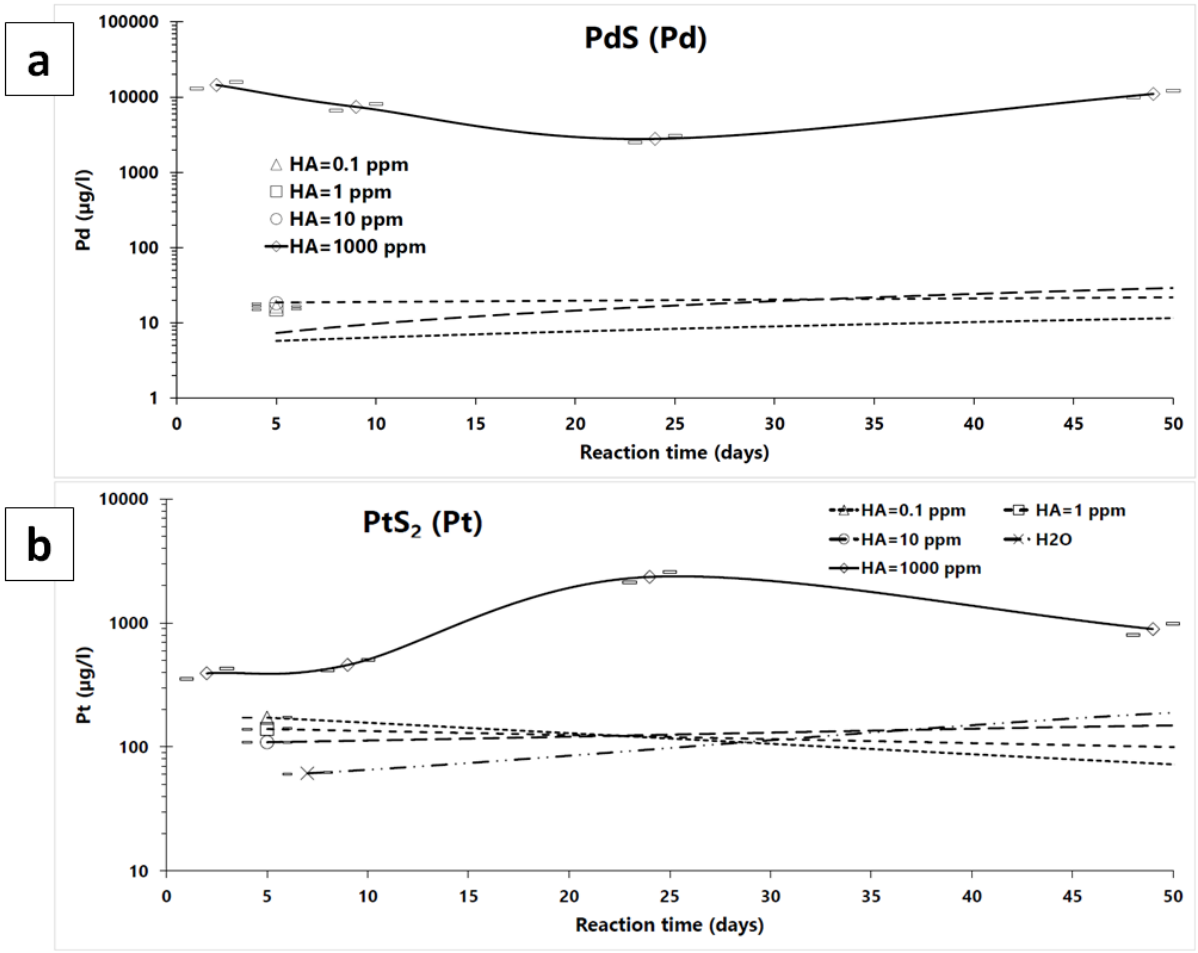

Figure 5.8: Comparison of the results of Pd and Pt mobility in this study with the long-term experiments of Chapter 4, which were carried out using the same substrates and lower concentrations of humic acid.

For the 50 days of reaction depicted in Fig. 5.8a, there is no drastic variation (in terms of orders of magnitude) for any of the different concentrations of humic acid. Since the three more diluted HA solutions continued to slowly increase in Pd over the whole experimental period, (see Chapter 4) we might expect similar behavior in this study; i.e. Pd will continue to increase over time, although not at a very rapid rate. The amount of Pd increase per day in a solution of 10 mg/l HA was calculated as only 0.5 µ/l (ibid.).

For Pt, a similar situation can be seen (Fig. 5.8b). The three solutions with lower amounts of humic acid varied in increase vs decrease of Pt after 50 days of reaction, while Pt in the 1 000 mg/l HA solution is observed to decrease. The starting pH of this solution was measured to be 10, but after 50 days of reaction, the pH of the solution exposed to PdS was 2.5 and the solu-

tion exposed to PtS_2 was 1.8. The solutions presented in Chapter 4 had a pH of about 8 at the beginning, and for both the PdS and PtS_2 solutions, the ending pH fell between 3.4 and 3.8. This change in pH probably took place because of hydrolysis of sulfur from the sulfide minerals and formation of sulfurous acid, as discussed in Chapter 4. The pH change in the solutions of this study was more drastic than in the previous study. A likely reason for this is that less water was added to the substrate powders of this study (only 50 ml, compared to 200 ml beforehand). More sulfur was likely also available from the PtS_2 molecule compared to PdS, explaining the bigger pH change in this solution. Under oxidizing conditions, Pt is considered to be mobile in water at pH <1 and >8 (Cabral et al., 2007). The starting pH and ending pH therefore both approach favorable conditions for Pt mobility, but the changing pH is not evident in the observed trends (Fig. 5.8b).

Dissolution of chromite

A study of Cr values in naturally occurring groundwater in the León Valley, Mexico (Robles-Camacho & Armienta, 2000) found up to 11.7 µg/l Cr in these waters, which is an unusually high concentration for natural waters. In the experiments previously described, the analyzed solutions resulting from crushed chromitite all had a roughly constant value of ± 100 µg/l Cr, whereas solutions resulting from whole chromitite contained 10x less Cr (± 10 µg/l). Naturally, the solutions from our experiments will contain more humic acid than what can be found in natural waters, but the fact that the value for whole chromitite is roughly the same as seen in water resulting from weathering of chromium-rich rocks (up to 11.7 µg/l) means that the Cr in our experiments could result only from interaction with water (no interaction with humic acid). The increased Cr values when chromitite was crushed indicate a faster mobilization of Cr due to a larger reactive surface on chromite grains; if chromitite has already undergone mechanical weathering, it can be taken into solution by water containing low amounts of humic acid. The concentration of humic acid was irrelevant with respect to those experiments

containing chromite concentrate; in all solutions, a maximum of ± 100 µg/l Cr was reached. However, with the experiments on chromitite tailings, (Figure 5.6) Cr was mobilized faster in the 1 000 mg/l HA experiment, compared to the solution containing only 10 mg/l HA. Only ~50 µg/l Cr was mobilized in the tailings experiments. The lower Cr concentrations in the tailings solutions are probably a consequence of the lower chromite (and thus also Cr) content in the tailings samples. The faster mobilization in the solution containing more HA indicates that HA plays a role in the mobilization rate of Cr. However, given that silicate minerals such as clinopyroxene and various phyllosilicates, which may naturally contain Cr as well, occur in greater amounts in the tailings material, the source of Cr may in fact be from silicate minerals rather than chromite. According to Garnier et al., (2008) all silicate minerals found in the studied soil overlying dunite rocks have been leached of their Cr, and this is the most probable source of Cr in soils; chromite weathers at a much lower rate than the silicates. Since the tailings sample also contains clay minerals, interaction of these with humic acid is likely (Liu & Gonzalez, 1999; Wang & Xing, 2004). These sources describe adsorption of humic acid onto the surfaces of clay minerals, and this process could have been active in the tailings solutions, possibly forming a Cr-clay-humic complex.

We can assume that all Cr present in chromite is in the oxidation state Cr(III), given the limitations of the spinel mineral structure (Barnes & Roeder, 2001). Associated silicate minerals are likely to have the same oxidation state of Cr. In this form, Cr is likely to be taken into solution by means of formation of the hydroxide complexes $CrOH_2^+$ and $Cr(OH)_3^0$, but is also readily mobilized as organic complexes (Richard & Bourg, 1991). It seems likely that the humic acid in our experimental solutions contributed to the mobilization of available Cr along with water, although it was not capable of leaching Cr from whole chromite grains. Once the silicate minerals associated with chromite have leached away at an advanced rate of weathering, the individual chromite grains will expose greater surfaces for weathering and thus Cr can be slowly mobilized (Garnier et al., 2008). This late-stage weathering of chromites would take

place in a soil environment, with exposure of the chromites to organic substances including humic acids. It is probably at this stage of the weathering process that humic complexes become an important factor in the weathering of chromitite lithologies.

The fate of palladium and platinum during weathering of chromitite

There was little difference seen in the Pt and Pd concentrations of crushed and uncrushed chromite concentrate (Figs. 5.3 and 5.4). After Pd and Pt were mobilized at ~1 µg/l in pure water, both fell rapidly to values close to the detection limit in subsequent aliquots (Fig. 5.3d). The weak humic acids, however, mobilized a maximum of just over 1 µg/l in all 6 solutions. In most of these, both Pt and Pd appear to be increasing slightly towards the end of the experiment. When subjected to reaction with 1 000 mg/l HA, the crushed chromite concentrate yielded a maximum of ~10 µg/l Pt and Pd to solution. For both Pt and Pd, this value dropped slightly in subsequent aliquots, then began to rise again. Pt and Pd do not appear to be greatly increasing in solution with time, but clearly higher concentrations of humic acid in solution encourage their mobilization. Crushing of the chromite concentrate increased the amount of Cr mobilized, but had no effect on Pt and Pd values, indicating that the majority of the Pt– and Pd-bearing minerals were not included in the chromite crystal lattice. For the chromite tailings, Pt and Pd reached maximum values of ~10 µg/l in the 1 000 mg/l HA solution and ~1 µg/l in the 10 mg/l HA solution. These values correspond closely to those for the chromite concentrate, indicating that there was little difference in PGM mineralogy between concentrate and tailings samples, or that the mobilization of Pt and Pd from these minerals at specific concentrations of HA reached their maximum value. Unlike the chromite concentrate solutions, the solutions exposed to the tailings sample appear to be decreasing for the duration of the experiment. A possible explanation for this is the presence of clay mineral aggregates in the tailings sample (see Fig. 5.2e). Humic acid may be adsorbed onto clay particles, which

may effectively cause the withdrawal of humic acid particles from solution, (Wang & Xing, 2005) taking any complexiated Pt and Pd out of solution as well.

5.5. Conclusion

Our results indicate that advanced weathering of chromitite is not necessary in order to liberate Pt– and Pd-bearing minerals and expose them to the weathering environment. Breakup of the original rock due to weathering of less-resistant silicate minerals would be sufficient to expose these PGM to leaching. Crushing of the chromite concentrate sample resulted in more Cr being mobilized, but the concentration of humic acid had no effect on chromium concentration. Platinum and palladium, however, were mobilized in greater amounts with concentrated humic acid (1 000 mg/l) compared to diluted humic acid (0.1-10 mg/l). The humic acid solutions are capable of keeping Pt and Pd in solution, unlike pure water, in which these two elements are initially taken into solution but then precipitated over a period of time. Palladium was found to be slightly more mobile than platinum. High concentrations of organic reagents in the natural weathering environment could lead to increased leaching of Pt and Pd through formation of organometallic complexes.

6. General discussion, conclusions and outlook for further studies

6.1. Discussion: Comparison of results from the three experimental series

6.1.1. Palladium tellurides

The short-term experiments (Chapter 3) showed that when subjected to reaction with palladium tellurides, humic acid is unlikely to mobilize Pd in significant amounts. Tellurium was preferentially mobilized rather than Pd, the total amount depending on the Pd:Te mineral ratio (more Te was mobilized from palladium ditelluride, compared to monotelluride). Pure water mobilized around ~ 1 500–2 000 µg/l Te in these experiments. Although the humic acids did mobilize some Pd, there was not a great difference between the HA solutions and water. Palladium showed a clear preference for remaining in the mineral residue.

The long-term experiments (Chapter 4) largely confirmed these results. An unexpected addition was the discovery of precipitated Te in the form of tellurium oxide crystals. Palladium was not significantly mobilized from the solutions of diluted HA, while after ~300 days, the water-control experiment mobilized ~9 µg/l Pd, which falls within the range of Pd values mobilized by water in the short-term experiments. The concentration of HA was found to play a role in mobilization of Te, particularly from PdTe. After ~300 days of reaction, Te was still increasing in the 10 mg/l HA solution, whereas it had begun to decrease in the 1 and 0.1 mg/l HA solutions. Fewer tellurium oxide crystals were found in the residues of this experiment, compared to the others, indicating that Te was not being actively precipitated. Te reached a maximum of ~2 800 µg/l in solution with 10 mg/l HA from $PdTe_2$, and lower values with the other two humic acid concentrations. Water was even lower, at ~600 µg/l. In the short-term experiments, water mobilized almost 4 times as much Te. It seems that over a long period of time, even low amounts of humic acid are capable of keeping tellurium in solution at higher

values compared to pure water. With the short-term experiments at a much higher concentration of HA, (~22.6 g/l) more Te was also mobilized (up to 10 000 µg/l for $PdTe_2$). Due to the presence of HCl in these experiments, however, it cannot conclusively be said that the humic acids were responsible for the high mobilization of Te, when anorganic chloride complexes could also be responsible. If Te is being transported as an organic complex, the lower pH of the short-term experiments clearly does not inhibit the formation of such a complex, indicating that it could be stable over a wide range of conditions.

The main finding of the long-term experiments, that the weathering of Te from these and similar minerals could result in upgrading of Pd in the weathering environment, is supported by the results of the short-term experiments.

6.1.2. Pd and Pt sulfide

The short-term experiments (Chapter 3) showed that hydrolysis of the sulfide molecule played a major role in the mobilization of Pd and Pt. Platinum was more mobile than palladium under the conditions of the short-term experiments, possibly because of its affinity for chloride complexes resulting from the HCl used in these experiments to fix pH. Platinum reached a maximum of ~1 300 µg/l in the humic acid solutions, compared to only ~700 µg/l for Pd.

The results of the long-term experiments (Chapter 4) confirmed that hydrolysis of sulfide had indeed taken place, and showed a marked difference in the behavior of Pd and Pt compared to the previous experiments. The total amount of Pd and Pt mobilized was much lower, but organic complexes are more likely to have been responsible for mobilization (compared to the previous experiments, where chloride complexes were probably responsible). Platinum mobility over time corresponded well with a change in pH caused by hydrolysis of sulfur. Palladium increased steadily with time, showing the highest amounts (~160 µg/l) with the strongest concentration of humic acid.

The final experiments ("Experiment 3" of Chapter 5) confirmed that it was likely that Pd and Pd could be mobilized by organic complexes at these experimental conditions, probably after hydrolysis of sulfide. About 10 000 µg/l of Pd and 1 500 µg/l Pt were mobilized by these experiments, showing a higher mobility of Pd over Pt. Because of the lower volume of fluid involved in these experiments, the lowering of pH due to hydrolysis was more extreme, and this probably caused Pt to remain mobile, since Pt is generally considered to be mobile in water at surficial conditions when the pH is above 8 and below 1 (Cabral et al., 2007). A notable effect of the humic acids regarding Pt in the long-term experiments was to slow down precipitation in conditions unfavorable for mobility. With a greater amount of humic substance present, this effect probably also helped prevent Pt precipitation with changing conditions in the final experiments.

Although the results for Pd and Pt seen in the short-term experiments were most likely produced by chloride complexiation, the subsequent experiments showed that the humic substances are indeed capable of mobilizing Pt and Pd. When chlorine is not present, Pt is less mobile than Pd. This agrees with studies that have found that under surficial weathering conditions, Pt tends to accumulate in soils, whereas Pd is removed from the environment (e.g. Traoré et al., 2006; Cabral et al., 2007). Chloride complexiation may be of interest under conditions where PGE minerals react with highly acidic and saline surface waters, and both Pd and Pt seem to show a preference for the chloride complex over an organic complex under such conditions. The high values seen in the final experiments, however, indicate that organic complexes may mobilize Pd and Pt efficiently when Cl is not present, over a range of pH conditions.

6.1.3. Chromitite

The short-term experiments (Chapter 3) showed that there was little difference in the trends of Cr, Pd or Pt between the original chromitite concentrate and the crushed chromitite concen-

trate, save for the possible loss of PGM due to crushing. The amount of Pt mobilized was less than 1 µg/l, while Pd was mobilized by HAP up to ~10 µg/l. There was a clear difference in trends for the humic acids versus pure water for all three elements; in all cases, the humic acids produced a higher mobilization. Palladium showed different trends for the two different humic acid types, (HASS and HAP) showing that the type of organic compound is relevant in Pd mobility. Chlorine was also present in these solutions, as with the synthetic minerals, but the low Pt values when compared to Pd indicate that chloride transport may not have been relevant, at least for Pt. This could be because the pH remained stable at 3-3.5 throughout the duration of the experiments. It is still possible that the mobility we see in these experiments was (partly) due to chloride complexiation rather than an organic complex, even with Pd.

The long-term experiments on chromitite (Chapter 5) showed that the crushed chromitite liberated more Cr, but there was no difference in Pd and Pt values between whole and crushed chromitite. Palladium and platinum values were very similar in these experiments, suggesting that the fixed pH of 3–3.5 in the previous, short-term experiments inhibited Pt mobility. The pH of the long-term solutions remained stable throughout the duration of the experiment at about 8, at which value Pt is considered mobile in water under surficial conditions. The long-term experiments did not mobilize as much Cr or Pd as the short-term experiments, but Pt was higher. The long-term experiment carried out with whole chromitite and pure water (Fig. 5.3d) only mobilized ~10 µg/l Cr, which was the same value for the humic acid solutions in these experiments. In comparison, water in the short-term experiments mobilized ~200 µg/l Cr, irrespective of whether the chromitite was crushed or whole. This indicates that the shaking of these experiments promoted chromium mobility and sped up the dissolution reactions.

The final experiments carried out on chromitite tailings material (Chapter 5) showed little difference when compared to the chromitite concentrate. A similar amount of both Pd and Pd was mobilized by both concentrations of humic acid, and this value was similar to the Pd and

Pt mobilized in chromitite concentrate experiments. Chromium showed differences depending on humic acid concentration, supporting the idea that it may be mobilized by an organic complex. The final experiment of 1 000 mg/l HA carried out on a sample of crushed chromitite concentrate, however, showed the same value of Cr as the previous chromitite concentrate experiments. It is likely that the chromium of the tailings material is in a more available form (i.e. not bound in the chemically resistant chromite mineral structure; possibly part of the associated silicate minerals found in the tailings material). Pt and Pd were mobilized in greater amounts with a greater concentration of humic acid, supporting the idea that these elements can be mobilized by organic substances.

6.2. Conclusions

Pd and Pt can be mobilized from PGE-bearing minerals by humic acids, although the total mobilization depends not only on the concentration of humic acid but also the mineral type (e.g. telluride vs. sulfide). Palladium is more easily mobilized by the humic acids than platinum. The mobility of platinum under simulated surficial conditions depends largely on the pH of the reacting solution, whereas Pd is mobile under a range of pH conditions. Compared to pure water, the humic acids mobilize Pd in greater amounts, and also Pt at a pH of above 8. The humic acids also slow down precipitation of Pd and Pt when conditions become unfavorable for mobilization; this can be seen by a gentler variation in Pd and Pt content over time when compared to water. Experiments on chromitite concentrate and tailings broadly reproduce results seen for synthetic PdS and PtS_2, with smaller absolute amounts of Pd and Pt. The results from the experiments on synthetic material agree with observations made on oxidized PGE deposits, namely that Pd and Pt can be precipitated at low temperatures as oxide or hydroxide minerals, that less mobile metals such as Pt can be upgraded in the weathering environment due to selective leaching of Pd, and that the palladium-platinum telluride minerals are destroyed in the weathering environment due to leaching and dispersion of Te. The exper-

iments on chromitite concentrate and tailings show that chromitite does not have to undergo an advanced stage of weathering in order to liberate PGE to the environment. Any PGM not bound inside chromite have the potential to be leached when the interstitial silicate minerals of the chromitite break down, and palladium and platinum can be mobilized by water and organic material, although with some mineral types, (tellurides) they are likely to preferentially remain in detrital minerals.

6.3. Outlook for further studies

The experiments done in this study have produced a wealth of information, and yet they have raised as many questions as they have answered. The exact nature of the PGE-organic complex has yet to be constrained, and a further question remains as to the role of microbial intervention in soil processes pertaining to the PGE, as mentioned by Cabral et al. (2011). The role of the humic substances in transport of other metals is also a potential new field of study to explore. This study revealed a great affinity of Te for the humic acids, which has not been studied in depth. Metals such as Au, Ag, and the other PGE may also reveal interactions with organic reagents. With analytical technology being capable of reporting values of metals well below 1 µg/l, new interactions between metals and natural organic material may yet be revealed. This study, along with others, may be important to the perspective of those who would study all aspects of the ore-forming system.

7. References

Ahmad, N. (1996). Chapter 10: Management of vertisols in rainfed conditions. In: Ahmad, N. & Mermut, A. (eds.), Vertisols and technologies for their management. Developments in soil science 24: 363-428. https://doi.org/10.1016/S0166-2481(96)80012-2.

Aiglsperger, T., Proenza, J. A., Zaccarini, F., Lewis, J. F., Garuti, G., Labrador, M. & Longo, F. (2015). Platinum group minerals (PGM) in the Falcondo Ni-laterite deposit, Loma Caribe peridotite (Dominican Republic). Mineralium Deposita 50: 105-123. https://doi.org/10.1007/s00126-014-0520-9.

American Elements (2015). Certificate of Analysis: PdS and PtS_2. Merelex Corporation, 10884 Weyburn Ave., Los Angeles, CA 90024, USA.

Andersen, J. C. Ø., Rasmussen, H., Nielsen, T. F. D. & Rønsbo, J. G. (1998). The Triple Group and the Platinova Gold and Palladium Reefs in the Skaergaard Intrusion: Stratigraphic and Petrographic Relations. Economic Geology 93: 488-509. https://doi.org/10.2113/gsecongeo.93.4.488.

Andersen, J. C. Ø., Thalhammer, O. A. R. & Schoenberg, R. (2006). Platinum-Group Element and Re-Os Isotope Variations of the High-Grade Kilvenjärvi Platinum-Group Element Deposit, Portimo Layered Igneous Complex, Finland. Economic Geology 101: 159-177. https://doi.org/10.2113/gsecongeo.101.1.159

Andrews, D. R. A. & Brenan, J. M. (2002). Phase-Equilibrium Constraints on the Magmatic Origin of Laurite + Ru-Os-Ir Alloy. Canadian Mineralogist 40: 1705-1716. https://doi.org/10.2113/gscanmin.40.6.1705.

Arndt, N., Czamanske, G., Walker, R., Chauvel, C. & Fedorenko, V. (2003). Geochemistry and Origin of the Intrusive Hosts of the Noril'sk-Talnakh Cu-Ni-PGE Sulfide Deposits. Economic Geology 98(3): 495-515. https://doi.org/10.2113/gsecongeo.98.3.495.

Augé, T. & Maurizot, P. (1995). Stratiform and Alluvial Platinum Mineralization in the New Caledonia Ophiolite Complex. Canadian Mineralogist 33: 1023-1045.

Azaroual, M., Romand, B., Freyssinet, P. & Disnar, J.-R. (2001). Solubility of platinum in aqueous solutions at 25°C and pHs 4 to 10 under oxidizing conditions. Geochimica et Cosmochimica Acta 65(24): 4453-4466. https://doi.org/10.1016/S0016-7037(01)00752-9.

Ballhaus, C. G. & Stumpfl, E. F. (1985). Occurrence and petrological significance of graphite in the Upper Critical Zone, western Bushveld Complex, South Africa. Earth and Planetary Science Letters 74: 58-68. https://doi.org/10.1016/0012-821X(85)90166-9.

Ballhaus, C. & Sylvester, P. (2000). Noble Metal Enrichment Processes in the Merensky Reef, Bushveld Complex. Journal of Petrology 41(4): 545-561. https://doi.org/10.1093/petrology/41.4.545.

Barkov, A., Fleet, M., Nixon, G. & Levson, V. (2005). Platinum-group minerals from five placer deposits in British Columbia, Canada. The Canadian Mineralogist 43: 1687-1710. https://doi.org/10.2113/gscanmin.43.5.1687.

Bazarkina, E. F., Pokrovski, G. S. & Hazemann, J.-L. (2014). Structure, stability and geochemical role of palladium chloride complexes in hydrothermal fluids. Geochimica et Cosmochimica Acta 146: 107-131. https://doi.org/10.1016/j.gca.2014.09.024.

Bencs, L., Ravindra, K. & Van Grieken, R. (2003). Methods for the determination of platinum group elements originating from the abrasion of automotive catalytic converters. Spectro-

chimica Acta Part B: Atomic Spectroscopy 58(10): 1723-1755. https://doi.org/10.1016/S0584-8547(03)00162-9.

Berglund, M. & Wieser, M. (2011). Isotopic compositions of the elements 2009 (IUPAC Technical Report). Pure Appl. Chem., 83(2): 397-410. https://doi.org/10.1351/PAC-REP-10-06-02.

Binnewies, M., Jöckel, M., Willner, H. & Rayner-Canham, G. (2004). Spektrum Lehrbuch: Allgemeine und Anorganische Chemie, 1st ed, Chapter 20, pp. 529-530. Elsevier.

Boudreau, A. E. & McCallum, I. S. (1992). Concentration of Platinum-Group Elements by Magmatic Fluids in Layered Intrusions. Economic Geology 87: 1830-1848. https://doi.org/10.2113/gsecongeo.87.7.1830.

Bowles, J. F. W. (1986). The Development of Platinum-Group Minerals in Laterites. Economic Geology 81: 1278-1285. https://doi.org/10.2113/gsecongeo.81.5.1278.

Bowles, J.F.W., Giże, A.P., Vaughan, D.J., Norris, S.J., 1994. Technical note: development of platinum-group minerals in laterites—initial comparison of organic and inorganic controls. Trans. Inst. Min. Metall. 103, B53–B56.

Bowles, J.F.W., Giże, A.P., Vaughan, D.J., Norris, S.J., 1995. Organic controls on platinum-group element (PGE) solubility in soils: initial data. Chronique de la Recherche Minière 520, 65–73.

Bowles, J. F. W., Suárez, S., Prichard, H. M. & Fisher, P. C. (2017). Weathering of PGE sulfides and Pt-Fe alloys in the Freetown Layered Complex, Sierra Leone. Mineralium Deposita 52: 1127-1144. https://doi.org/10.1007/s00126-016-0706-4.

Bowles, J.F.W., Bowles, J.H., Giże, A.P., 2018. C14–22 n-Alkanes in soil from the Freetown layered intrusion, Sierra Leone: products of Pt catalytic breakdown of natural longer chain n-alkanes? Minerals 8 (3), 105. https://doi.org/10.3390/min8030105.

Cabral, A. R., Beaudoin, G., Choquette, M., Lehmann, B. & Polônia, J. C. (2007). Supergene leaching and formation of platinum in alluvium: evidence from Serro, Minas Gerais, Brazil. Mineralogy and Petrology 90: 141-150. https://doi.org/10.1007/s00710-006-0171-3.

Cabral, A. R., Galbiatti, H. F., Kwitko-Ribeiro, R. & Lehmann, B. (2008). Platinum enrichment at low temperatures and related microstructures, with examples of hongshiite (PtCu) and empirical 'Pt_2HgSe_3' from Itabira, Minas Gerais, Brazil. Terra Nova 20: 32-37. https://doi.org/10.1111/j.1365-3121.2007.00783.x.

Cabral, A., Radtke, M., Munnik, F., Lehmann, B., Reinholz, U., Riesemeier, H., Tupinambá, M. & Kwitko-Ribeiro, R. (2011). Iodine in alluvial platinum–palladium nuggets: Evidence for biogenic precious-metal fixation. Chemical Geology 281: 125-132. https://doi.org/10.1016/j.chemgeo.2010.12.003.

Cabri, L. J., Rowland, J. F., LaFlamme, J. H. G. & Stewart, J. M. (1979). Keithconnite, telluropalladinite and other Pd-Pt tellurides from the Stillwater Complex, Montana. Canadian Mineralogist 17: 589-594.

Cawthorn, R. G. & McCarthy, T. S. (1985). Incompatible Trace Element Behavior in the Bushveld Complex. Economic Geology 80: 1016–1026. https://doi.org/10.2113/gsecongeo.80.4.1016.

Cawthorn, R. G., Lee, C. A., Schouwstra, R. P. & Mellowship, P. (2002). Relationship Between PGE and PGM in the Bushveld Complex. Canadian Mineralogist 40: 311-328. https://doi.org/10.2113/gscanmin.40.2.311.

Cousins, C. A. (1966). The Merensky Reef of the Bushveld Igneous Complex. In: Wilson, H. D. B. (ed). Magmatic Ore Deposits, a Symposium, 12-13 November 1966: 239-251.

Cousins, C. A. & Kinloch, E. D. (1976). Some observations on textures and inclusions in alluvial platinoids. Economic Geology 71(7): 1377-1398. https://doi.org/10.2113/gsecongeo.71.7.1377.

Creamer, M. (2006). The uses of platinum-group metals. From: Creamer Media's Mining Weekly. Retrieved on 30.06.2019 from https://m.miningweekly.com/article/the-uses-of-platinumgroup-metals-2006-11-10/rep_id:3861.

Daltry, V. D. C. & Wilson, A. H. (1997). Review of platinum-group mineralogy: compositions and elemental associations of the PG-minerals and unidentified PGE-phases. Mineralogy and Petrology 60: 185-229. https://doi.org/10.1007/BF01173709.

Dare, S. A., Barnes, S.-J., Prichard, H. M. & Fisher, P. C. (2011). Chalcophile and platinum-group element (PGE) concentrations in the sulfide minerals from the McCreedy East deposit, Sudbury, Canada, and the origin of PGE in pyrite. Mineralium Deposita 46: 381-407. https://doi.org/10.1007/s00126-011-0336-9.

Downard, K. (2004). Mass Spectrometry—A Foundation Course. Cambridge UK: Royal Society of Chemistry.

Dudal, R. (1963). Dark clay soils of tropical and subtropical regions. Soil Science 95(4): 264-270. https://doi.org/10.1097/00010694-196304000-00008.

European Commission (2014). Report on critical raw materials for the EU. From: European Commission: Internal Market, Industry, Entrepreneurship and SMEs. Retrieved on 16.07.2019 from https://ec.europa.eu/growth/sectors/raw-materials/specific-interest/critical_en.

Evans, D. M. & Spratt, J. (2000). Platinum and palladium oxides/hydroxides from the Great Dyke, Zimbabwe, and thoughts on their stability and possible extraction. In: Rammelmair, D. et al. (eds). Applied Mineralogy Research Economy, CRC Press, pp. 289−292.

Fuchs, W. A. & Rose, A. W. (1974). The Geochemical Behavior of Platinum and Palladium in the Weathering Cycle in the Stillwater Complex, Montana. Economic Geology 69(3): 332-346. https://doi.org/10.2113/gsecongeo.69.3.332.

Gain, S. (1985). The Geologic Setting of the Platiniferous UG-2 Chromitite Layer on the Farm Maandagshoek, Eastern Bushveld Complex. Economic Geology 80: 925-943. https://doi.org/10.2113/gsecongeo.80.4.925.

Garuti, G. & Zaccarini, F. (1997). In Situ Alteration of Platinum-Group Minerals at Low Temperature: Evidence from Serpentinized and Weathered Chromitite of the Vouinos Complex, Greece. Canadian Mineralogist 35: 611-626.

Godel, B. & Barnes, S.-J. (2008). Platinum-group elements in sulfide minerals and the whole rocks of the J-M Reef (Stillwater Complex): Implication for the formation of the reef. Chemical Geology 248: 272-294. https://doi.org/10.1016/j.chemgeo.2007.05.006.

Grayson, R., Tumenbayar, B., Batbayar, M., Altanzul, B. (2000). Platinum & gold placers of Late Cretaceous and Quaternary Age in the Gobi Desert, Mongolia. World Placer J. 1, 129-133.

Haworth, R. D. (1971). The Chemical Nature of Humic Acid. Soil Science 11(1): 71-79. https://doi.org/10.1097/00010694-197101000-00009.

Holwell, D. A. & McDonald, I. (2007). Distribution of platinum-group elements in the Platreef at Overysel, northern Bushveld Complex: a combined PGM and LA-ICP-MS study.

Contributions to Mineralogy and Petrology 154(2): 171-190. https://doi.org/10.1007/s00410-007-0185-9.

Ihlenfield, C. & Keays, R. (2011). Crustal contamination and PGE mineralization in the Platreef, Bushveld Complex, South Africa: evidence for multiple contamination events and transport of magmatic sulfides. Mineralium Deposita 46: 813-832. https://doi.org/10.1007/s00126-011-0340-0.

Johan, Z. (2006). Platinum-group minerals from placers related to the Nizhni Tagil (Middle Urals, Russia) Uralian-Alaskan-type ultramafic complex: ore-mineralogy and study of silicate inclusions in (Pt, Fe) alloys. Mineralogy and Petrology 87: 1-30. https://doi.org/10.1007/s00710-005-0117-1.

Junge, M., Oberthür, T. & Melcher, F. (2014). Cryptic Variation of Chromite Chemistry, Platinum Group Element and Platinum Group Mineral Distribution in the UG-2 Chromitite: An Example from the Karee Mine, Western Bushveld Complex, South Africa. Economic Geology 100: 795-810. https://doi.org/10.2113/econgeo.109.3.795.

Kinloch, E. D. (1982). Regional Trends in the Platinum-Group Mineralogy of the Critical Zone of the Bushveld Complex, South Africa. Economic Geology 77: 1328-1347. https://doi.org/10.2113/gsecongeo.77.6.1328.

Köllensperger, G., Hann, S. & Stingeder, G. (2000). Determination of Rh, Pd and Pt in environmental silica containing matrices: capabilities and limitations of ICP-SFMS. Journal of Analytical Atomic Spectrometry 15: 1553-1557. https://doi.org/10.1039/B006695H.

Kullerud, G. (1971). Experimental Techniques in Dry Sulfide Research. In: Ulmer G.C. (eds). Research Techniques for High Pressure and High Temperature. Springer, Berlin, Heidelberg, pp. 289-315. https://doi.org/10.1007/978-3-642-88097-1_11.

Kweiyang Institute of Geochemistry, Academia Sinica (1974): Tellurostibnide of palladium and nickel and other new minerals and varieties of platinum metals. Geochimica 3: 169-181 (in Chinese, with English abstract). In: Fleischer, M., Pabst, A., Mandarino, J.A., Chao, G.Y., Cabri, L.J. (1976): New mineral names. American Mineralogist: 61: 182.

Liu, A. & Gonzalez, R. (1999). Adsorption/Desorption in a System Consisting of Humic Acid, Heavy Metals, and Clay Minerals. Journal of Colloid and Interface Science 218(1): 225–232. https://doi.org/10.1006/jcis.1999.6419.

Locmelis, M., Melcher, F. & Oberthür, T. (2010). Platinum-group element distribution in the oxidized Main Sulfide Zone, Great Dyke, Zimbabwe. Mineralium Deposita 45: 93-109. https://doi.org/10.1007/s00126-009-0258-y.

McCallum, M. E., Loucks, R. R., Carlson, R. R., Cooley, E. F. & Doerge, T. A. (1976). Platinum metals associated with hydrothermal copper ores of the New Rambler Mine, Medicine Bow Mountains, Wyoming. Economic Geology 71(7): 1429-1450. https://doi.org/10.2113/gsecongeo.71.7.1429.

McDonald, I., Ohnenstetter, D., Rowe, J., Tredoux, M., Pattrick, R. & Vaughan, D. (1999). Platinum precipitation in the Waterberg deposit, Naboomspruit, South Africa. South African Journal of Geology 102(3): 184-191.

Meisel, T., Fellner, N. & Moser, J. (2003). A simple procedure for the determination of platinum group elements and rhenium (Ru, Rh, Pd, Re, Os, Ir and Pt) using ID-ICP-MS with an inexpensive on-line matrix separation in geological and environmental materials. Journal of Analytical Atomic Spectrometry 18(7): 720-726. https://doi.org/10.1039/B301754K.

Melcher, F., Oberthür, T. & Lodziak, J. (2005). Modification of Detrital Platinum-Group Minerals from the Eastern Bushveld Complex, South Africa. Canadian Mineralogist 43: 1711-1734. https://doi.org/10.2113/gscanmin.43.5.1711.

Mountain, B. & Wood, S. (1988). Chemical Controls on the Solubility, Transport, and Deposition of Platinum and Palladium in Hydrothermal Solutions: A Thermodynamic Approach. Economic Geology 83, 492-510. https://doi.org/10.2113/gsecongeo.83.3.492.

Naldrett, A., Wilson, A., Kinnaird, J. & Chunnett, G. (2009). PGE Tenor and Metal Ratios within and below the Merensky Reef, Bushveld Complex: Implications for its Genesis. Journal of Petrology 50(4): 625-659. https://doi.org/10.1093/petrology/egp015.

Ndjigui, P.-D. & Bilong, P. (2010). Platinum-group elements in the serpentinite lateritic mantles of the Kongo–Nkamouna ultramafic massif (Lomié region, South-East Cameroon). Journal of Geochemical Exploration 107(1): 63-76. https://doi.org/10.1016/j.gexplo.2010.06.008.

Oberthür, T., Weiser, T. W. & Gast, L. (2003). Geochemistry and mineralogy of platinum-group elements at Hartley Platinum Mine, Zimbabwe, Part 2: Supergene redistribution in the oxidized Main Sulfide Zone of the Great Dyke, and alluvial platinum-group minerals. Mineralium Deposita 38: 344-355. https://doi.org/10.1007/s00126-002-0337-9.

Oberthür, T., Melcher, F., Gast, L., Wöhrl, C. & Lodziak, J. (2004). Detrital Platinum-Group Minerals in Rivers Draining the Eastern Bushveld Complex, South Africa. Canadian Mineralogist 42: 563-582. https://doi.org/10.2113/gscanmin.42.2.563.

Oberthür, T., Melcher, F., Buchholz, P. & Locmelis, M. (2013). The oxidized ores of the Main Sulfide Zone, Great Dyke, Zimbabwe: turning resources into minable reserves—mineralogy is the key. Journal of the South African Institute of Mining and Metallurgy 113: 191-201.

Oberthür, T., Junge, M., Rudashevsky, N., De Meyer, E. & Gutter, P. (2016). Platinum-group minerals in the LG and MG chromitites of the eastern Bushveld Complex, South Africa. Mineralium Deposita 51(1): 71-87. https://doi.org/10.1007/s00126-015-0593-0.

Oppermann, L., Junge, M., Schuth, S., Holtz, F., Schwarz-Schampera, U. & Sauheitl, L. (2017). Mobility and distribution of palladium and platinum in soils above Lower and Middle Group chromitites of the western Bushveld Complex, South Africa. South African Journal of Geology 120(4): 511-524. https://doi.org/10.25131/gssajg.120.4.511.

Oszczepalski, S., Nowak, G.J., Bechtel, A., Zák, K., (2002). Evidence of oxidation of the Kupferschiefer in the Lubin-Sieroszowice deposit, Poland: implications for Cu-Ag and Au-Pt-Pd mineralisation. Geol. Q. 46 (1), 1–23.

Richard, F. & Bourg, A. (1991). Aqueous geochemistry of chromium: A review. Water Research 25(7): 807-816. https://doi.org/10.1016/0043-1354(91)90160-R.

Robb, L. (2005). Surficial and supergene ore-forming processes. In: Robb, L. Introduction to Ore-Forming Processes, Blackwell Publishing, 219–245.

Robles-Camacho, J. & Armienta, M. (2000). Natural chromium contamination of groundwater at León Valley, México. Journal of Geochemical Exploration 68: 167–181. https://doi.org/10.1016/S0375-6742(99)00083-7.

Sassani, D. & Shock, E. (1998). Solubility and transport of platinum-group elements in supercritical fluids: Summary and estimates of thermodynamic properties for ruthenium, rhodium, palladium, and platinum solids, aqueous ions, and complexes to 1 000 °C and 5 kbar. Geochimica et Cosmochimica Acta 62(15), 2643–2671. https://doi.org/10.1016/S0016-7037(98)00049-0.

Schiffries, C. M. (1982). The petrogenesis of a platiniferous dunite pipe in the Bushveld Complex; infiltration metasomatism by a chloride solution. Economic Geology 77(6): 1439-1453. https://doi.org/10.2113/gsecongeo.77.6.1439.

Schnitzer, M. (1978). Humic Substances: Chemistry and Reactions. Developments in Soil Science 8: 1–64. https://doi.org/10.1016/S0166-2481(08)70016-3.

Shackleton, N. J., Malysiak, V. & O'Connor, C. T. (2007). Surface characteristics and flotation behavior of platinum and palladium tellurides. Minerals Engineering 20: 1232-1245. https://doi.org/10.1016/j.mineng.2007.05.004.

Shaffer, C. (2015). What Are the Platinum Group Metals and Why Do They Matter? From: ThermoFisher Scientific. Retrieved on 30.06.2019 from https://www.thermofisher.com/blog/metals/what-are-the-platinum-group-metals-and-why-do-they-matter.

Sluzhenikin, S. F. & Mokhov, A. V. (2015). Gold and silver in PGE–Cu–Ni and PGE ores of the Noril'sk deposits, Russia. Mineralium Deposita 50(4): 465-492. https://doi.org/10.1007/s00126-014-0543-2.

Strome, D.J., & Miller, M.C. (1978). Photolytic changes in dissolved humic substances. Int. Ver. Theor. Angew. Limnol. Verh. 20: 1248-1254. https://doi.org/10.1080/03680770.1977.11896681.

Switzer, G. & Swanson, H. (1960). News and notes: paratellurite, a new mineral from Mexico. American Mineralogist 45: 1272-1274.

Tarkian, M. & Stumpfl, E. F. (1975). Platinum Mineralogy of the Driekop Mine, South Africa. Mineralium Deposita 10: 71-85. https://doi.org/10.1007/BF00207462.

Tarkian, M. (1987). Compositional Variations and Reflectance of the Common Platinum-Group Minerals. Mineralogy and Petrology 36: 169-190. https://doi.org/10.1007/BF01163258.

Thanabalasingam, P. & Pickering, W. F. (1986). Arsenic Sorption by Humic Acids. Environmental Pollution (Series B) 12: 233-246. https://doi.org/10.1016/0143-148X(86)90012-1.

Thomas, R. (2002). A Beginner's Guide to ICP-MS, Part XII—A Review of Interferences. Spectroscopy 17(10): 24-31.

Tolstykh, N., Foley, J., Sidorov, E., & Laajoki, K. (2002). Composition of the platinum-group minerals in the Salmon River placer deposit, Goodnews Bay, Alaska. The Canadian Mineralogist 40: 463-471. https://doi.org/10.2113/gscanmin.40.2.463.

Traoré, D., Beauvais, A., Augé, T., Chabaux, F., Parisot, J.-C., Cathelineau, M., Peiffert, C., Colin, F., 2006. Platinum and palladium mobility in supergene environment: the residual origin of the Pirogues River mineralization, New Caledonia. J. Geochem. Explor. 88, 350–354. https://doi.org/10.1016/j.gexplo.2005.08.073.

Turner, A., Crussell, M., Millward, G. E., Cobelo-Garcia, A. & Fisher, A. S. (2006). Adsorption Kinetics of Platinum Group Elements in River Water. Environmental Science Technology 40: 1524-1531. https://doi.org/10.1021/es0518124.

Van Middlesworth, J. M. & Wood, S. A. (1999). The stability of palladium(II) hydroxide and hydroxy–chloride complexes: an experimental solubility study at 25–85°C and 1 bar. Geochimica et Cosmochimica Acta 63(11-12): 1751-1765. https://doi.org/10.1016/S0016-7037(99)00058-7.

Verryn, S. M. C. & Merkle, R. K. W. (1994). Compositional variation of cooperite, braggite, and vysotskite from the Bushveld Complex. Mineralogical Magazine 58: 223-234. https://doi.org/10.1180/minmag.1994.058.391.05.

Vymazalová, A., Ondrus, P. & Drábek, M. (2005). Synthetic palladium tellurides, their structures and mineralogical significance. In: Mao, J. & Bierlein, F. P. (eds.). Mineral Deposit Re-

search: Meeting the Global Challenge: Proceedings of the Eighth Biennial SGA Meeting Beijing, China, 18–21 August 2005. https://doi.org/10.1007/3-540-27946-6_366.

Wang, K. & Xing, B. (2005). Structural and Sorption Characteristics of Adsorbed Humic Acid on Clay Minerals. Journal of Environmental Quality 34(1): 342-349. https://doi.org/10.2134/jeq2005.0342.

Warwick, P., Inam, E. and Evans, N. (2005). Arsenic's Interaction with Humic Acid. Environ. Chem. 2: 119-124. https://doi.org/10.1071/EN05025.

Wood, S. A. (1990). The Interaction of Dissolved Platinum with Fulvic Acid and Simple Organic Acid Analogues in Aqueous Solutions. Canadian Mineralogist 28: 665-673.

Wood, S. A. (1996). The role of humic substances in the transport and fixation of metals of economic interest (Au, Pt, Pd, U, V). Ore Geology Reviews 11: 1-31. https://doi.org/10.1016/0169-1368(95)00013-5.

Wood, S. A., Tait, C. D., Vlassopoulos, D. & Janecky, D. R. (1994). Solubility and spectroscopic studies of the interaction of palladium with simple carboxylic acids and fulvic acid at low temperature. Geochimica et Cosmochimica Acta 58(2): 625-637. https://doi.org/10.1016/0016-7037(94)90493-6.

8. Appendix

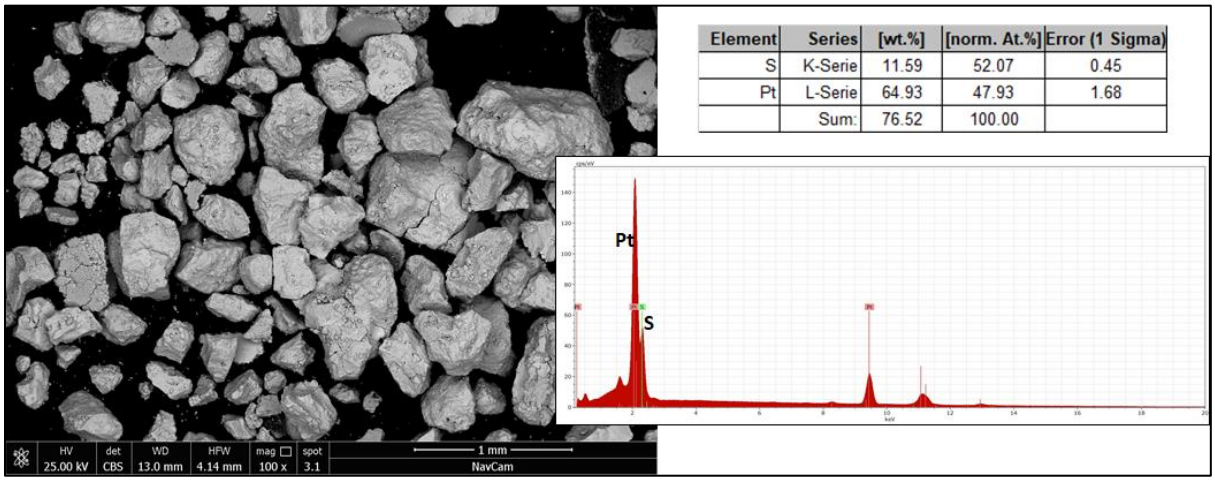

Figure 8.1:Image of PtS residue (after reaction with 10 mg/l HA) (left) and analysis of residue (absolute concentrations, top right; spectra, bottom right).

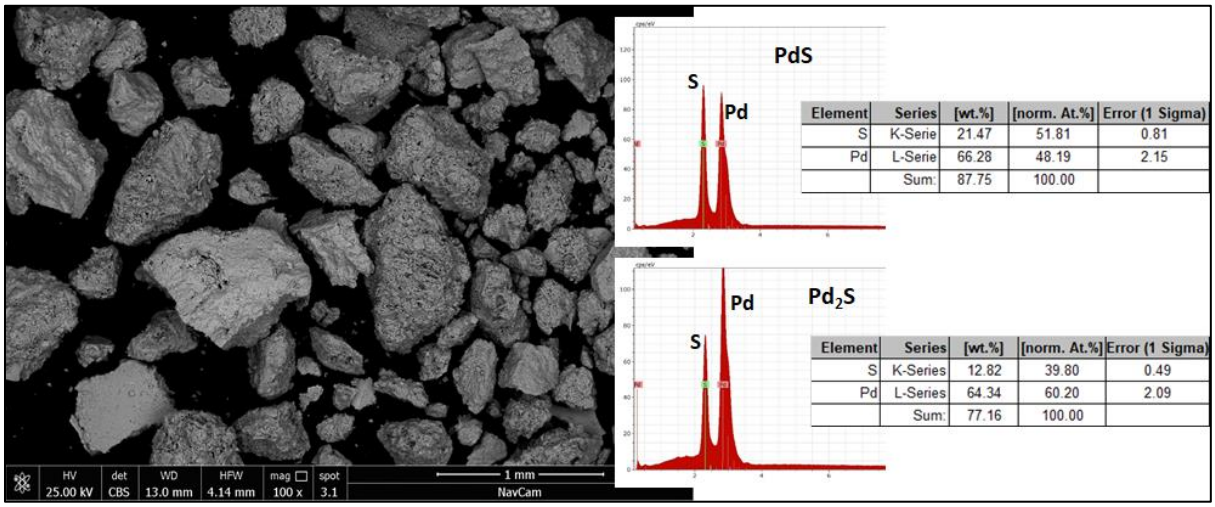

Figure 8.2: Image of PdS residue (after reaction with 10 mg/l HA) (left) and analysis of residues indicating differences in Pd:S ratio (absolute concentrations, right; spectra, middle).

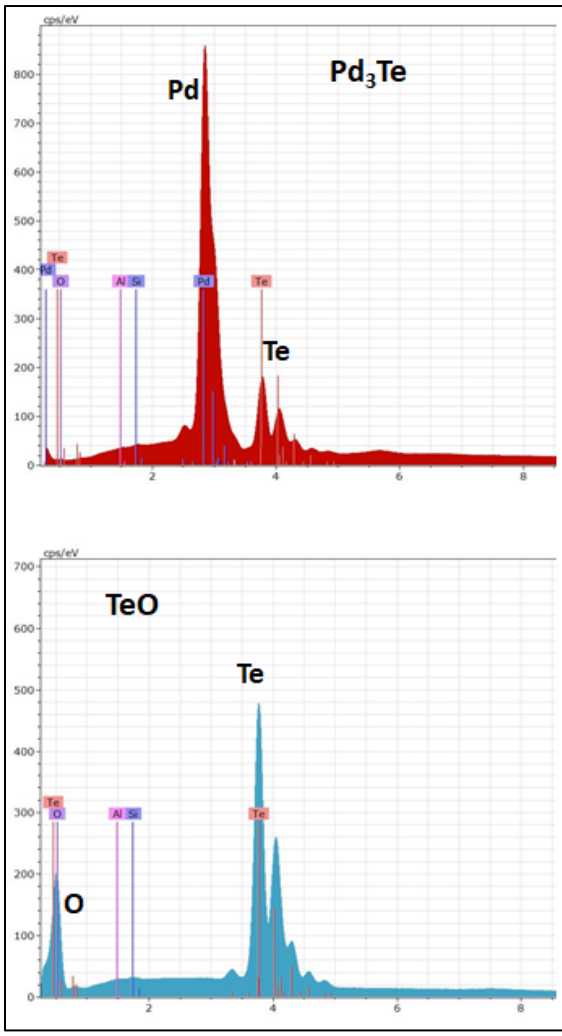

Element	Series	[wt.%]	[norm. At.%]	Error (1 Sigma)
O	K-Series	0.38	3.12	0.08
Al	K-Series	0.16	0.80	0.03
Si	K-Series	0.12	0.56	0.03
Pd	L-Series	57.43	71.44	1.87
Te	L-Series	23.20	24.07	0.69
	Summe:	81.30	100.00	

Element	Series	[wt.%]	[norm. At.%]	Error (1 Sigma)
O	K-Series	11.96	61.44	1.28
Al	K-Series	0.12	0.35	0.03
Si	K-Series	0.07	0.20	0.03
Te	L-Series	58.99	38.00	1.70
	Sum:	71.14	100.00	

Figure 8.3: Results of analysis for residual palladium telluride grains after experiment (top) and newly formed crystals found encrusting these grains (bottom)

Table 8.1: Analyses of short-term experiments (synthetics and chromitites).

			Concentration (µg/l) + (isotopes used)			
Sample name	**Reagent**	**Reaction time**	**Cr** (52, 53)	**Pd** (105, 106, 108)	**Te** (125, 128)	**Pt** (194, 195)
Chromitite						
TSh-MNR(HO)	H_2O	1 hour	1.43	0.29		≤0.005
TSh-MNR(HO)II	H_2O	1 hour	51.68	0.31		0.02
TSh-MNR100(HO)	H_2O	1 hour	43.19	0.38		0.01
TSh-MNR100(HO)II	H_2O	1 hour	20.12	0.37		≤0.005
TSh-MNR(HS)	HASS	1 hour	1274.44	1.19		0.14
TSh-MNR(HS)II	HASS	1 hour	1427.43	2.04		0.15
TSh-MNR100(HS)	HASS	1 hour	960.79	1.10		0.14
TSh-MNR100(HS)II	HASS	1 hour	895.33	0.63		0.11
TSh-MNR(HP)	HAP	1 hour	603.04	0.81		0.25
TSh-MNR(HP)II	HAP	1 hour	432.04	1.79		0.38
TSh-MNR100(HP)	HAP	1 hour	896.34	1.48		0.32
TSh-MNR100(HP)II	HAP	1 hour	492.39	0.79		0.19
TSd-MNR(HO)	H_2O	20 hours	13.78	≤0.01		0.01
TSd-MNR(HO)II	H_2O	20 hours	19.53	≤0.01		0.01
TSd-MNR100(HO)	H_2O	20 hours	11.60	≤0.01		0.01
TSd-MNR100(HO)II	H_2O	20 hours	7.94	≤0.01		≤0.005
TSd-MNR(HS)	HASS	20 hours	434.66	0.53		0.03
TSd-MNR(HS)II	HASS	20 hours	346.19	0.49		0.02
TSd-MNR100(HS)	HASS	20 hours	383.53	0.47		0.04
TSd-MNR100(HS)II	HASS	20 hours	480.35	0.49		0.04
TSd-MNR(HP)	HAP	20 hours	417.51	1.06		0.02
TSd-MNR(HP)II	HAP	20 hours	375.60	0.98		0.04
TSd-MNR100(HP)	HAP	20 hours	350.91	1.01		0.10
TSd-MNR100(HP)II	HAP	20 hours	458.93	1.01		0.06
TSw-MNR(HO)	H_2O	100 hours	212.78	0.43		0.20
TSw-MNR(HO)II	H_2O	100 hours	259.33	0.44		≤0.005
TSw-MNR100(HO)	H_2O	100 hours	41.56	0.52		≤0.005
TSw-MNR100(HO)II	H_2O	100 hours	174.49	0.43		≤0.005
TSw-MNR(HS)	HASS	100 hours	943.74	1.19		≤0.005

TSw-MNR(HS)II	HASS	100 hours	1026.32	4.09		-
TSw-MNR100(HS)	HASS	100 hours	1224.27	1.55		0.06
TSw-MNR100(HS)II	HASS	100 hours	1050.86	1.02		0.05
TSw-MNR(HP)	HAP	100 hours	-	10.71		0.18
TSw-MNR(HP)II	HAP	100 hours	628.86	5.85		0.97
TSw-MNR100(HP)	HAP	100 hours	310.97	3.19		0.03
TSw-MNR100(HP)II	HAP	100 hours	-	3.20		0.27
PdTe						
TSh-PdT1(HO)	H_2O	1 hour		2.55	825.43	
TSh-PdT1(HO)II	H_2O	1 hour		2.36	1113.03	
TSh-PdT1(HS)	HASS	1 hour		1.94	188.11	
TSh-PdT1(HS)II	HASS	1 hour		2.23	259.17	
TSh-PdT1(HP)	HAP	1 hour		2.76	11.67	
TSh-PdT1(HP)II	HAP	1 hour		2.34	13.91	
TSd-PdT1(HO)	H_2O	20 hours		51.30	1261.79	
TSd-PdT1(HO)II	H_2O	20 hours		1.70	1349.25	
TSd-PdT1(HS)	HASS	20 hours		9.80	132.87	
TSd-PdT1(HS)II	HASS	20 hours		1.22	78.14	
TSd-PdT1(HP)	HAP	20 hours		24.24	212.89	
TSd-PdT1(HP)II	HAP	20 hours		5.56	72.35	
TSw-PdT1(HO)	H_2O	100 hours		≤0.01	1290.99	
TSw-PdT1(HO)II	H_2O	100 hours		≤0.01	1247.40	
TSw-PdT1(HS)	HASS	100 hours		2.10	1019.21	
TSw-PdT1(HS)II	HASS	100 hours		2.54	869.49	
TSw-PdT1(HP)	HAP	100 hours		1.18	1130.63	
TSw-PdT1(HP)II	HAP	100 hours		0.30	165.51	
$PdTe_2$						
TSh-PdT2(HO)	H_2O	1 hour		0.11	1287.34	
TSh-PdT2(HO)II	H_2O	1 hour		0.14	1294.00	
TSh-PdT2(HS)	HASS	1 hour		4.44	4844.12	
TSh-PdT2(HS)II	HASS	1 hour		4.46	4982.87	
TSh-PdT2(HP)	HAP	1 hour		2.62	2256.41	
TSh-PdT2(HP)II	HAP	1 hour		2.83	1169.70	
TSd-PdT2(HO)	H_2O	20 hours		3.78	2606.50	

TSd-PdT2(HO)II	H_2O	20 hours		2.48	-	
TSd-PdT2(HS)	HASS	20 hours		5.49	2055.74	
TSd-PdT2(HS)II	HASS	20 hours		2.28	2394.29	
TSd-PdT2(HP)	HAP	20 hours		1.62	1211.29	
TSd-PdT2(HP)II	HAP	20 hours		1.35	1942.43	
TSw-PdT2(HO)	H_2O	100 hours		0.43	1540.52	
TSw-PdT2(HO)II	H_2O	100 hours		-	1480.43	
TSw-PdT2(HS)	HASS	100 hours		2.95	7272.04	
TSw-PdT2(HS)II	HASS	100 hours		3.77	5840.11	
TSw-PdT2(HP)	HAP	100 hours		2.64	7553.06	
TSw-PdT2(HP)II	HAP	100 hours		7.32	9549.85	
PdS						
TSh-PdS(HO)	H_2O	1 hour		145.42		
TSh-PdS(HO)II	H_2O	1 hour		217.35		
TSh-PdS(HS)	HASS	1 hour		36.21		
TSh-PdS(HS)II	HASS	1 hour		18.17		
TSh-PdS(HP)	HAP	1 hour		7.12		
TSh-PdS(HP)II	HAP	1 hour		36.97		
TSd-PdS(HO)	H_2O	20 hours		2801.67		
TSd-PdS(HO)II	H_2O	20 hours		1601.00		
TSd-PdS(HS)	HASS	20 hours		525.52		
TSd-PdS(HS)II	HASS	20 hours		357.11		
TSd-PdS(HP)	HAP	20 hours		125.98		
TSd-PdS(HP)II	HAP	20 hours		60.04		
TSw-PdS(HO)	H_2O	100 hours		454.54		
TSw-PdS(HO)II	H_2O	100 hours		8.72		
TSw-PdS(HS)	HASS	100 hours		206.47		
TSw-PdS(HS)II	HASS	100 hours		65.38		
TSw-PdS(HP)	HAP	100 hours		200.25		
TSw-PdS(HP)II	HAP	100 hours		635.22		
PtS						
TSh-PtS(HO)	H_2O	1 hour				45.66
TSh-PtS(HO)II	H_2O	1 hour				201.33
TSh-PtS(HS)	HASS	1 hour				252.68

TSh-PtS(HS)II	HASS	1 hour				371.23
TSh-PtS(HP)	HAP	1 hour				28.69
TSh-PtS(HP)II	HAP	1 hour				35.74
TSd-PtS(HO)	H_2O	20 hours				2677.25
TSd-PtS(HO)II	H_2O	20 hours				2096.29
TSd-PtS(HS)	HASS	20 hours				304.18
TSd-PtS(HS)II	HASS	20 hours				105.34
TSd-PtS(HP)	HAP	20 hours				40.15
TSd-PtS(HP)II	HAP	20 hours				133.58
TSw-PtS(HO)	H_2O	100 hours				1287.23
TSw-PtS(HO)II	H_2O	100 hours				6355.17
TSw-PtS(HS)	HASS	100 hours				1228.98
TSw-PtS(HS)II	HASS	100 hours				1122.62
TSw-PtS(HP)	HAP	100 hours				326.11
TSw-PtS(HP)II	HAP	100 hours				801.60

Table 8.2: Long-term synthetic samples analyzed, showing isotopes used, concentration and error reported as standard deviation percentage.

		Isotopes used for analysis			Concentration (µg/l)			Error (%)		
Sample name	**Reaction time**	**Pd**	**Te**	**Pt**	**Pd**	**Te**	**Pt**	**Pd**	**Te**	**Pt**
PdTe										
HA=0.1ppm										
LOa-PdT1(01)	6 days	105, 106	125, 128		0.61	128.48		0.28	0.54	
LOb-PdT1(01)	64 days	105, 106, 108	125, 128		0.73	1537.37		0.83	0.25	
LOc-PdT1(01)	90 days	106, 108	125, 128		0.65	1070.75		0.96	0.42	
LOd-PdT1(01)	149 days	105, 106	125, 128		0.72	1132.45		0.39	0.64	
LOe-PdT1(01)	307 days	106, 108	125, 128		1.40	731.68		3.51	1.63	
HA=1ppm										
LOa-PdT1(1)	6 days	105, 106, 108	125, 128		0.68	72.23		0.33	0.53	
LOb-PdT1(1)	64 days	105, 106	125, 128		0.59	262.33		0.24	0.42	
LOc-PdT1(1)	90 days	105, 106	125, 128		0.59	465.33		0.43	0.50	
LOd-PdT1(1)	149 days	105, 108	125, 128		0.77	1745.27		0.35	1.01	
LOe-PdT1(1)	307 days	105, 106, 108	125, 128		0.30	1249.89		5.10	1.70	
HA=10ppm										
LOa-PdT1(10)	6 days	106, 108	125, 128		0.49	120.65		0.48	0.38	
LOb-PdT1(10)	64 days	105, 106	125, 128		0.66	177.54		0.26	0.42	
LOc-PdT1(10)	90 days	105, 106	125, 128		0.62	270.06		0.49	0.58	
LOd-PdT1(10)	149 days	105, 108	125, 128		0.69	741.72		0.31	0.88	
LOe-PdT1(10)	307 days	105, 106	125, 128		0.59	3498.88		8.44	6.91	
$PdTe_2$										
HA=0.1ppm										

LOa-PdT2(01)	6 days	106, 108	125, 128		1.17	970.14		9.09	0.36	
LOb-PdT2(01)	64 days	105, 108	125, 128		0.87	925.78		0.93	1.05	
LOc-PdT2(01)	90 days	105, 106	125, 128		0.63	934.49		0.62	0.21	
LOd-PdT2(01)	149 days	105, 106	125, 128		0.91	889.02		3.41	0.95	
LOe-PdT2(01)	307 days	105, 106	125, 128		3.05	760.85		2.81	2.88	
HA=1ppm										
LOa-PdT2(1)	6 days	105, 106	125, 128		2.68	800.52		11.75	0.61	
LOb-PdT2(1)	64 days	106, 108	125, 128		4.24	1265.73		0.36	0.34	
LOc-PdT2(1)	90 days	106, 108	125, 128		0.91	1323.69		7.25	0.90	
LOd-PdT2(1)	149 days	106, 108	125, 128		1.03	1304.58		1.32	1.85	
LOe-PdT2(1)	307 days	-	125, 128		bdl	1026.02		-	3.62	
HA=10ppm										
LOa-PdT2(10)	6 days	105, 106	125, 128		0.87	539.16		1.32	0.41	
LOb-PdT2(10)	64 days	105, 106	125, 128		1.55	2701.04		1.90	0.35	
LOc-PdT2(10)	90 days	105, 106	125, 128		1.00	2448.40		1.62	0.27	
LOd-PdT2(10)	149 days	105, 106	125, 128		0.97	2627.89		2.53	1.43	
LOe-PdT2(10)	307 days	106, 108	125, 128		1.70	2669.39		4.20	4.38	
H_2O										
LOa-PdT2(B)	7 days	-	125, 128		bdl	1087.34		-	0.36	
LOb-PdT2(B)	65 days	105, 106	125, 128		2.42	656.70		0.64	0.52	
LOc-PdT2(B)	91 days	106, 108	125, 128		2.37	642.46		0.15	0.30	
LOd-PdT2(B)	150 days	105, 106	125, 128		2.98	695.34		0.55	1.22	
LOe-PdT2(B)	308 days	106, 108	125, 128		9.00	604.25		3.66	3.79	
PdS										

HA=0.1ppm										
LOa-PdS(01)	5 days	105, 106			16.55			0.26		
Lob-PdS(01)	63 days	-			outlier			-		
LOc-PdS(01)	89 days	105, 106			17.38			1.36		
LOd-PdS(01)	148 days	105, 106, 108			24.47			1.94		
LOe-PdS(01)	306 days	105, 106, 108			46.97			3.31		
HA=1ppm										
LOa-PdS(1)	5 days	106, 108			15.03			0.46		
LOb-PdS(1)	63 days	105, 108			22.36			0.94		
LOc-PdS(1)	89 days	105, 106			25.78			1.75		
LOd-PdS(1)	148 days	105, 106, 108			34.77			0.94		
LOe-PdS(1)	306 days	105, 106			36.90			2.68		
HA=10ppm										
LOa-PdS(10)	5 days	105, 106			18.26			1.84		
LOb-PdS(10)	63 days	105, 106			30.87			0.64		
LOc-PdS(10)	89 days	106			52.36			13.40		
LOd-PdS(10)	148 days	105, 108			56.73			44.59		
LOe-PdS(10)	306 days	105, 108			162.08			2.19		
PtS										
HA=0.1ppm										
LOa-PtS(01)	5 days			194, 195			172.53			0.28
LOb-PtS(01)	63 days			194, 195			57.78			0.83
LOc-PtS(01)	89 days			194, 195			46.97			0.99
LOd-PtS(01)	148 days			194, 195			69.20			1.48

LOe-PtS(01)	306 days			194, 195			39.14			1.90
HA=1ppm										
LOa-PtS(1)	5 days			194, 195			139.61			0.71
LOb-PtS(1)	63 days			194, 195			91.00			0.31
LOc-PtS(1)	89 days			194, 195			78.90			0.99
LOd-PtS(1)	148 days			194, 195			86.95			1.56
LOe-PtS(1)	306 days			194, 195			77.51			4.29
HA=10ppm										
LOa-PtS(10)	5 days			194, 195			109.19			0.59
LOb-PtS(10)	63 days			194, 195			155.17			0.66
LOc-PtS(10)	89 days			194, 195			103.85			1.07
LOd-PtS(10)	148 days			194, 195			72.22			1.00
LOe-PtS(10)	306 days			194, 195			93.54			3.51
H_2O										
LOa-PtS(B)	7 days			194, 195			61.23			2.02
LOb-PtS(B)	65 days			194, 195			208.76			1.37
LOc-PtS(B)	91 days			194, 195			18.65			1.00
LOd-PtS(B)	150 days			194, 195			49.73			2.89
LOe-PtS(B)	308 days			194, 195			118.06			4.20

Table 8.4: pH at start and end of experiments.

	pH at start	pH at end
PdTe + 0.1 mg/l HA	7.8	7.8
PdTe + 1 mg/l HA	7.2	7.2
PdTe + 10 mg/l HA	7.7	7.7
$PdTe_2 + H_2O$	6.8	6.8
$PdTe_2$ + 0.1 mg/l HA	7.8	7.8
$PdTe_2$ + 1 mg/l HA	7.2	7.2
$PdTe_2$ + 10 mg/l HA	7.7	7.7
PdS + 0.1 mg/l HA	7.8	3.5
PdS + 1 mg/l HA	7.2	3.7
PdS + 10 mg/l HA	7.7	3.8
$PtS + H_2O$	6.8	3.4
PtS + 0.1 mg/l HA	7.8	3.5
PtS + 1 mg/l HA	7.2	3.3
PtS + 10 mg/l HA	7.7	3.4

Table 8.5: Analyses of long-term experiments on chromitite.

		Concentration (µg/l) + (isotopes used)		
Sample name	**Reaction time**	**Cr** (52, 53)	**Pd** (105, 106, 108)	**Pt** (194, 195)
HA=0.1 ppm				
LOa-MNR(01)	7 days	2.07	≤0.01	0.38
LOa-MNR100(01)	6 days	99.61	0.39	0.04
LOb-MNR(01)	65 days	6.57	≤0.01	0.28
LOb-MNR100(01)	64 days	199.10	0.03	0.09
LOc-MNR(01)	91 days	4.47	0.02	0.30
LOc-MNR100(01)	90 days	77.39	0.13	0.03
LOd-MNR(01)	150 days	3.24	≤0.01	0.18
LOd-MNR100(01)	149 days	31.87	≤0.01	0.02
LOe-MNR(01)	308 days	10.32	0.36	0.19
LOe-MNR100(01)	307 days	1080.39	0.07	0.23

HA=1 ppm				
LOa-MNR(1)	7 days	2.36	≤0.01	1.76
LOa-MNR100(1)	6 days	69.07	0.03	0.50
LOb-MNR(1)	65 days	6.11	≤0.01	1.92
LOb-MNR100(1)	64 days	15.41	≤0.01	0.03
LOc-MNR(1)	91 days	4.02	0.03	1.69
LOc-MNR100(1)	90 days	10.97	0.02	0.03
LOd-MNR(1)	150 days	3.57	0.02	0.99
LOd-MNR100(1)	149 days	9.06	≤0.01	0.02
LOe-MNR(1)	308 days	22.74	0.10	0.82
LOe-MNR100(1)	307 days	25.47	0.06	2.25
HA=10 ppm				
LOa-MNR(10)	7 days	3.48	≤0.01	0.02
LOa-MNR100(10)	5 days	144.50	0.57	0.04
LOb-MNR(10)	65 days	8.85	0.02	0.03
LOb-MNR100(10)	63 days	70.37	0.02	0.02
LOc-MNR(10)	91 days	7.87	≤0.01	0.03
LOc-MNR100(10)	98 days	65.67	0.03	0.01
LOd-MNR(10)	150 days	6.06	≤0.01	0.07
LOd-MNR100(10)	148 days	56.30	≤0.01	0.01
LOe-MNR(10)	308 days	30.98	0.07	0.11
LOe-MNR100(10)	306 days	102.36	0.05	0.01
H_2O				
LOa-MNR(B)	7 days	9.49	0.03	0.01
LOb-MNR(B)	65 days	-	1.94	0.30
LOc-MNR(B)	91 days	8.00	≤0.01	0.02
LOd-MNR(B)	150 days	5.71	≤0.01	0.01
LOe-MNR(B)	308 days	2.91	≤0.01	≤0.005

Table 8.6: Analyses of final experiments with diluted and concentrated HA

		Concentration (µg/l) + (isotopes used)		
Sample name	**Reaction time**	**Cr** (52, 53)	**Pd** (105, 106, 108)	**Pt** (194, 195)
Tailings material				
HA=10 ppm				
LAa-TAIL10	2 days	7.12	0.37	1.92
LAb-TAIL10	9 days	8.08	1.47	0.95
LAc-TAIL10	24 days	4.39	0.41	0.01
LAd-TAIL10	49 days	45.14	0.30	0.06
HA=1 000 ppm				
LAa-TAIL1000	2 days	42.81	1.22	2.66
LAb-TAIL1000	9 days	47.71	0.86	9.17
LAc-TAIL1000	24 days	33.44	2.18	0.30
LAd-TAIL1000	49 days	32.78	0.49	0.11
Chromitite				
HA=1 000 ppm				
LAa-MNR1000	2 days	61.28	4.18	5.46
LAb-MNR1000	9 days	61.02	0.66	0.26
LAc-MNR1000	24 days	71.32	3.60	0.19
LAd-MNR1000	49 days	66.09	2.45	0.46
PdS				
HA=1 000 ppm				
LAa-PdS1000	2 days		14528.68	
LAb-PdS1000	9 days		7428.32	
LAc-PdS1000	24 days		2787.79	
LAd-PdS1000	49 days		11033.99	
PtS				
HA=1 000 ppm				
LAa-PtS1000	2 days			392.68
LAb-PtS1000	9 days			458.61
LAc-PtS1000	24 days			2355.78
LAd-PtS1000	49 days			894.45

CV: Emmylou Kotzé

Personal information

Tel. number:	+49 174 2872 406
E-Mail:	emmyktz@gmail.com
Born:	13 April 1990, South Africa
Current residence:	Germany
First language:	English

Education and employment

Since 2015	Ph.D. position at Leibniz University in Hannover (Germany)
2012-2015	M.Sc. at the University of the Free State (South Africa)
2011	Student geologist at Bokoni Platinum Mine, Limpopo, South Africa
2008-2011	Bachelor of Science (Honours) in Geology
2007	Matriculation from high school (Bloemfontein, South Africa)

Publications

Kotzé, E., Schuth, S., Goldmann, S., Winkler, B., Botcharnikov, R.E. & Holtz, F. (2019). The mobility of palladium and platinum in the presence of humic acids: an experimental study. Chemical Geology 514, pp. 65-78. https://doi.org/10.1016/j.chemgeo.2019.03.028.